Analysis of Selected Legacy ^{85}Kr Samples

Fuel Cycle Research & Development

Prepared for
U.S. Department of Energy
Material Recovery and Waste Form Development Campaign
R. T. Jubin and S. H. Bruffey
Oak Ridge National Laboratory

September 2, 2016
FCRD-MRWFD-2016-000047 (L2)
FCRD-MRWFD-2016-000299 (L3)
ORNL/TM-2016/350

Approved for public release.
Distribution is unlimited.

DISCLAIMER

This information was prepared as an account of work sponsored by an agency of the U.S. Government. Neither the U.S. Government nor any agency thereof, nor any of their employees, makes any warranty, expressed or implied, or assumes any legal liability or responsibility for the accuracy, completeness, or usefulness, of any information, apparatus, product, or process disclosed, or represents that its use would not infringe privately owned rights. References herein to any specific commercial product, process, or service by trade name, trade mark, manufacturer, or otherwise, does not necessarily constitute or imply its endorsement, recommendation, or favoring by the U.S. Government or any agency thereof. The views and opinions of authors expressed herein do not necessarily state or reflect those of the U.S. Government or any agency thereof.

ACKNOWLEDGMENTS

The authors of this report wish to acknowledge the many researchers at the U.S. Department of Energy national laboratories who are part of the Off-Gas Sigma Team and who have contributed information in support of this effort. This includes D. Brashear [Oak Ridge National Laboratory (ORNL)], T. G. Garn [Idaho National Laboratory (INL)], T. J. Garino [Sandia National Laboratories (SNL)], M. R. Greenhalgh (INL), D. L. Lee (ORNL), T. M. Nenoff (SNL), N. Soelberg (INL), and G. W. Wright (ORNL). Special thanks go to Z. Burns, C. Baldwin, T. Gerczak, and C. Silva, all from ORNL, for their efforts to recover, sample and perform the detailed analysis of these samples.

SUMMARY

Legacy samples composed of ^{85}Kr encapsulated in solid zeolite 5A material and five small metal tubes containing a mixture of the zeolite combined with a glass matrix resulting from hot isostatic pressing have been preserved. The samples were a result of krypton R&D encapsulation efforts in the late 1970s performed at the Idaho Chemical Processing Plant.

These samples were shipped to Oak Ridge National Laboratory (ORNL) in mid-FY 2014. Upon receipt the outer shipping package was opened and the inner package removed and placed in a radiological hood. The individual capsules were double bagged as they were removed from the inner shipping pig and placed into individual glass sample bottles for further analysis.

The five capsules were then x-ray imaged. Capsules 1 and 4 appear intact and to contain an amorphous mass within the capsules. Capsule 2 clearly shows the saw marks on the capsule and a quantity of loose pellet or bead-like material remaining in the capsule. Capsule 3 shows similar bead-like material within the intact capsule. Capsule 5 had been opened at an undetermined time in the past. The end of this capsule appears to have been cut off, and there are additional saw marks on the side of the capsule. X-ray tomography allowed the capsules to be viewed along the three axes. Of most interest was determining whether there was any residual material in the closed end of Capsule 5. The images confirmed the presence of residual material within this capsule. The material appears to be compacted but still retains some of the bead-like morphology.

Based on the nondestructive analysis (NDA) results, a proposed path forward was formulated to advance this effort toward the original goals of understanding the effects of extended storage on the waste form and package. Based on the initial NDA and the fact that there are at least two breached samples, it was proposed that exploratory tests be conducted with the breached specimens before opening the three intact capsules. Portions of these would be analyzed to determine the fraction of krypton/xenon remaining in the matrix and the amount of rubidium remaining in the matrix. The inner surface of the breached capsules would be examined for corrosion.

The materials contained in Capsules 2 and 5 have been examined. There appears to be a relatively uniform distribution of Kr and Rb throughout the pellets examined. The chemical composition of the pellets appears to be consistent with 5A molecular sieves. The material contained within Capsule 5 showed ~1 at. % lead. The origin of the Pb is currently indeterminate. X-ray diffraction analysis shows a significant shift from the 5A structure, most likely due to the Kr encapsulation / sintering process that occurred when the samples were made.

The capsule walls were also examined and showed extensive corrosion throughout. Elemental mapping of the capsule material appeared consistent with carbon steel, while the weld material appeared consistent with a stainless steel. The interior surface of the capsule appeared to have a layer of material containing Al, Si, and Ca similar to the 5A molecular sieve. Analysis for Rb within the corrosion sites was inconclusive.

CONTENTS

ACKNOWLEDGMENTS iii
SUMMARY iv
ACRONYMS xv
1. INTRODUCTION 1
2. BACKGROUND 2
3. SUMMARY OF NDA RESULTS AND ANALYSIS PLANS FOR SELECTED CAPSULES / MATERIALS 5
3.1 Analysis of Loose Material from Capsule 2 10
3.2 Analysis of Capsule 2 10
3.3 Analysis of Capsule 5 10
4. ANALYSIS OF LOOSE MATERIAL FROM CAPSULE 2 10
4.1 Optical Analysis 10
4.2 SEM Analysis 10
4.3 Chemical Analysis 23
5. ANALYSIS OF CAPSULE 2 26
5.1 Optical Analysis 26
5.2 SEM Analysis 31
6. ANALYSIS OF CAPSULE 5 49
6.1 Optical Analysis 49
6.2 SEM Analysis of Zeolite Material Recovered from Capsule 5 56
6.3 Chemical Analysis 76
7. ANALYSIS OF CAPSULE 5 CONTAINER 79
7.1 Optical Analysis 79
7.2 SEM Analysis 81
8. XRD ANALYSIS OF MATERIAL RECOVERED FROM CAPSULES 2 AND 5 115
9. DISCUSSION AND PATH FORWARD 117
9.1 Discussion 117
9.2 Path Forward 118
10. REFERENCES 118

FIGURES

Figure 1: Graphical depiction of the Kr-85 decay chain. Kr-85 with a 10.752 y half life decays by emitting a beta particle. About 0.43 percent of the beta decays (red line) produce Rb-85, in the second ground state at 0.514 MeV which subsequently decays to the ground state, Rb-85, by emitting a gamma ray. About 99.56 percent of the decays (blue line) produce Rb-85 directly. Ru-85 is stable. 1

Figure 2: Photo of the loose zeolite material in a Ziploc bag. 3

Figure 3: Photo of a metal tube, presumably containing potentially un-HIPed loose zeolites. 3

Figure 4: Kr-85 Capsules (Top, L-R: Capsule 1, Capsule 2; Middle, L-R: Capsule 3, Capsule 4; Bottom: Capsule 5). 4

Figure 5: Photo of squashed metal tubes. 5

Figure 6: General sequence for the samples. 6

Figure 7: Capsule 2. 7

Figure 8: Capsule 5. 7

Figure 9: Loose material from Capsule 2. 8

Figure 10: X-ray image of Capsule 2. 8

Figure 11: X-ray image of Capsule 5. 9

Figure 12: X-ray tomographic images of Capsule 5 cutting across the capsule in the vertical plane. Image sequence begins in upper left and proceeds clockwise ending in lower left. 9

Figure 13: Cross section of recovered pellets from Kr-85 legacy waste form Capsule 2 as seen through an optical microscope. 11

Figure 14: Cross section of selected recovered pellet from Kr-85 legacy waste form Capsule 2 as seen through an optical microscope at low magnification. 12

Figure 15: Cross section of selected recovered pellet from Kr-85 legacy waste form Capsule 2 as seen through an optical microscope at higher magnification. 12

Figure 16: Secondary electron image of cross section of pellet recovered from Capsule 2 at 35× magnification (Image 4302) [Sample K3]. 13

Figure 17: Backscatter electron image of cross section of pellet recovered from Capsule 2 at 35× magnification (Image 4303) [Sample K3]. 13

Figure 18: Detailed images of area near center of pellet recovered from Capsule 2 at 250× to 2500× magnification. SEI images on left and backscatter images on the right (Images 4304 – 4309) [Sample K3]. 14

Figure 19: Elemental maps of area shown in bottom images of Figure 18 for pellet recovered from Capsule 2 [Sample K3]. 15

Figure 20: SEM-EDS of the area shown in the elemental maps for Image 4310 near center of pellet recovered from Capsule 2 [Sample K3]. 16

Figure 21: Detailed images of area near midpoint between center and edge of pellet recovered from Capsule 2 at 250× to 2500× magnification. SEI images on the left and backscatter images on the right (Images 4310 – 4315) [Sample K3]. 17

Figure 22: Elemental maps of area shown in bottom images of Figure 21 for pellet recovered from Capsule 2 [Sample K3]. 18

Figure 23: SEM-EDS of the area shown in the elemental maps for Image 4315 near midpoint between center and edge of pellet recovered from Capsule 2 [Sample K3]. 19

Figure 24: Detailed images of area near outer edge of pellet recovered from Capsule 2 at 250× to 2500× magnification. SEI images on left and backscatter images on the right (Images 4316 – 4321) [Sample K3]. 20

Figure 25: Elemental maps of area shown in bottom images of Figure 24 for pellet recovered from Capsule 2 [Sample K3]. 21

Figure 26: SEM-EDS of the area shown in the elemental maps for Image 4321 near outer edge of pellet recovered from Capsule 2 [Sample K3]. 22

Figure 27: SEM-EDS line data for pellet recovered from Capsule 2 [Sample K3]. 23

Figure 28: Section “A” of Capsule 2 looking through cell window. 27

Figure 29: Composite optical microscope image of Section “A” of Capsule 2. 27

Figure 30: Composite optical microscope image of Section “B” of Capsule 2. 28

Figure 31: Detail optical microscope image of Section “A” of Capsule 2 at low magnification. 28

Figure 32: Optical microscope image of Section “A” of Capsule 2 (Image MM2B2-0MS-001). 29

Figure 33: Optical microscope image at 50× magnification of Section “A” of Capsule 2 (Image MM2B2-050X-002). 29

Figure 34: Optical microscope image at 200× magnification of Section “A” of Capsule 2 (Image MM2B2-0200X-014). 30

Figure 35: Detail optical microscope image at 400× magnification of Section “A” of Capsule 2 at higher magnification(Image MM2B2-400X-021). 30

Figure 36: Optical microscope image series with focus plane above the polish surface (a), on surface (b), and below surface (c) for Section the “A” of Capsule 2 (images MM2B2-200x-016-18). 31

Figure 37: Annotated optical microscope image of Section “A” of Capsule 2 showing locations that were examined by SEM (Image MM2B2-0MS-001). 32

Figure 38: Detailed images of the wall of Capsule 2 at 50× to 200× magnification at Location 1. SEI images on the left and BEC images on the right (Images 4406 – 4409) [Sample 2B2]. 33

Figure 39: Elemental maps of area shown in bottom images of Figure 38 for Area 1 of the wall segment from Capsule 2 [Sample 2B2]. 34

Figure 40: EDS layer image for bottom images of Figure 38 for Area 1 of the wall segment from Capsule 2. Sub-areas for localized spectral analysis are annotated [Sample 2B2]. 35

Figure 41: SEM-EDS spectra for the three sub-areas of the Capsule 2 wall segment shown in Figure 40 [Sample 2B2]. 36

Figure 42: Detailed images of the wall of Capsule 2 at 30× to 150× magnification at Location 2. SEI images on the left and BEC images on the right (Images 4410 – 4415) [Sample 2B2]. 37

Figure 43: Elemental maps of area shown in bottom images of Figure 42B for Area 2 of the wall segment from Capsule 2 [Sample 2B2]. 38

Figure 44: EDS layer image for bottom images of Figure 42B for Area 2 of the wall segment from Capsule 2. Sub-areas for localized spectral analysis are annotated [Sample 2B2]. 38

Figure 45. SEM-EDS spectra for the two sub-areas of the Capsule 2 wall segment shown in Figure 44 [Sample 2B2]. 39

Figure 46: Detailed images of the wall of Capsule 2 at 75× to 150× magnification at Location 3. SEI images on the left and BEC images on the right (Images 4416 – 4419) [Sample 2B2]. 40

Figure 47: Elemental maps of area shown in bottom images of Figure 46 for Area 3 of the wall segment from Capsule 2 [Sample 2B2]. 41

Figure 48: EDS layer image for bottom images of Figure 46 for Area 3 of the wall segment from Capsule 2. Sub-areas for localized spectral analysis are annotated [Sample 2B2]. 42

Figure 49: SEM-EDS spectra for the two sub-areas of the Capsule 2 wall segment shown in Figure 48 [Sample 2B2]. 42

Figure 50: Detailed images of the wall of Capsule 2 at 50× to 200× magnification at Location 4. SEI images on the left and BEC images on the right (Images 4420 – 4425) [Sample 2B2]. 43

Figure 51: Elemental maps of area shown in middle images of Figure 50A for Area 4 of the exterior surface of the wall segment from Capsule 2 [Sample 2B2]. 44

Figure 52: Elemental maps of area shown in bottom images of Figure 50B for Area 4 of the interior of the wall segment from Capsule 2 [Sample 2B2]. 45

Figure 53: EDS layer image for bottom images of Figure 50B for Area 4 of the wall segment from Capsule 2. Sub-areas for localized spectral analysis are annotated [Sample 2B2]. 46

Figure 54: SEM-EDS spectra for the five sub-areas of the Capsule 2 wall segment shown in Figure 53 [Sample 2B2]. 47

Figure 55: Section “A” of Capsule 5 looking through cell window. 50

Figure 56: Composite optical microscope image of Section “A” of Capsule 5. 51

Figure 57: Composite optical microscope image of Section “B” of Capsule 5. 52

Figure 58: Detail optical microscope image of Section “A” of Capsule 5. 53

Figure 59: Optical microscope image of Section “A” of Capsule 5 (Image MM5A2-0MS-001). 53

Figure 60: Optical microscope image at 50× magnification of section “A” of Capsule 5 with possible zeolite material attached to wall (Image MM5A2-050X-004). 54

Figure 61: Optical microscope image at 50× magnification of Section “A” of Capsule 5 showing suspected weld area (Image MM5A2-050X-010). 54

Figure 62: Optical microscope image at 200× magnification of Section “A” of Capsule 5 (Image MM5A2-0200X-011). 55

Figure 63: Detail optical microscope image at 400× magnification of Section "A" of Capsule 5 at higher magnification(Image MM5A2-400X-013). 55

Figure 64: Secondary electron image of cross section of pellet recovered from Capsule 5 at 35× magnification (Image 4322) [Sample K5]. 57

Figure 65: Backscatter electron image of cross section of pellet recovered from Capsule 5 at 35× magnification (Image 4323) [Sample K5]. 57

Figure 66: Detailed images of area near center of pellet recovered from Capsule 5 at 250× to 2500× magnification. SEI images on the left and backscatter images on the right (Images 4324–4329) [Sample K5]. 58

Figure 67: Elemental maps of area shown in bottom images of Figure 66 for pellet recovered from Capsule 5 [Sample K5]. 59

Figure 68: SEM-EDS of the area shown in the elemental maps for Image 4329 near center of pellet recovered from Capsule 5 [Sample K5]. 60

Figure 69: Detailed images of area near midpoint between center and edge of pellet recovered from Capsule 5 at 250× to 2500× magnification. SEI images on the left and backscatter images on the right (Images 4336–4341) [Sample K5]. 61

Figure 70: Elemental maps of area shown in bottom images of Figure 69 for pellet recovered from Capsule 5 [Sample K5]. 62

Figure 71: SEM-EDS of the area shown in the elemental maps for Image 4341 near midpoint between center and edge of pellet recovered from Capsule 5 [Sample K5]. 63

Figure 72: Detailed images of area near outer edge of pellet recovered from Capsule 5 at 250× to 2500× magnification. SEI images on the left and backscatter images on the right (Images 4342–4347) [Sample K5]. 64

Figure 73: Elemental maps of area shown in bottom images of Figure 72 for pellet recovered from Capsule 5 [Sample K5]. 65

Figure 74: SEM-EDS of the area shown in the elemental maps for Image 4347 near the outer edge of pellet recovered from Capsule 5 [Sample K5]. 66

Figure 75: Detailed images of high-Z area near center of pellet recovered from Capsule 5 at 250× to 2500× magnification. SEI images on the left and backscatter images on the right (Images 4330–4335) [Sample K5]. 67

Figure 76: Elemental maps of area shown in bottom images of Figure 75 for pellet recovered from Capsule 5 [Sample K5]. 68

Figure 77: SEM-EDS of the high-Z area shown in the elemental maps for Image 4335 near center and edge of pellet recovered from Capsule 5 [Sample K5]. 69

Figure 78: SEM-EDS line data for pellet recovered from Capsule 5 [Sample K5]. 70

Figure 79: Secondary electron image of surface showing interface between two HIPed pellets recovered from Capsule 5 at 250× magnification (Image 4348) [Sample K5]. 71

Figure 80: Secondary electron image of surface showing interface between two HIPed pellets recovered from Capsule 5 at 750× magnification (Image 4349) [Sample K5]. 71

Figure 81: Backscatter electron image of interface area for HIPed pellet recovered from Capsule 5 at 750× magnification showing location for EDS point scans shown in Figures 82-85 (Image 4349) [Sample K5]. 72

Figure 82: EDS point scan spectrum 13 for location noted in Figure 81 (Image 4349) [Sample K5]. 73

Figure 83: EDS point scan spectrum 14 for location noted in Figure 81 (Image 4349) [Sample K5]. 74

Figure 84: EDS point scan spectrum 15 for location noted in Figure 81 (Image 4349) [Sample K5]. 75

Figure 85: EDS point scan spectrum 16 for location noted in Figure 81 (Image 4349) [Sample K5]. 76

Figure 86: Detail optical microscope image of Section "A" of Capsule 5. 79

Figure 87: Detail optical microscope image of Section "A" of Capsule 5. 80

Figure 88: Annotated optical microscope image of Section "A" of Capsule 5 showing locations that were examined by SEM (Image MM5A2-0MS-001). 82

Figure 89: Detailed images of the wall of Capsule 5 at 50× to 200× magnification at location 5. SEI images on the left and BEC images on the right (Images 4426–4429) [Sample 5AB2]. 83

Figure 90: Elemental maps of area shown in bottom images of Figure 89 for area 5 of the wall segment from Capsule 5 [Sample 5A2]. 84

Figure 91: EDS layer image for bottom images of Figure 89 for area 5 of the wall segment from Capsule 5. Sub-areas for localized spectral analysis are annotated [Sample 5A2]. 85

Figure 92: SEM-EDS spectra for the six sub-areas of the Capsule 5 wall segment shown in Figure 91 [Sample 5A2]. 86

Figure 93: Detailed images of the wall of Capsule 5 at 50× to 150× magnification at location 6. SEI images on the left and BEC images on the right (Images 4431–4434) [Sample 5A2]. 87

Figure 94: Elemental maps of area shown in bottom images of Figure 93 for area 6 of the wall segment from Capsule 5 [Sample 5A2]. 88

Figure 95: EDS layer image for bottom images of Figure 93 for area 6 of the wall segment from Capsule 5. Sub-areas for localized spectral analysis are annotated [Sample 5A2]. 89

Figure 96. SEM-EDS spectra for the four sub-areas of the Capsule 5 wall segment shown in Figure 95 [Sample 5A2]. 90

Figure 97: Detailed images of the wall of Capsule 5 at 50× to 150× magnification at location 7. SEI images on the left and BEC images on the right (Images 4435–4438) [Sample 5A2]. 92

Figure 98: Elemental maps of area shown in bottom images of Figure 97 for area 7 of the wall segment from Capsule 7 [Sample 5A2]. 93

Figure 99: EDS layer image for bottom images of Figure 97 for area 7 of the wall segment from Capsule 5. Sub-areas for localized spectral analysis are annotated [Sample 5A2]. 93

Figure 100: SEM-EDS spectra for the three sub-areas of the Capsule 5 wall segment shown in Figure 99 [Sample 5A2.]. 94

Figure 101: Detailed images of the wall of Capsule 5 at 50× to 200× magnification at location 8. SEI images on the left and BEC images on the right (Images 4439–4442) [Sample 5A2]. 95

Figure 102: Detailed images of the wall of Capsule 5 at 50× to 200× magnification at location 8. SEI images on the left and BEC images on the right (Images 4457–4458) [Sample 5A2]. 95

Figure 103: Elemental maps of area shown in middle images of Figure 102 for area 8 of the exterior surface of the wall segment from Capsule 5 [Sample 5A2]. 96

Figure 104: EDS layer image for bottom images of Figure 102 for area 8 of the wall segment from Capsule 5. Sub-areas for localized spectral analysis are annotated [Sample 5A2]. 96

Figure 105: SEM-EDS spectra for the five sub-areas of the Capsule 5 wall segment shown in Figure 102 [Sample 5A2]. 97

Figure 106: Detailed images of the wall of Capsule 5 at 50× to 150× magnification at location 9. SEI images on the left and BEC images on the right (Images 4443–4448) [Sample 5A2]. 98

Figure 107: Elemental maps of area shown in middle images of Figure 106A for area 9 of the interior surface of the wall segment from Capsule 5 [Sample 5A2]. 99

Figure 108: EDS layer image for middle images of Figure 106A for area 9 of the wall segment from Capsule 5. Sub-areas for localized spectral analysis are annotated [Sample 5A2]. 100

Figure 109: SEM-EDS spectra for the four sub-areas of the Capsule 5 wall segment shown in Figure 108 [Sample 5A2]. 101

Figure 110: Elemental maps of area shown in bottom images of Figure 106B for area 9 of the exterior surface of the wall segment from Capsule 5 [Sample 5A2]. 102

Figure 111: EDS layer image for bottom images of Figure 106B for area 9 of the wall segment from Capsule 5. Sub-areas for localized spectral analysis are annotated [Sample 5A2]. 103

Figure 112: SEM-EDS spectra for the six sub-areas of the Capsule 5 wall segment shown in Figure 111 [Sample 5A2]. 104

Figure 113: Detailed images of the wall of Capsule 5 at 50× to 150× magnification at location 10. SEI images on the left and BEC images on the right (Images 4449–4451) [Sample 5A2]. 105

Figure 114: Elemental maps of area shown in bottom images of Figure 113 for area 10 of the exterior surface of the wall segment from Capsule 5 [Sample 5A2]. 106

Figure 115: EDS layer image for bottom images of Figure 113 for area 10 of the wall segment from Capsule 5. Sub-areas for localized spectral analysis are annotated [Sample 5A2]. 107

Figure 116: SEM-EDS spectra for the four sub-areas of the Capsule 5 wall segment shown in Figure 115 [Sample 5A2]. 108

Figure 117: Detailed images of the wall of Capsule 5 at 50× to 150× magnification at location 11. SEI images on the left and BEC images on the right (Images 4452–4455) [Sample 5A2]. 109

Figure 118: Elemental maps of area shown in bottom images of Figure 116 for area 11 of the exterior surface of the wall segment from Capsule 5 [Sample 5A2]. 110

Figure 119: EDS layer image for bottom images of Figure 116 for area 11 of the wall segment from Capsule 5. Sub-areas for localized spectral analysis are annotated [Sample 5A2]. 111

Figure 120: SEM-EDS spectra for the five sub-areas of the Capsule 5 wall segment shown in Figure 119 [Sample 5A2]. 112

Figure 121: Experimental XRD pattern of fresh 5A zeolite sample (black color) and the reference pattern for zeolite 5A (red color lines). Asterisks indicate the reflections corresponding to Si standard. 116

Figure 122: A comparison of XRD patterns of irradiated Kr-85 zeolite samples with 5A MS base metal sample and the sample holder. Asterisks indicate the reflections corresponding to Si standard. Full XRD patterns from 5–70° 2Θ range are shown in the left side figure, and a focused range of 5–30° 2Θ is shown on the right side. 116

TABLES

Table 1: Compositional analyis of zeolite material, noble gases and Rb from Capsule 2 based on EDS data 25

Table 2: Compositional analyis of selected area of the Capsule 2 wall sample based on EDS data 48

Table 3: Compositional analyis of zeolite material, noble gases and Rb from Capsule 5 based on EDS data 78

Table 4: Compositional analyis of selected area of the Capsule 5 wall sample based on EDS data 113

ACRONYMS

BEC	backscatter electron imaging
EDS	energy dispersive spectroscopy
HFEF	Hot Fuels Examination Facility
HIP	hot isostatic press
ICP-MS	inductively coupled plasma mass spectrometry
ICPP	Idaho Chemical Processing Plant
INL	Idaho National Laboratory
MS	molecular sieve
NDA	nondestructive analysis
ORNL	Oak Ridge National Laboratory
SEM/EDX	scanning electron microscope/energy dispersive x-ray
SEI	secondary electron imaging
STP	standard temperature and pressure
TEM	transmission electron microscopy
XAS	x-ray absorption spectroscopy
XPS	x-ray photoelectron spectroscopy
XRD	x-ray diffraction

MATERIAL RECOVERY AND WASTE FORM DEVELOPMENT CAMPAIGN

ANALYSIS OF SELECTED LEGACY ^{85}KR SAMPLES

1. INTRODUCTION

Legacy samples composed of ^{85}Kr encapsulated in solid zeolite 5A material and five small metal tubes containing a mixture of the zeolite combined with a glass matrix resulting from hot isostatic pressing have been preserved. The samples are a result of krypton R&D encapsulation efforts in the late 1970s performed at the Idaho Chemical Processing Plant (ICPP). The samples were retrieved from archive storage and transported to the Hot Fuels Examination Facility (HFEF) within the Materials Fuels Complex at the Idaho National Laboratory (INL). Examination of such samples can lead to invaluable information on the long-term stability of ^{85}Kr waste forms. These samples are unique in the sense that these have undergone decay of three plus half-lives of the ^{85}Kr while in storage. Kr-85 decays with about a 10.75 year half-life by emitting a beta particle. About 99.56 percent of the decays produce Rb-85 in the ground state while about 0.44% result in a 0.514 MeV gamma emission via the pathways depicted in Figure 1.

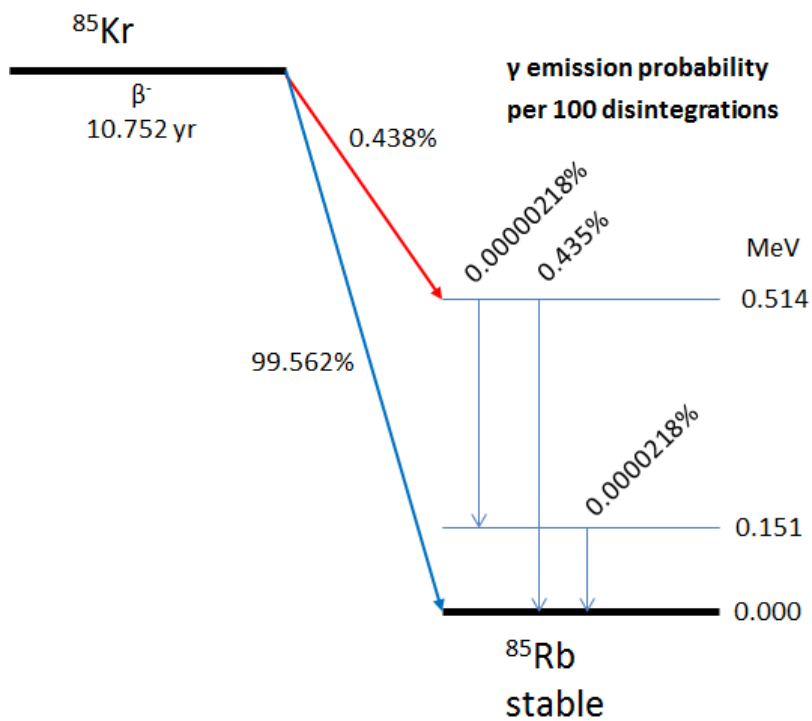

Figure 1: Graphical depiction of the Kr-85 decay chain. Kr-85 with a 10.752 y half life decays by emitting a beta particle. About 0.43 percent of the beta decays (red line) produce Rb-85, in the second ground state at 0.514 MeV which subsequently decays to the ground state, Rb-85, by emitting a gamma ray. About 99.56 percent of the decays (blue line) produce Rb-85 directly. Ru-85 is stable.

There are two areas of particular interest relative to these capsules. The first is to determine the location of the Rb decay daughter and its impact (since it is highly corrosive[1]) on the storage capsule. The second is to gain insight into the long-term performance of the Kr loaded zeolite. The zeolite was loaded or encapsulated by immobilizing the krypton in a solid matrix by sintering it at high temperatures and pressures. This would include determining the amount of Kr remaining and the behavior of the Rb decay daughter (i.e., where is it, and its impact on the zeolite structure). Numerous analytical options are available to investigate sample aging characteristics. These options include, but are not limited to, neutron radiography, scanning electron microscope/energy dispersive x-ray spectroscopy (SEM/EDX), transmission electron microscopy (TEM), x-ray diffraction (XRD), x-ray photoelectron spectroscopy (XPS), and x-ray absorption spectroscopy (XAS). To that end, a phased analysis approach was developed in FY 2011[2] and updated in FY 2015[3] to begin the more detailed analysis of the capsules following the nondestructive analysis (NDA) that had been completed on these samples.

2. BACKGROUND

The background regarding the origin of these samples is detailed by Garn et al.[2] and repeated here in an abbreviated form for completeness. In the late 1970s, an R&D effort to study ^{85}Kr encapsulation and leakage was performed at INL by Christensen et al.[4-7] Off-gas resulting from fuel dissolution underwent treatment, with the fission products sent to the Rare Gas Plant at ICPP where the ^{85}Kr along with stable krypton was recovered via cryogenic distillation and collected in gas cylinders. A cylinder containing the ^{85}Kr mixture was transferred to the Multi-Curie Cell where the encapsulation studies were completed.

The ^{85}Kr R&D encapsulation effort incorporated numerous materials, including sodalite, “thirsty” glass, and zeolite 5A, with zeolite 5A reportedly showing the best results. The R&D effort included evaluation of ^{85}Kr leakage, resulting in numerous samples of each material being cut apart to measure ^{85}Kr leakage via thermogravimetric analysis. Because the testing included numerous materials, there is a question as to the exact nature of the legacy samples. Because the zeolite 5A material showed the most promise, it is assumed that these samples represent the zeolite material. Further support of this assumption was a recent verbal communication with one of the original researchers (retired), who stated that the samples included “loose” zeolite 5A encapsulating ^{85}Kr and zeolites hot isostatic pressed (HIPed) in a glass matrix contained in squashed metal tubes.[8] This statement was based on inspection of photographs of the samples transported to the HFEF. Photographs showing the loose zeolite and the squashed metal tubes are found in Figures 2–5.

Figure 2: Photo of the loose zeolite material in a Ziploc bag.

Figure 3: Photo of a metal tube, presumably containing potentially un-HIPed loose zeolites.

Figure 4: Kr-85 Capsules (Top, L-R: Capsule 1, Capsule 2; Middle, L-R: Capsule 3, Capsule 4; Bottom: Capsule 5).

Figure 5: Photo of squashed metal tubes.

3. SUMMARY OF NDA RESULTS AND ANALYSIS PLANS FOR SELECTED CAPSULES / MATERIALS

The general sequence of the work as originally planned was in three stages as shown in Figure 6. Stage 1 included NDA characterization of the samples (radiation levels, contamination levels, and gamma signature) and neutron imaging. The results of stage 1 evaluations are given below.

Figures 7 and 8 show capsules 2 and 5, respectively, as they were removed from the shipping package and shielding. Figure 9 shows the loose material that fell out of capsule 2.

Figures 10 and 11 are the x-ray images of Capsules 2 and 5, respectively. Figure 10 clearly shows the saw marks on the capsule and a quantity of loose pellet or bead-like material remaining in Capsule 2. Figure 11 shows the opened Capsule 5. The end of this capsule appears to have been cut off, and there are additional saw marks on the side of the capsule. There appears to be a shadow of some sort at the closed end of the capsule that might indicate the presence of residual material.

X-ray tomography allowed the capsules to be viewed along the three axes. X-ray tomography was used in place of the originally planned neutron tomography due to greater availability of the instrument. Determining whether there was any residual material in the closed end of Capsule 5 was of most interest. Figure 12 shows slices taken along the x-axis of Capsule 5. Progressing from one image to the next sections is shown as sequential planes passing through the capsule. The heavy light gray lines on either side of the capsule are the walls of the glass jar containing the capsule. The light curving lines are the metal walls of the capsule. These images confirm the presence of residual material within this capsule. The material appears to be compacted but still retains some of the bead-like morphology.

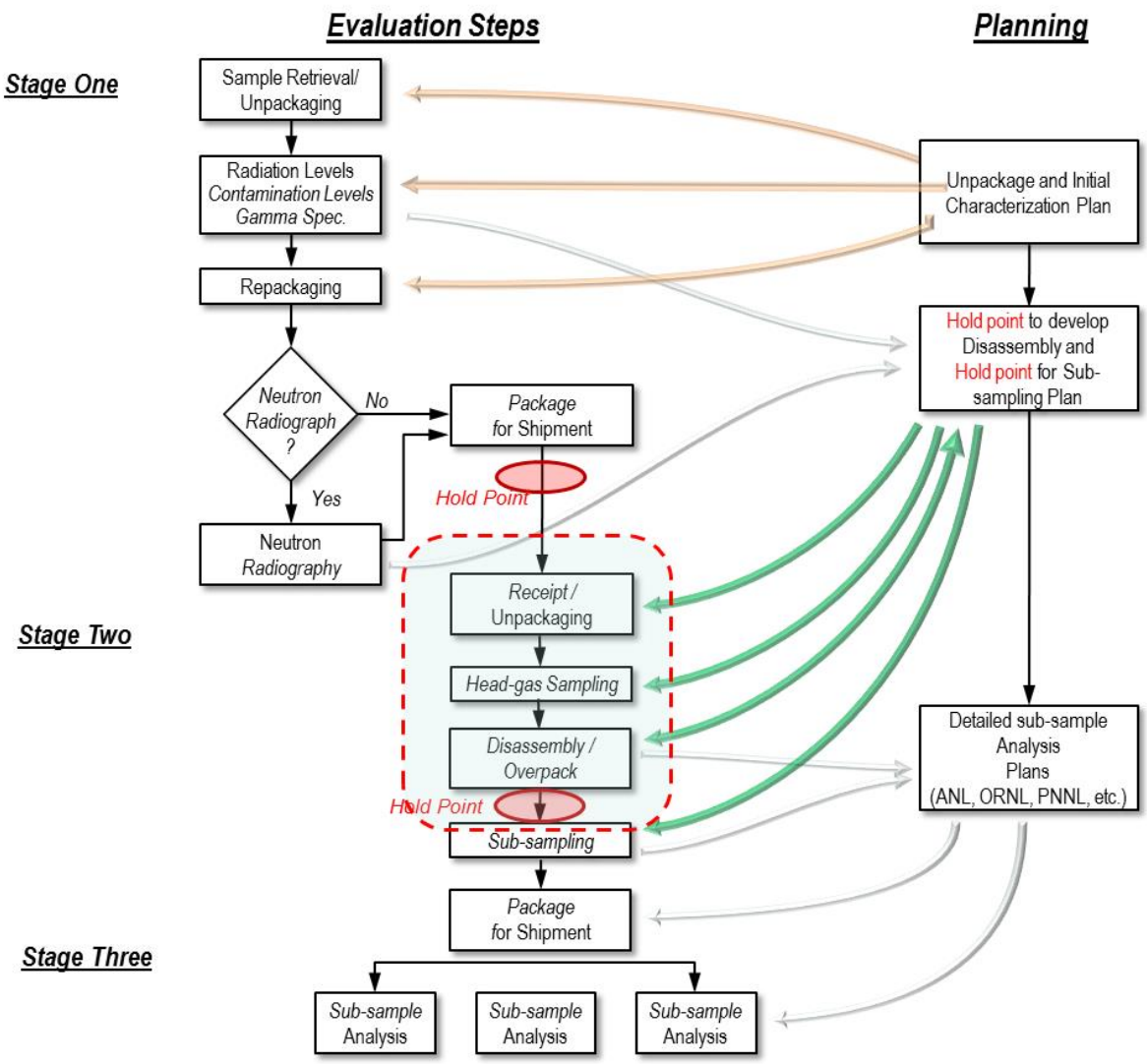

Figure 6: General sequence for the samples.

Figure 7: Capsule 2.

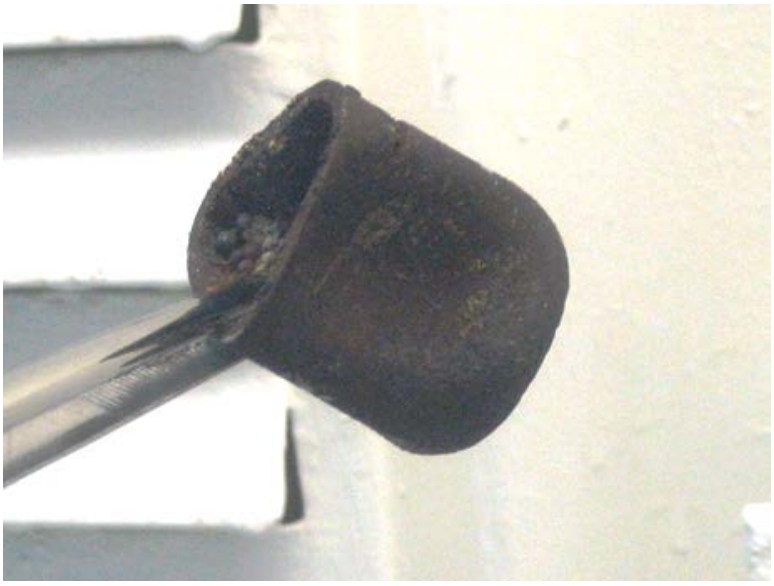

Figure 8: Capsule 5.

Figure 9: Loose material from Capsule 2.

Figure 10: X-ray image of Capsule 2.

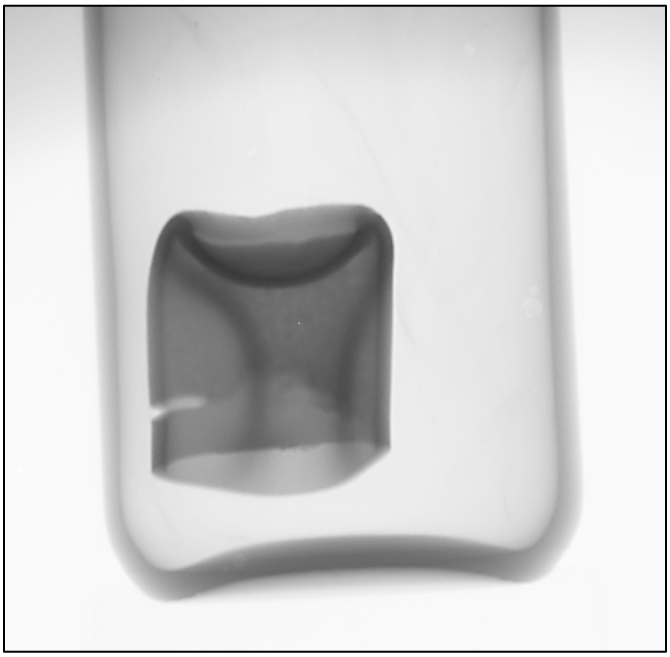

Figure 11: X-ray image of Capsule 5.

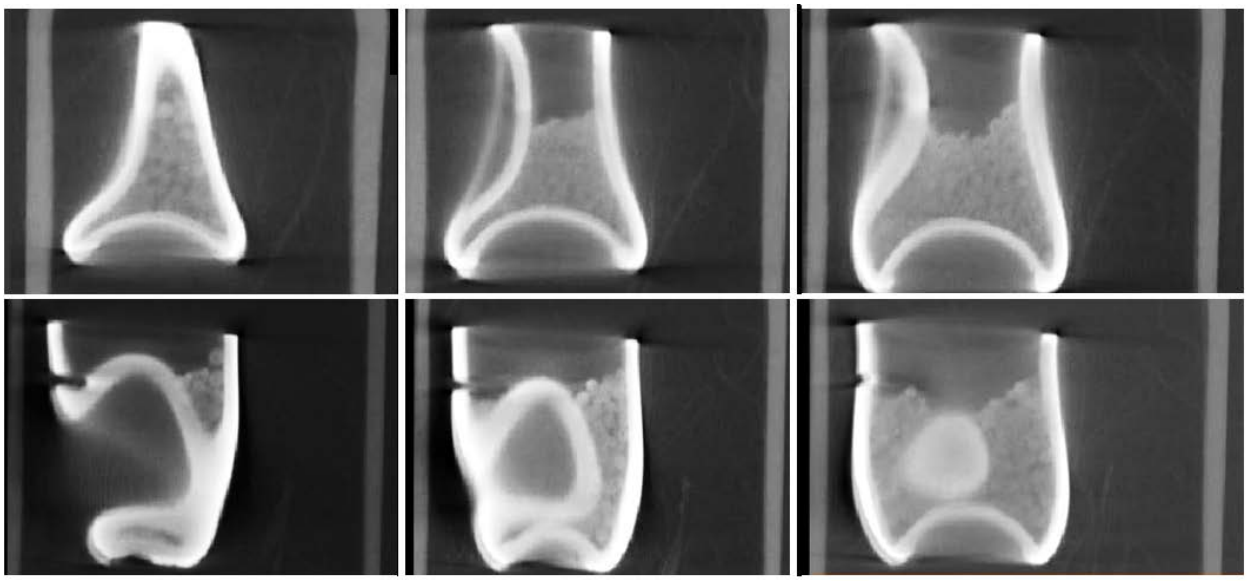

Figure 12: X-ray tomographic images of Capsule 5 cutting across the capsule in the vertical plane. Image sequence begins in upper left and proceeds clockwise ending in lower left.

A hold point was established at the completion of the NDA characterization to review the results and develop the detailed plans for the next phase of analysis that would involve opening the capsule and sub-sampling. It was determined that the first two capsules to be examined would be Capsules 2 and 5 since these were previously compromised. The analysis of these two compromised capsules should yield valuable preliminary data on the materials and will also be extremely useful in refining the techniques to be used on the remaining samples. The proposed analysis steps are discussed in the following subsections.

3.1 Analysis of Loose Material from Capsule 2

It was proposed that several of the loose pellets/beads would be analyzed. SEM/EDS and XRD would be used to determine chemical composition, morphology, and structure. Several pellets would be dissolved, and the effluent (liquid and gas) would be analyzed by inductively coupled plasma mass spectrometry (ICP-MS) and rare gas analysis to determine, if possible, the fraction of krypton/xenon remaining in the un-HIPed zeolite matrix. The rubidium content in the matrix would also be determined.

3.2 Analysis of Capsule 2

Since Capsule 2 was already breached when received, it was proposed that the capsule would be fully opened and the remaining loose material recovered. The inner surface of the capsule would be examined for corrosion. The results are intended to be compared at a later date to those for the inner surfaces of the intact capsules.

3.3 Analysis of Capsule 5

This capsule would to be cut lengthwise to reveal the residual compressed material and the sorbent-capsule interface. One half of this sample would be examined by SEM. Of particular interest is the interface between the zeolite matrix and the metal capsule. Analysis of the inner surface of the metal capsule would also be performed to compare the surface in direct contact with the zeolite matrix with the noncontact surface.

It was proposed that material would be recovered from the other half of the sample for powder XRD and chemical analysis. SEM/EDS and XRD would be used to determine chemical composition, morphology, and structure. A portion of the recovered material would be dissolved, and the effluent (liquid and gas) would be analyzed by ICP-MS and rare gas analysis to determine the fraction of krypton/xenon remaining in the HIPed zeolite matrix, if possible. The rubidium content in the matrix would also be determined.

4. ANALYSIS OF LOOSE MATERIAL FROM CAPSULE 2

4.1 Optical Analysis

Seven pellets removed from Capsule 2 have been mounted, and the cross sections as seen by optical microscope are shown in Figures 13-15. The recovered pellets were observed to have two layers: an external ceramic-like hard layer, and the center of the pellets found to be a softer almost powder-like material.

4.2 SEM Analysis

The SEM analysis was performed on a JEOL-6390LV W-filament SEM with an Oxford X-Max 50 Silicon Drift Detector for energy dispersive spectroscopy (EDS) analysis. Energy dispersive spectroscopy analysis was performed using the Oxford AZtec acquisition software using both point-ID and mapping applications. Secondary electron imaging (SEI) and backscatter electron imaging (BEC) at an accelerating voltage of 20 kV was performed on the samples. The SEI imaging signal is surface sensitive and allows for identification of topographical surface features. The BEC imaging signal is sensitive to the atomic mass of the incident substrate and is therefore compositionally dependent. The EDS analysis was also performed in parallel with the SEI and BEC imaging.

One of the pellets recovered from Capsule 2 was mounted and ground to the midpoint of the pellet. This surface was coated with an ~7-µm layer of carbon. This sample was designated K3. A second pellet was also recovered and mounted but was not carbon coated. This sample is designated K2.

The surface of K3 was examined by SEM. First, the sample was examined at low magnification. The SEI revealed the presence of some surface pitting (Fig. 16). The BEC of the same area is shown in Figure 17. Three areas across the diameter of the pellet were selected for further examination at higher magnifications. At each location, elemental maps were prepared using EDS, and a spectrum was collected to determine the approximate elemental composition. Finally an EDS line analysis was completed from the center point to the outer edge of the pellet. The SEM images taken near the center of the pellet are shown in Figure 18. The elemental mapping of the selected point near the center of the pellet is shown in Figure 19. The brightness of the color in the elemental map correlates with the concentration of the element being mapped. The EDS spectrum is presented in Figure 20. The SEM images taken near the midpoint between the center and the edge of the pellet are shown in Figure 21. The corresponding elemental mapping of the selected point is shown in Figure 22, and the EDS spectrum is presented in Figure 23. The SEM images taken near outer edge of the pellet are shown in Figure 24. The corresponding elemental mapping of the selected point is shown in Figure 25, and the EDS spectrum is presented in Figure 26.

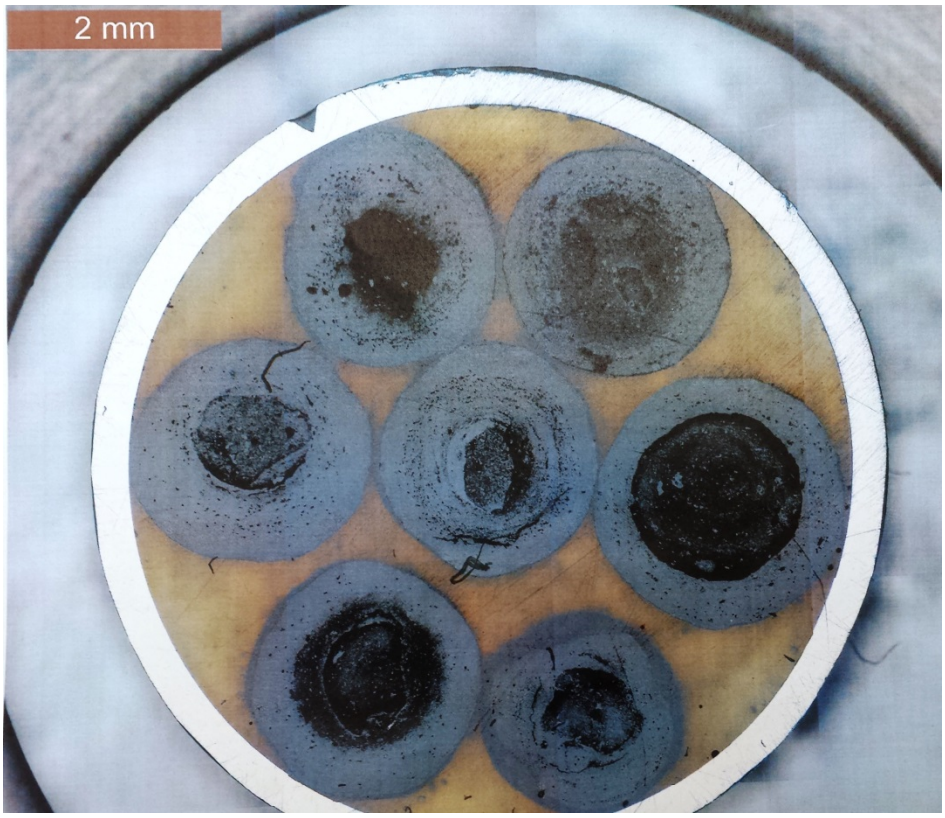

Figure 13: Cross section of recovered pellets from Kr-85 legacy waste form Capsule 2 as seen through an optical microscope.

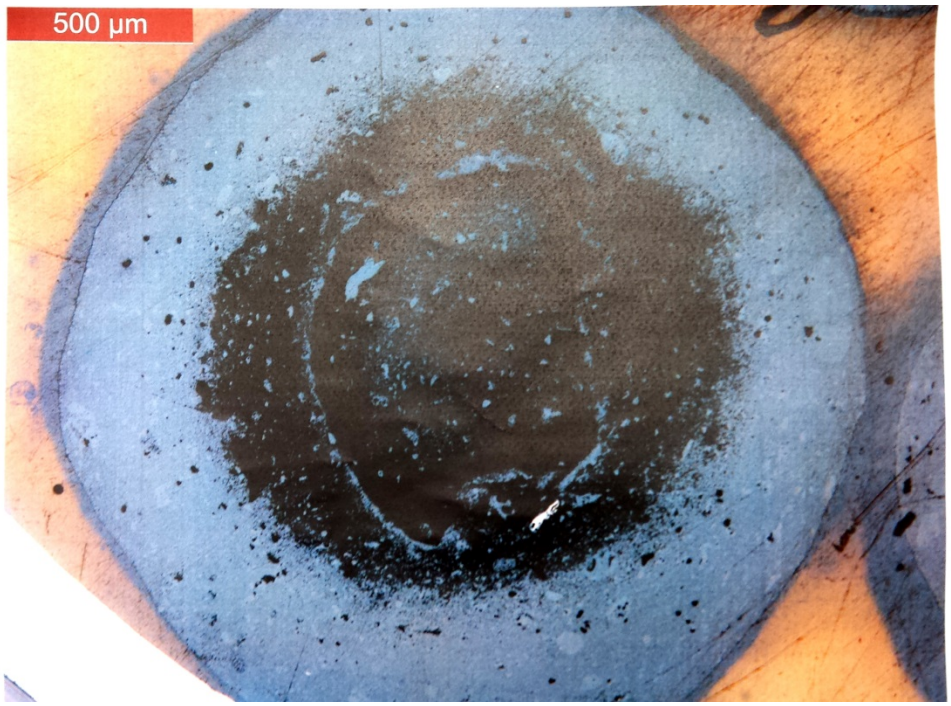

Figure 14: Cross section of selected recovered pellet from Kr-85 legacy waste form Capsule 2 as seen through an optical microscope at low magnification.

Figure 15: Cross section of selected recovered pellet from Kr-85 legacy waste form Capsule 2 as seen through an optical microscope at higher magnification.

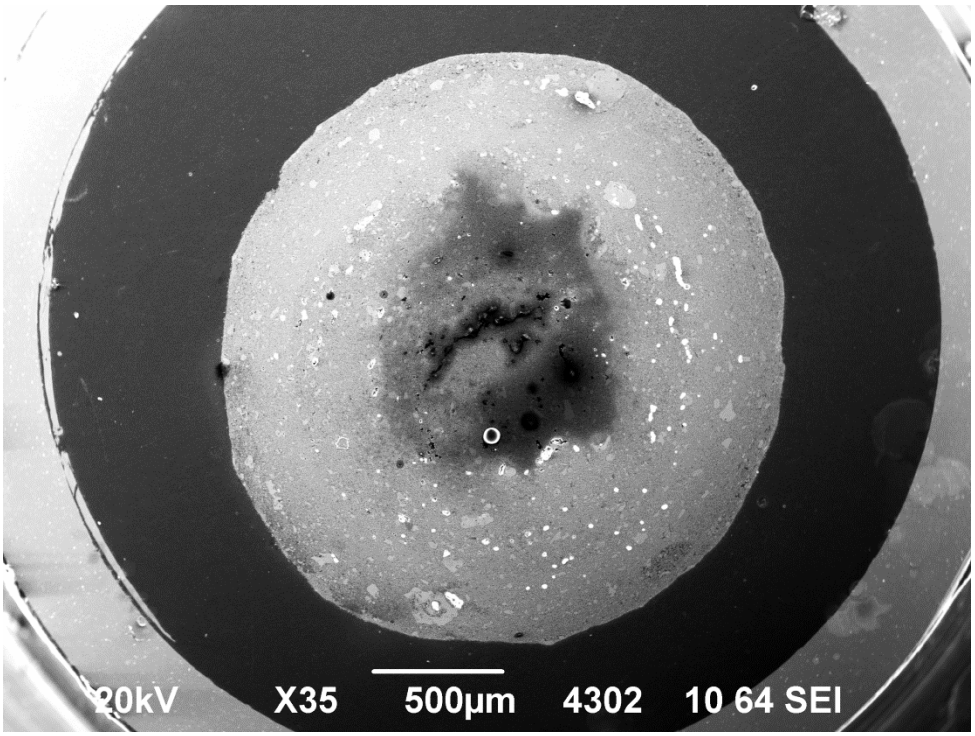

Figure 16: Secondary electron image of cross section of pellet recovered from Capsule 2 at 35× magnification (Image 4302) [Sample K3].

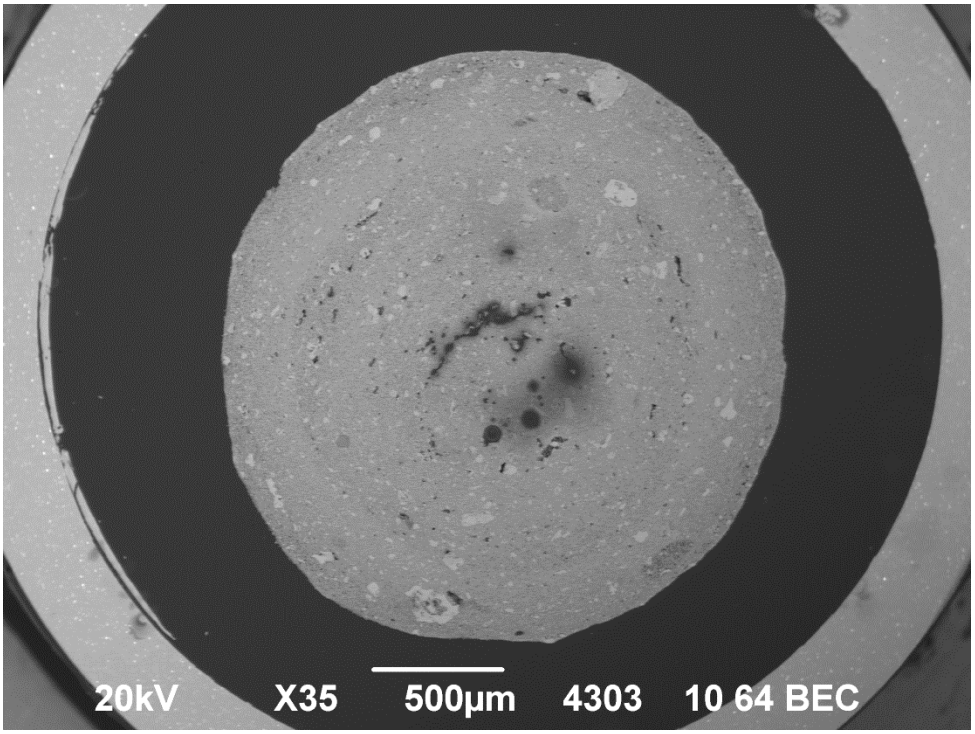

Figure 17: Backscatter electron image of cross section of pellet recovered from Capsule 2 at 35× magnification (Image 4303) [Sample K3].

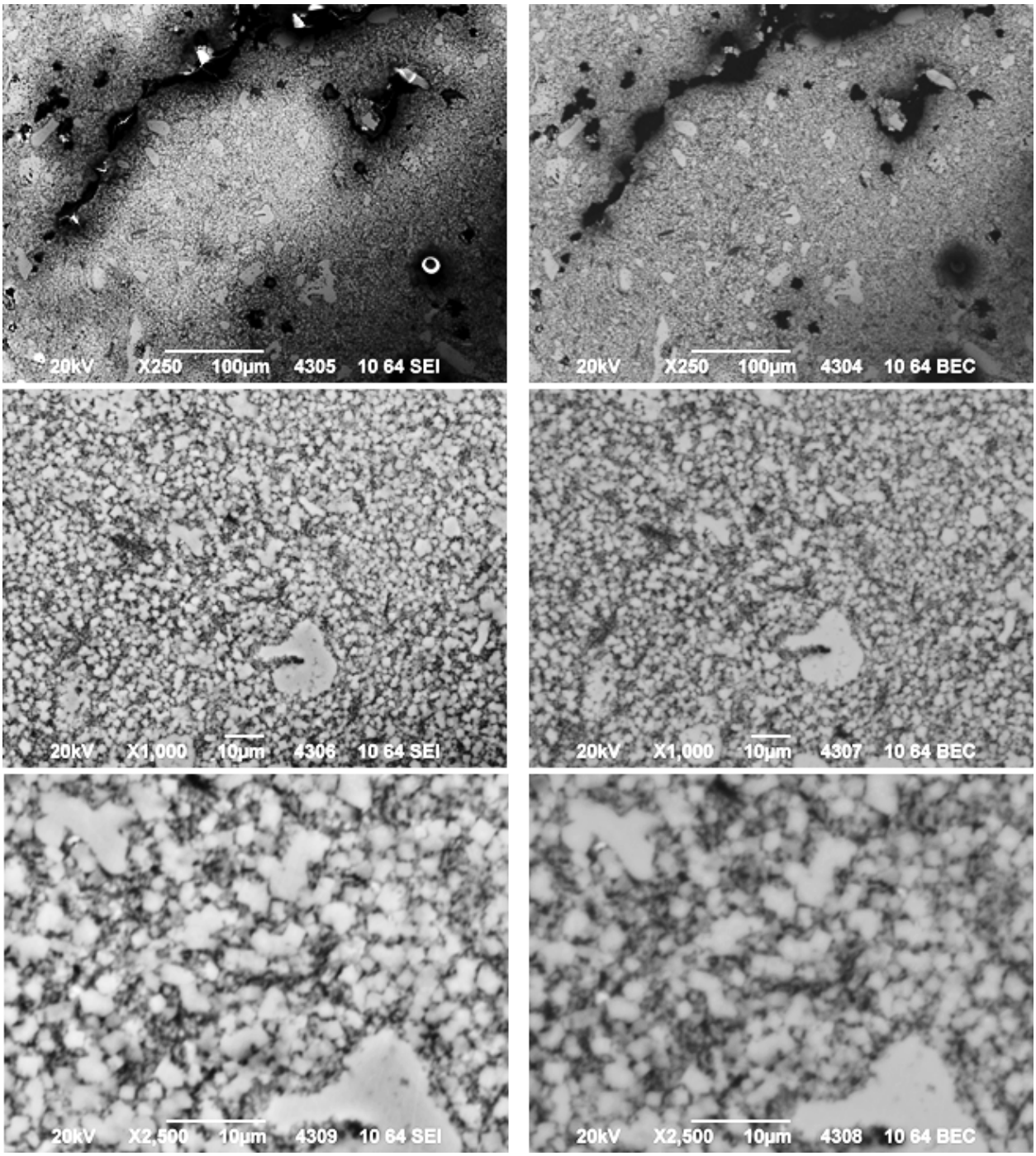

Figure 18: Detailed images of area near center of pellet recovered from Capsule 2 at 250× to 2500× magnification. SEI images on left and backscatter images on the right (Images 4304 – 4309) [Sample K3].

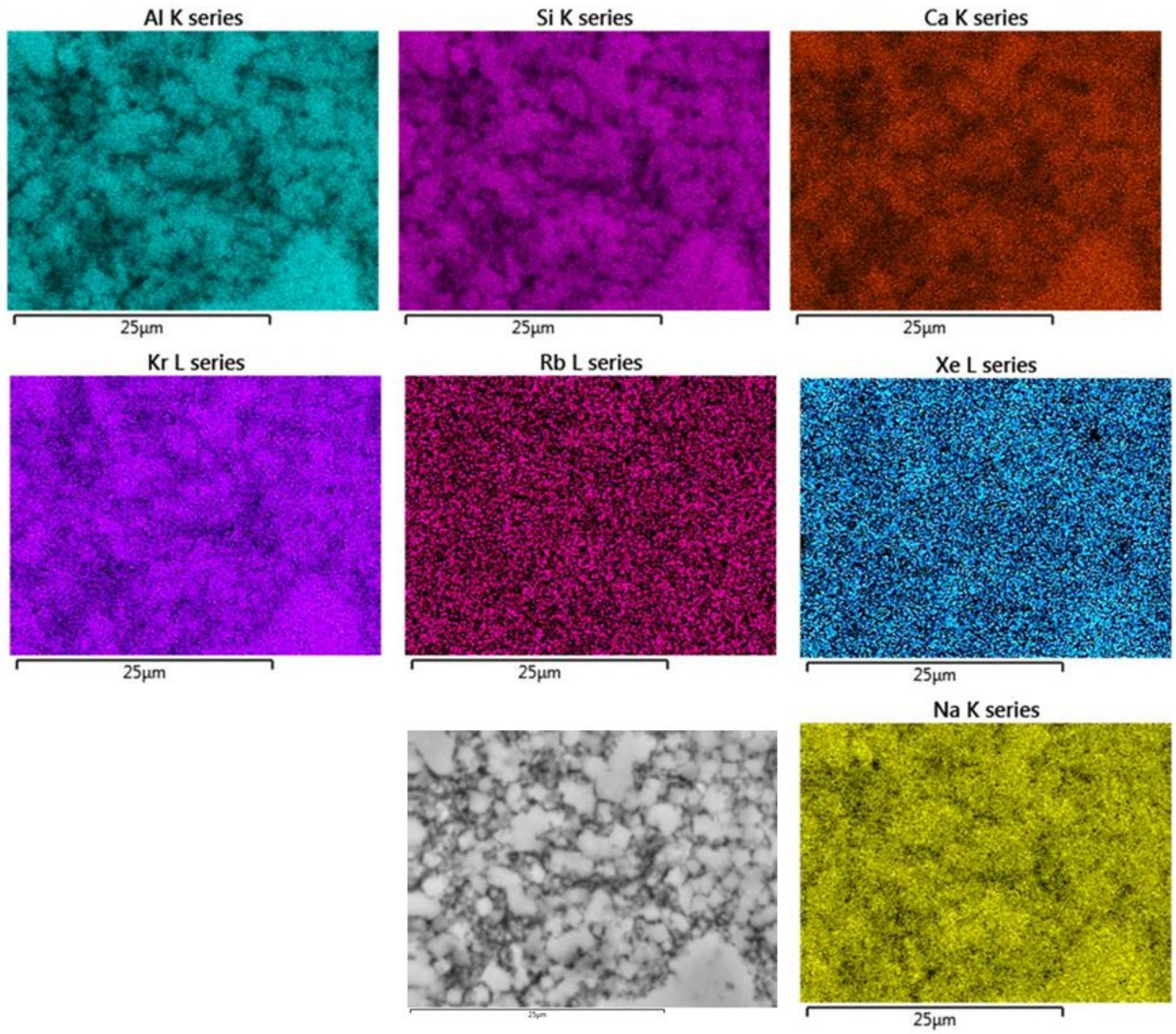

Figure 19: Elemental maps of area shown in bottom images of Figure 18 for pellet recovered from Capsule 2 [Sample K3].

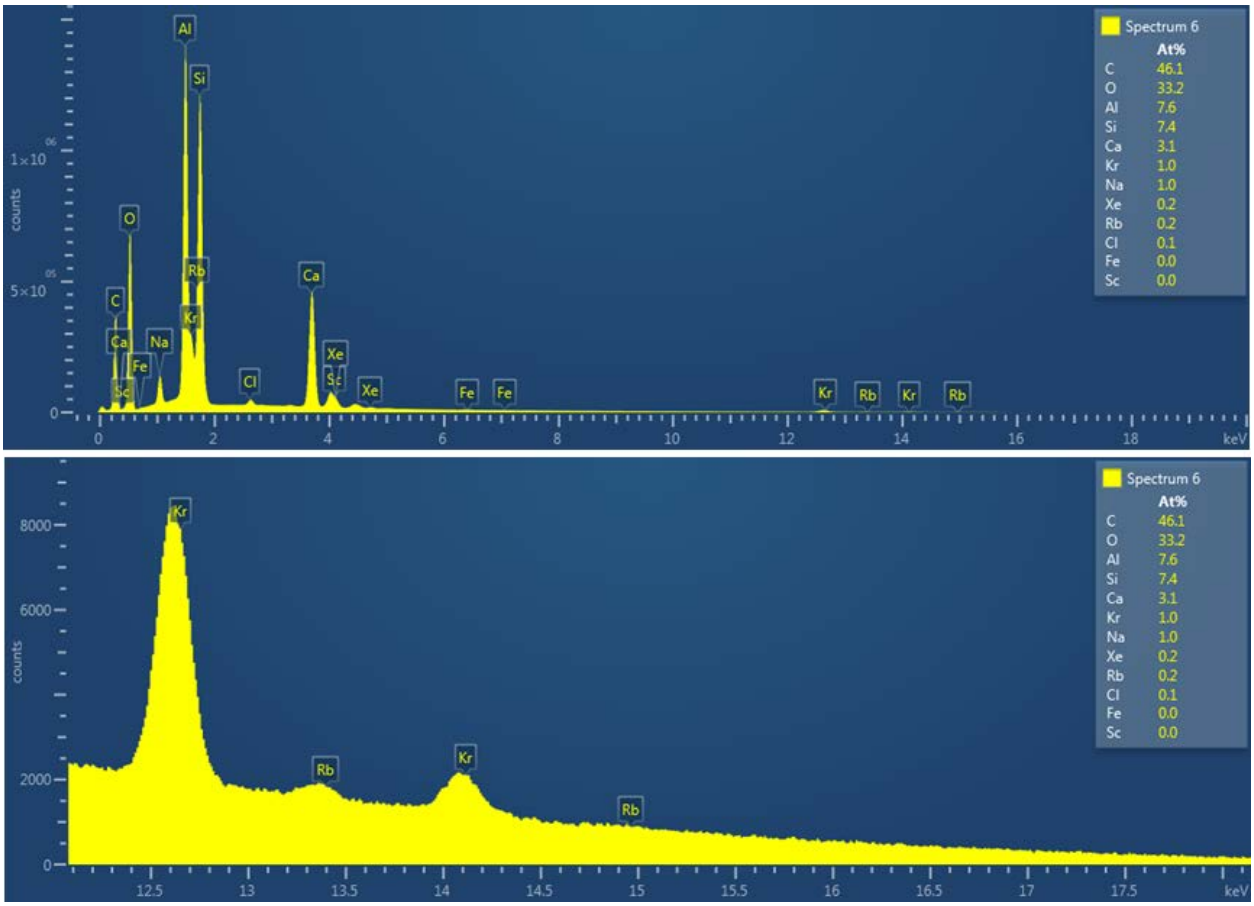

Figure 20: SEM-EDS of the area shown in the elemental maps for Image 4310 near center of pellet recovered from Capsule 2 [Sample K3].

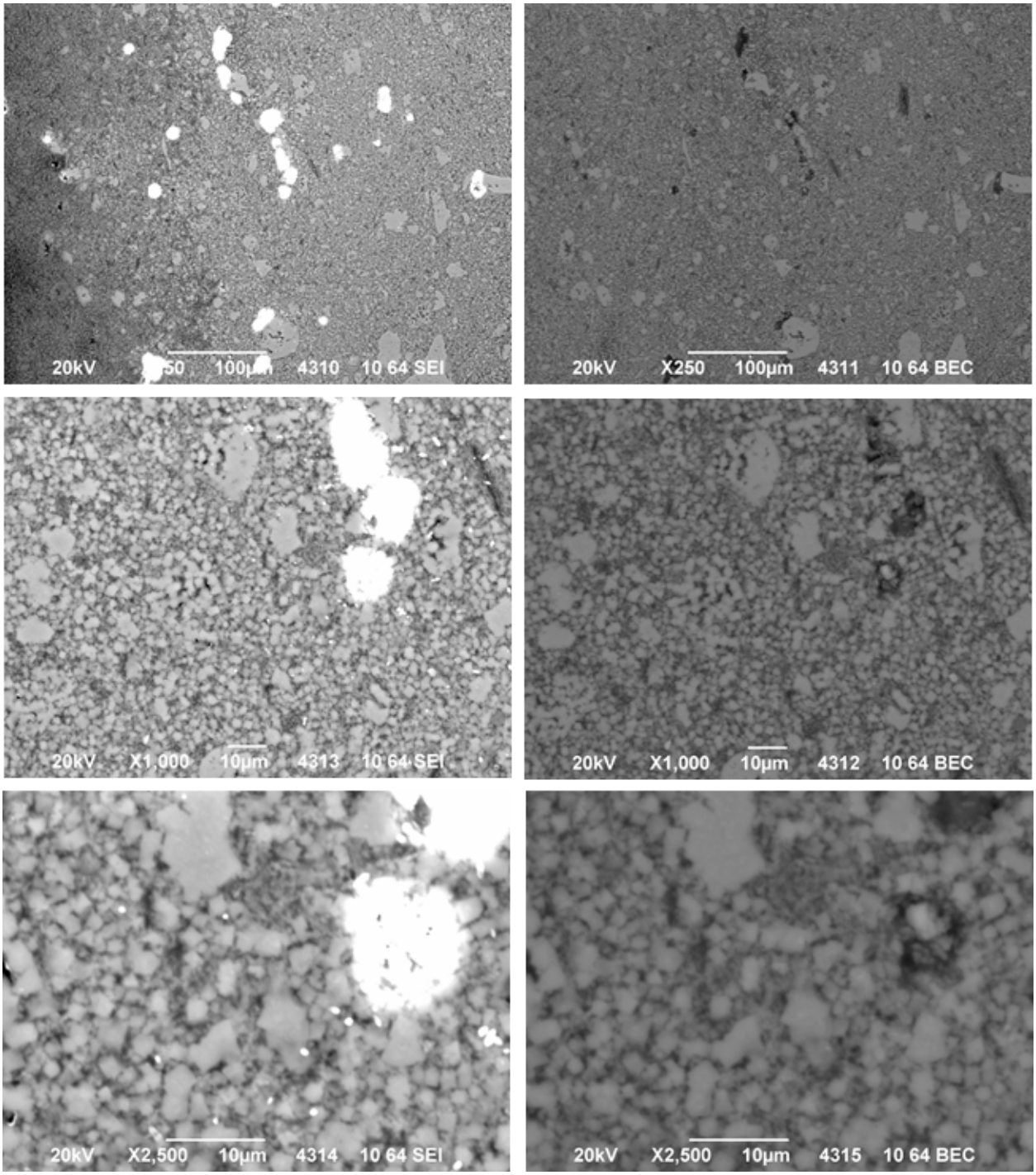

Figure 21: Detailed images of area near midpoint between center and edge of pellet recovered from Capsule 2 at 250× to 2500× magnification. SEI images on the left and backscatter images on the right (Images 4310 – 4315) [Sample K3].

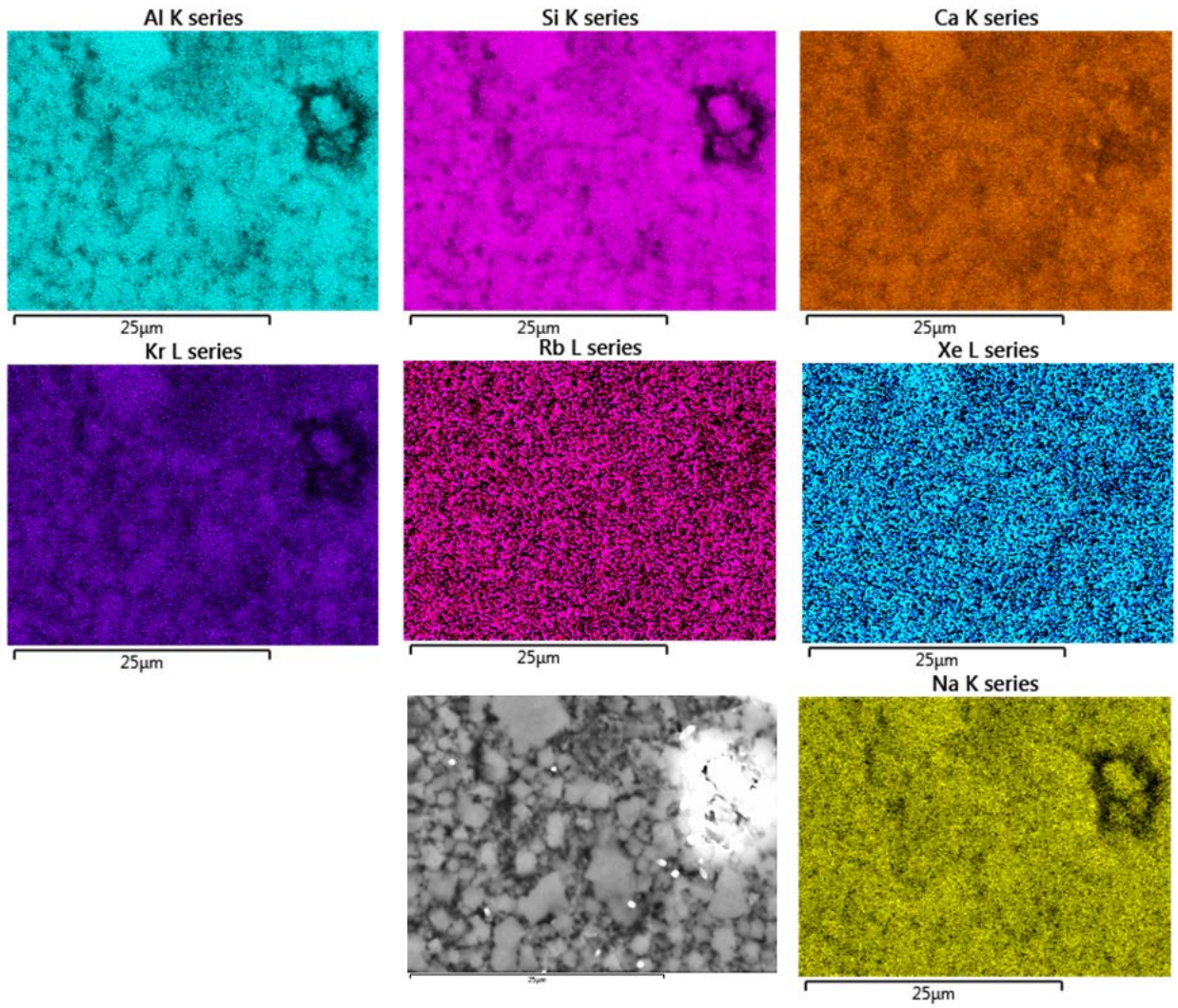

Figure 22: Elemental maps of area shown in bottom images of Figure 21 for pellet recovered from Capsule 2 [Sample K3].

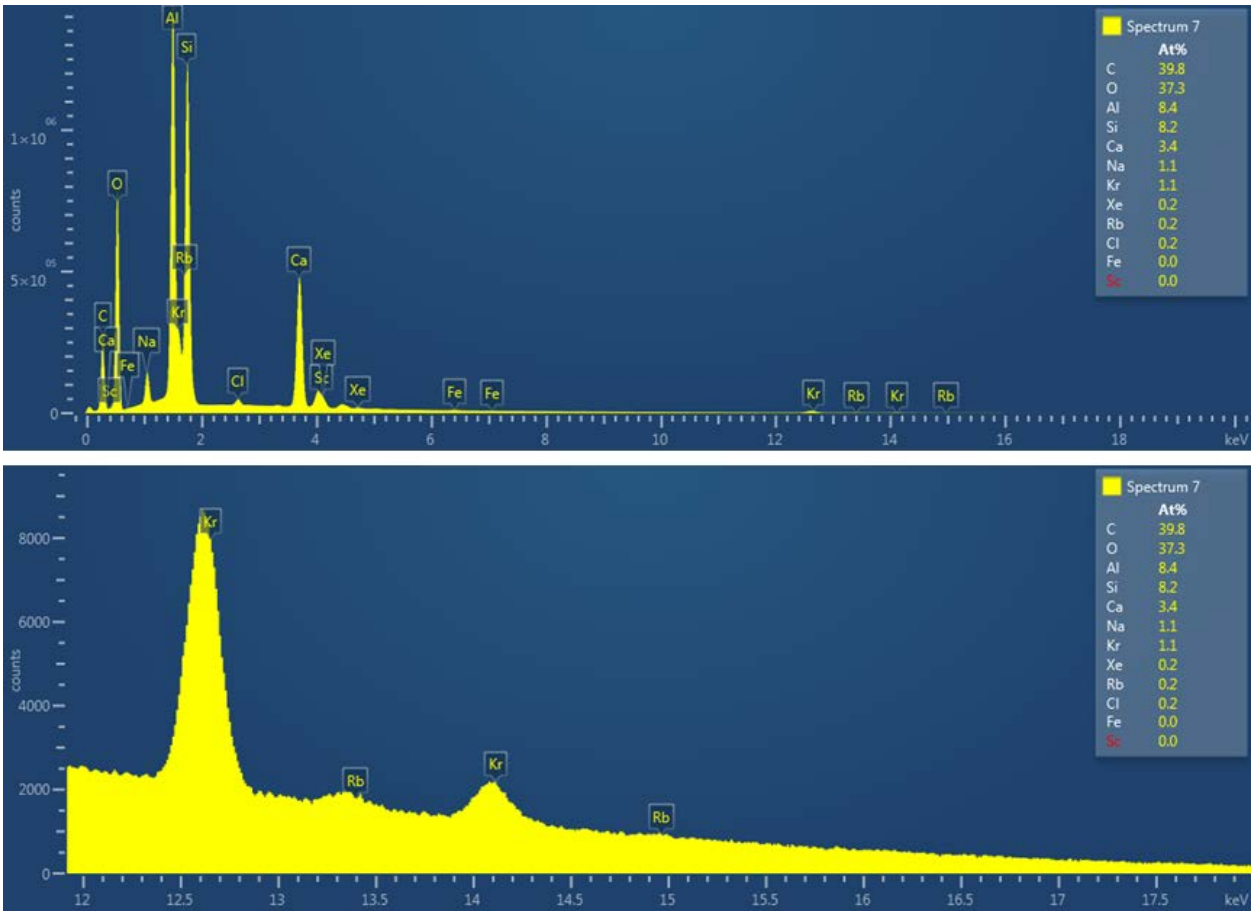

Figure 23: SEM-EDS of the area shown in the elemental maps for Image 4315 near midpoint between center and edge of pellet recovered from Capsule 2 [Sample K3].

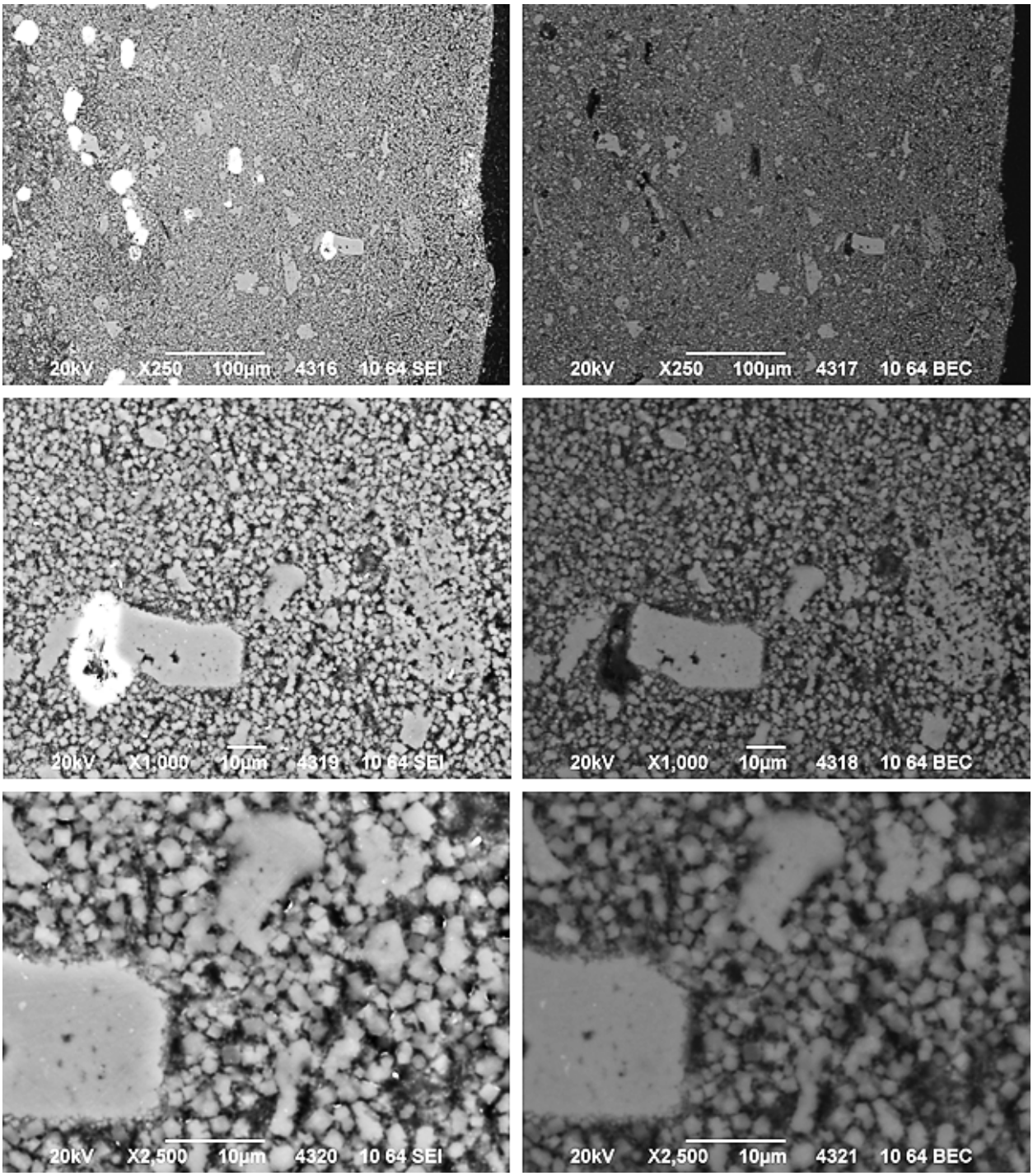

Figure 24: Detailed images of area near outer edge of pellet recovered from Capsule 2 at 250× to 2500× magnification. SEI images on left and backscatter images on the right (Images 4316 – 4321) [Sample K3].

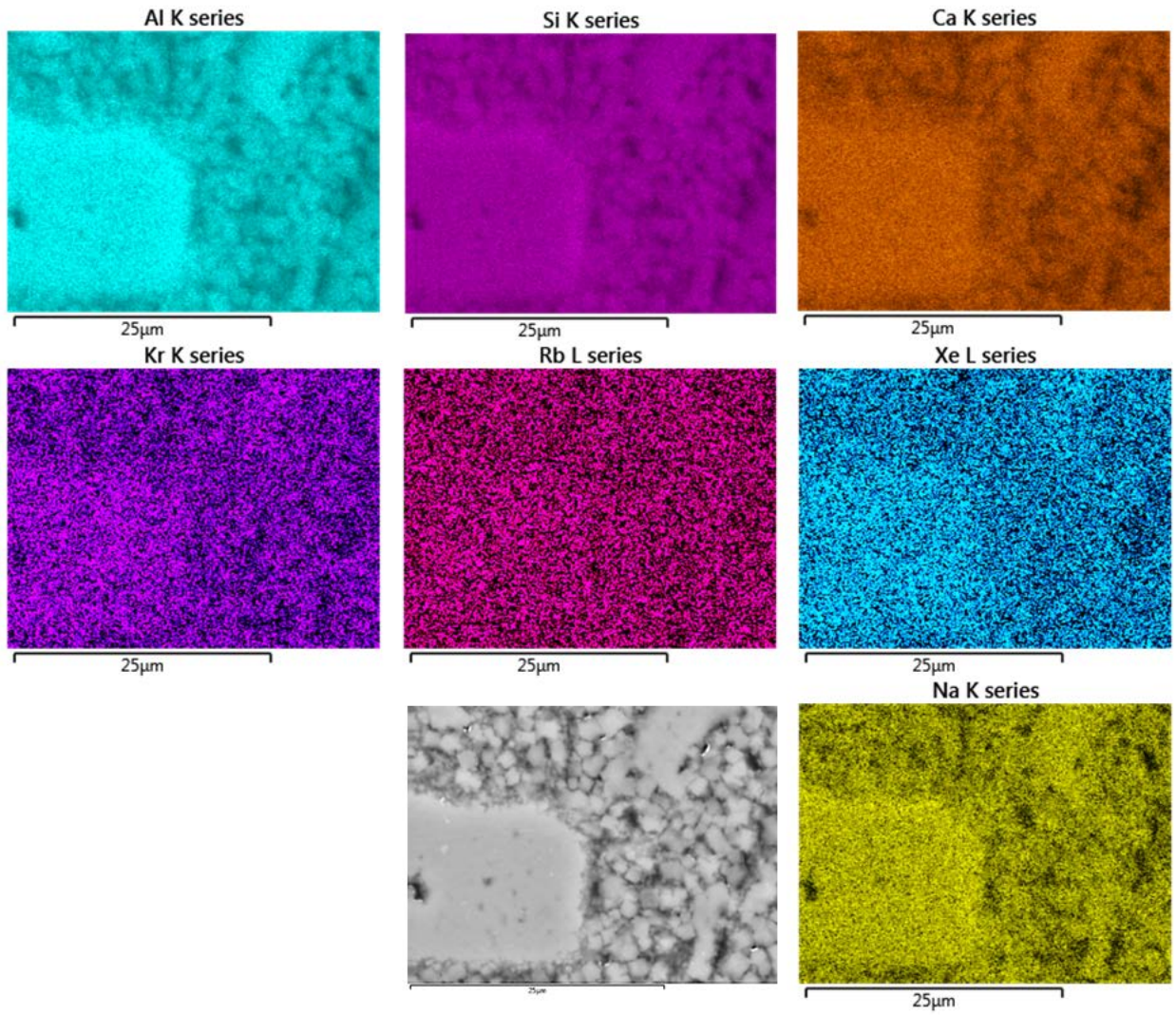

Figure 25: Elemental maps of area shown in bottom images of Figure 24 for pellet recovered from Capsule 2 [Sample K3].

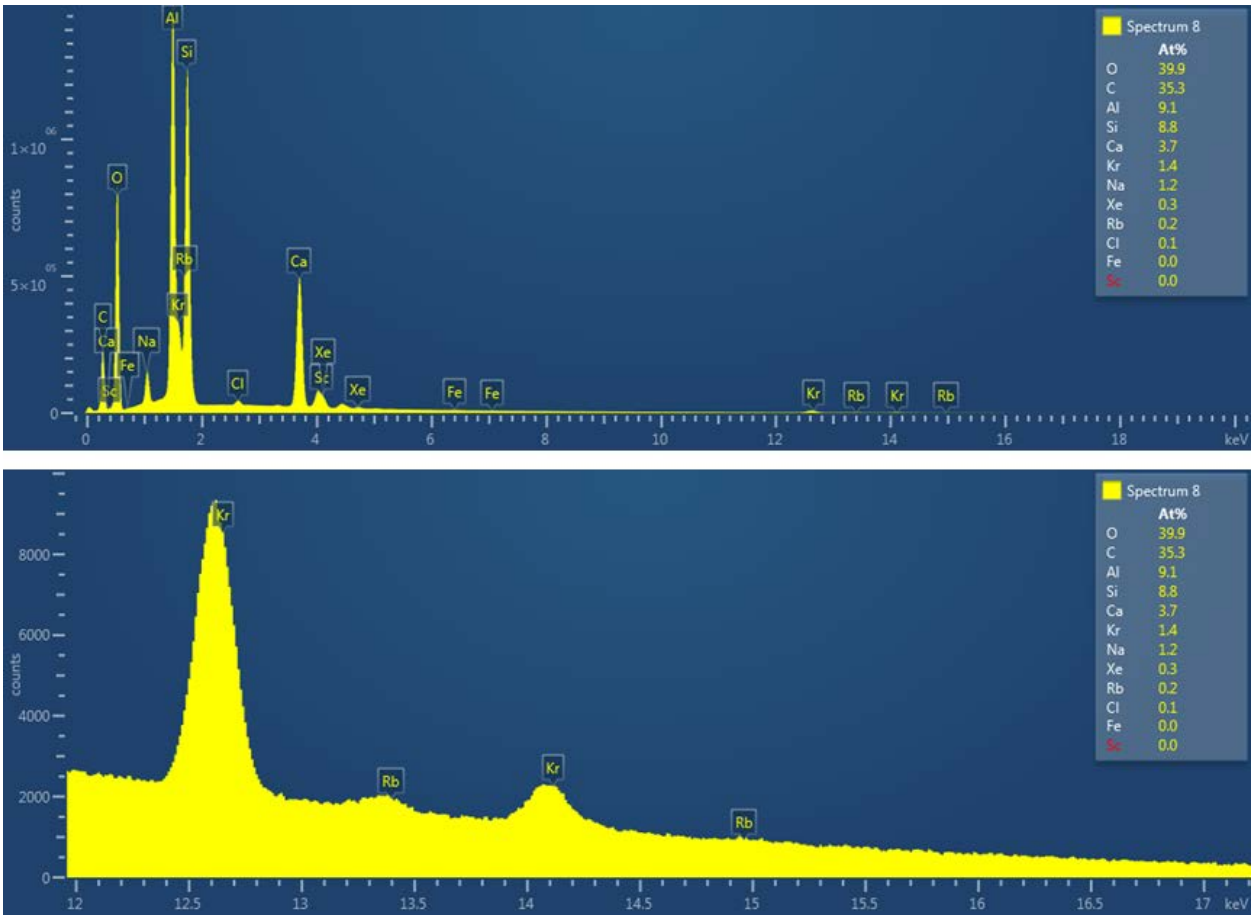

Figure 26: SEM-EDS of the area shown in the elemental maps for Image 4321 near outer edge of pellet recovered from Capsule 2 [Sample K3].

The SEM images appear to indicate an area of lower density material near the center of the pellet. During the polishing of the pellets shown in Figures 13-16 it was observed that the center was relatively soft, and great care had to be applied to not pull out this material. In all cases, the elemental mapping of the three points across the pellets showed that the Al, Si, and Ca were coincident with each other. The approximate atom % numbers obtained from the EDS analysis are consistent with the composition of 5A molecular sieves. The presence of some Na is also consistent with the production of 5A MS from 4A with the exchange of Ca for Na in the 4A molecular sieve[4]. A type A zeolite has an oxide formula of $Na_2O \cdot Al_2O_3 \cdot 2SiO_2 \cdot 4.5\ H_2O$. In 3A molecular sieves, the Na is replaced with K, and in 5A the Na is replaced with Ca. The Kr and Xe elemental maps are also coincident with the Al, Si, and Ca, which is indicative of the Kr being trapped in the zeolite structure. The Kr:Xe atom % numbers would indicate that the Kr that was loaded into the zeolite had some Xe impurities, ~20% Xe. Note that carbon is present in all samples because it was used to coat the sample in preparation for SEM examination and is ignored when considering the composition of the sample by creating ratios of the remaining elements to each other.

With regard to the presence and distribution of the Rb, the EDS spectra clearly show that it is present based on the peak at ~13.4 KeV, and the elemental maps also show that it is widely dispersed and also appears to be coincident with the Kr.

The EDS line scan (Figure 27) covering the area between the center of the pellet and the outer edge also showed significant correlation between the 5A MS structural elements and the Kr, Xe, and to a slightly lesser degree the Rb. It is worth noting that between 200 and 400 µm on the line scan there appears to be a void that was filled with the coating carbon (low in Al, Si, Ca, Na, Kr, Xe). The spike in Cl at ~300 µm is from the epoxy mounting material.

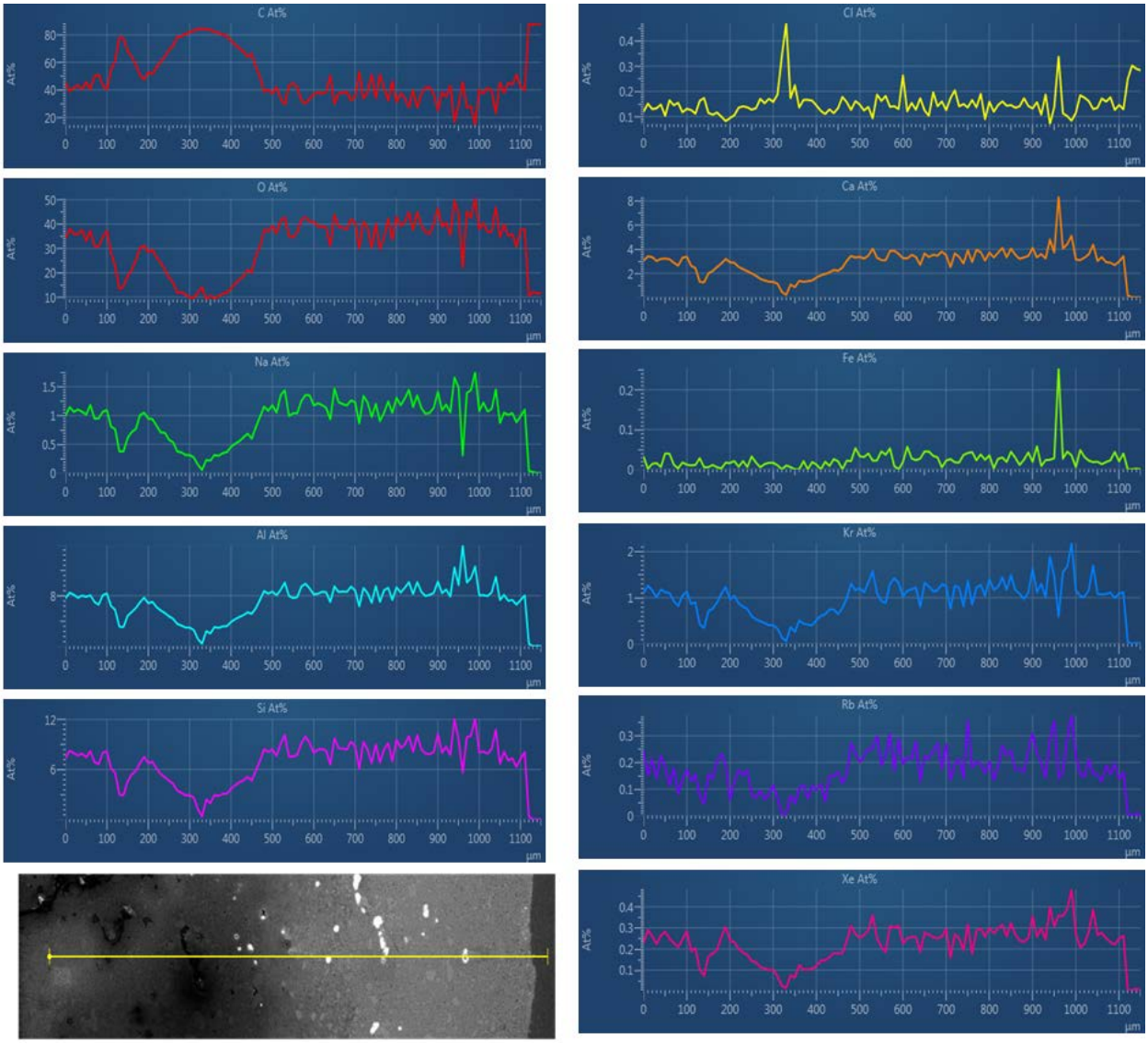

Figure 27: SEM-EDS line data for pellet recovered from Capsule 2 [Sample K3].

4.3 Chemical Analysis

Chemical analysis of the pellet was based on the EDS data (see Table 1). Starting with the Ca, Na, Si, and Al data from the three positions that were examined within the pellet, several points can be made. First, the average ratio of Si to Al is 0.97. The average ratio of Ca to Na is 3.10. Christensen et al.[5], indicated that one of the starting materials was a 5A zeolite obtained from W. R. Grace Co. in the form of 2-mm spheres, which was produced by a 67% exchange of calcium for sodium in zeolite 4A. The typical formula for A type zeolites is $Na_2O \cdot Al_2O_3 \cdot 2SiO_2 \cdot 4.5H_2O$. From this formula, it is clear that the ratio

of Si to Al should be 1, and the ratio of Na to either Al or Si should also be 1. However if Ca^{+2} is exchanged for Na^{+1}, then the ratio of (2Ca + Na) to either Al to Si should also be 1. For this sample, the ratio of (2Ca + Na) to Al was 0.94, and to Si the ratio was 0.97. All of this supports the initial assumption that these samples were formed using a 5A zeolite. It does appear that the Ca for Na exchange was significantly greater than 67% with closer to 87% of the sodium removed.

The average Kr atom % for these same three points is 1.17%. The molecular weight for the 5A zeolite with the Ca exchange based on the EDS data and no waters of hydration is 278.8. Christensen et al.[5], indicated that the 5A material used contained 0.8% water. This would increase the effective molecular weight to 281 g/mol. Since there are 2 mol of Si or Al per mole of zeolite, the molar ratio of Kr to 5A could be determined. For this pellet, the average atom % values for Kr and (Si+Al)/4 yields 1.17/4.125. Back calculation from the 1.2 at. % Kr + Xe would indicate a loading of 27 cm^3 at standard temperature and pressure (STP)/g solid. Reported data indicated that loading of 30 to 50 cm^3 STP Kr/g could be achieved.

Typically ^{85}Kr comprises about 5% of the total Kr from reprocessing of five year cooled fuel. At discharge, the ^{85}Kr could be as high as 6.5% of the total Kr. Assuming that the Kr used to make these samples contained 5% ^{85}Kr and that three half-lives have passed, the Rb content in the pellet should be 4.6% of the total Kr concentration. The observed Rb content is between 15 and 20% of the total Kr content. However, the Rb value from EDS is only at the ~0.2 at. %, and the level of detection is ~0.1 at. %. With only one significant figure reported, this value could have 50 to 75% error.

Table 1: Compositional analyis of zeolite material, noble gases and Rb from Capsule 2 based on EDS data

	Atom %							*Atom % ratios*						
Sample Point (Image No.)	Ca	Na	Si	Al	Kr	Xe	Rb	Ca:Na	Si:Al	Ca:Al	(2Ca+Na):Al	(2Ca+Na):Si	Kr:Xe	Kr:Rb
4310	3.1	1	7.4	7.6	1	0.2	0.2	3.10	0.97	0.41	0.95	0.97	5.0	5.0
4315	3.4	1.1	8.2	8.4	1.1	0.2	0.2	3.09	0.98	0.40	0.94	0.96	5.5	5.5
4321	3.7	1.2	8.8	9.1	1.4	0.3	0.2	3.08	0.97	0.41	0.95	0.98	4.7	7.0
Ave	3.40	1.10	8.13	8.37	1.17	0.23	0.20	3.09	0.97	0.41	0.94	0.97	5.1	5.8

5. ANALYSIS OF CAPSULE 2

5.1 Optical Analysis

Capsule 2 was sectioned vertically, i.e., cutting down through the stem and down the vertical sides of the right circular cylinder using a diamond rotary saw. Water was used to cool the blade during cutting. The sectioned capsule (Figure 28) was examined visually with the aid of an optical microscope within the hot cell. Composite images from the optical microscope showing the interior of a halved Capsule 2 are shown in Figures 29 and 30. These figures show areas of probable corrosion damage on the inside of Capsule 2. Figure 31 is a magnification of the lower portion of Section A of the capsule that shows pitting and corrosion at multiple points on the Capsule 2 inner walls. Figure 29 also shows areas of apparent corrosion around the cut that was made on the capsule at an unknown time before the capsule was sent to Oak Ridge National Laboratory (ORNL). Note that both this capsule and Capsule 5 have been open to the atmosphere for extended periods of time, and any observations must be interpreted within that context. One potential concern is that the capsule may be reacting with the water and with air that was used while polishing was performed. Figures 29-31 also appear to show discoloration or potential areas of corrosion on the capsule wall cross section. This does not appear to be uniform across all of the cross-section area, with the weld areas showing far less discoloration or corrosion.

One half of this capsule was then cut in to smaller sections that would allow it to be mounted for SEM analysis. The mounted sample from Capsule 2 is identified as MM2B2 and is shown in Figure 32. This section is from the lower right portion of the section shown in Figure 29. The mount was polished to a 1-µm finish. Results from the optical analysis of the capsule are striking. The extensive corrosion that had been observed in the macro images taken through the stereo-microscope appear to extend through the entire wall thickness. At 50× magnification (Figure 33), the extent of the corrosion is obvious. In the image taken at 200× magnification (Figure 34), there appears to be a film of some sort that may be on the order of 30 µm in thickness. There appear to be several breaks in this film. Figure 35 at 400× magnification shows what appears to be some type of “grain” structure. By adjusting the focus it was possible to determine that there are structures that are well below the polished surface. In addition to these “pits,” there were also small elevated areas. The sequence of images in Figure 36 is of the same area with focal plane above the polished surface in image (a), on the polished surface (b), and in one of the “pits” in image (c). From these images, it would appear to indicate that there may be ongoing corrosion as new areas are exposed to the atmosphere. Literature data on rubidium, the decay daughter of ^{85}Kr indicates that it is extremely reactive[1]. However, it is not known what, if any, role Rb has played in the observed corrosion.

This sample was further analyzed using SEM techniques, and the results are shown in Sect. 5.2.

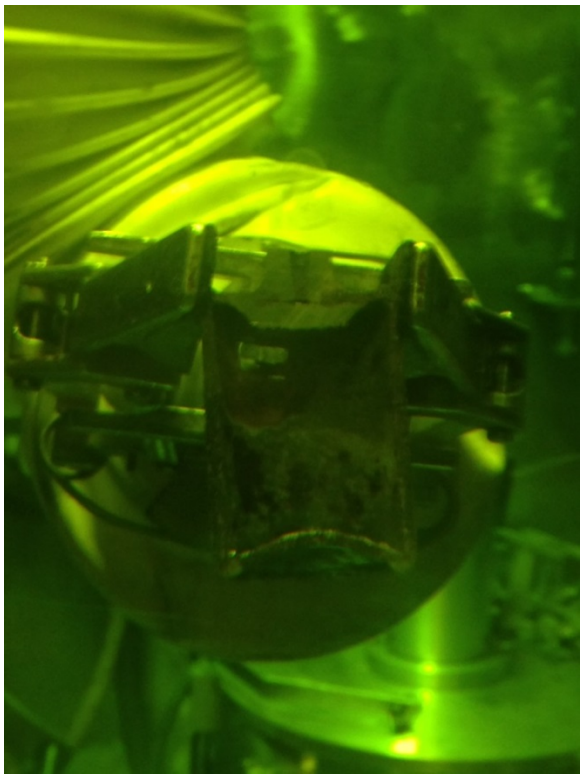

Figure 28: Section "A" of Capsule 2 looking through cell window.

Figure 29: Composite optical microscope image of Section "A" of Capsule 2.

Figure 30: Composite optical microscope image of Section "B" of Capsule 2.

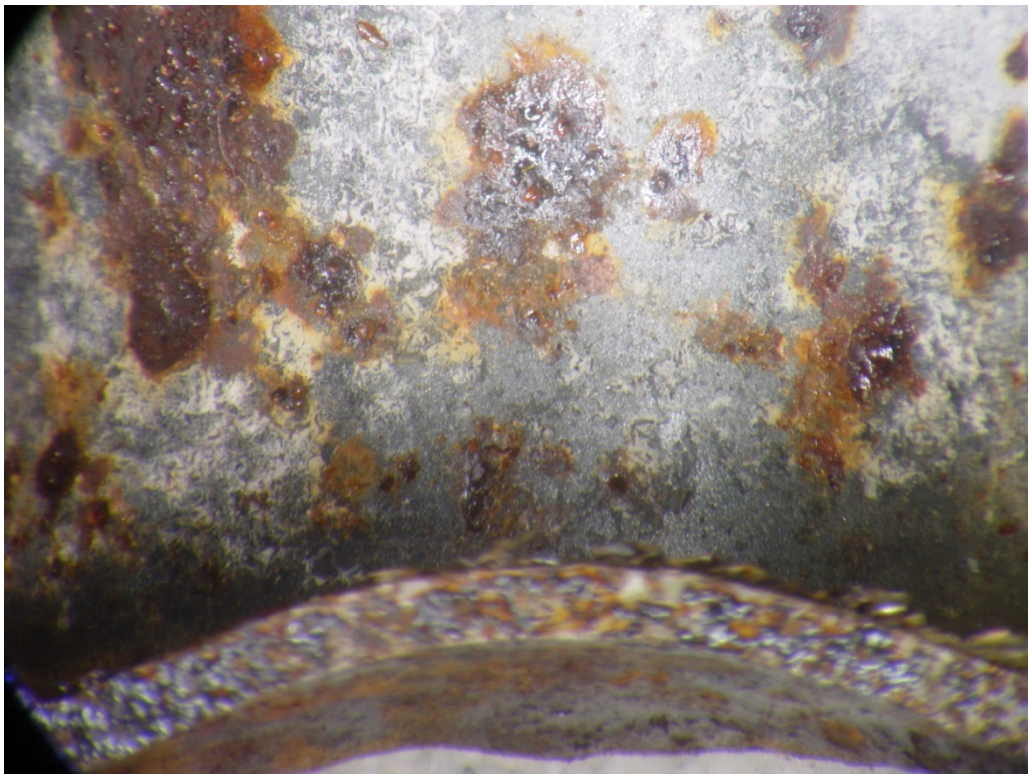

Figure 31: Detail optical microscope image of Section "A" of Capsule 2 at low magnification.

Figure 32: Optical microscope image of Section "A" of Capsule 2 (Image MM2B2-0MS-001).

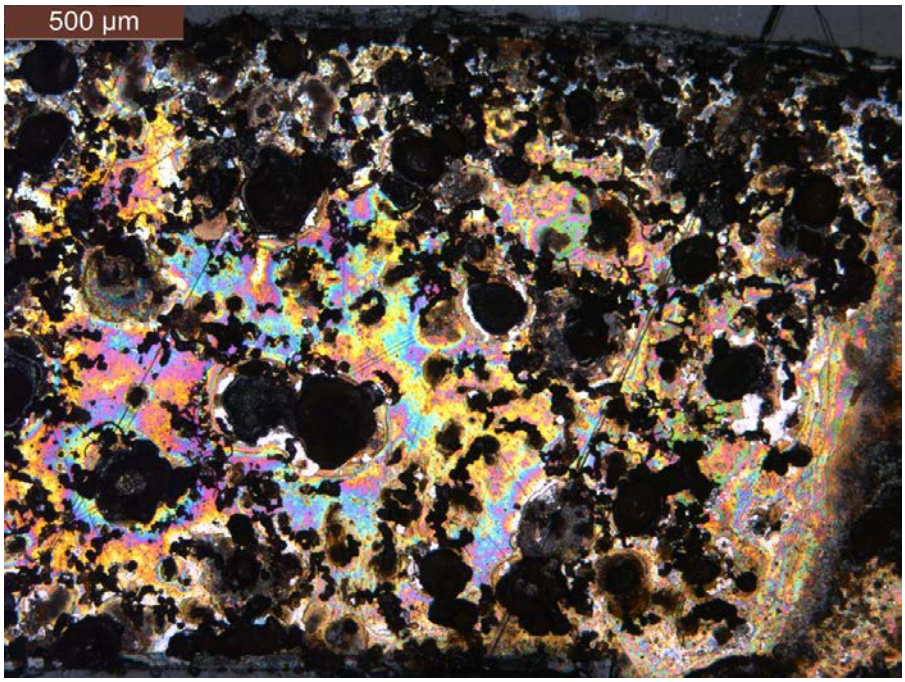

Figure 33: Optical microscope image at 50× magnification of Section "A" of Capsule 2 (Image MM2B2-050X-002).

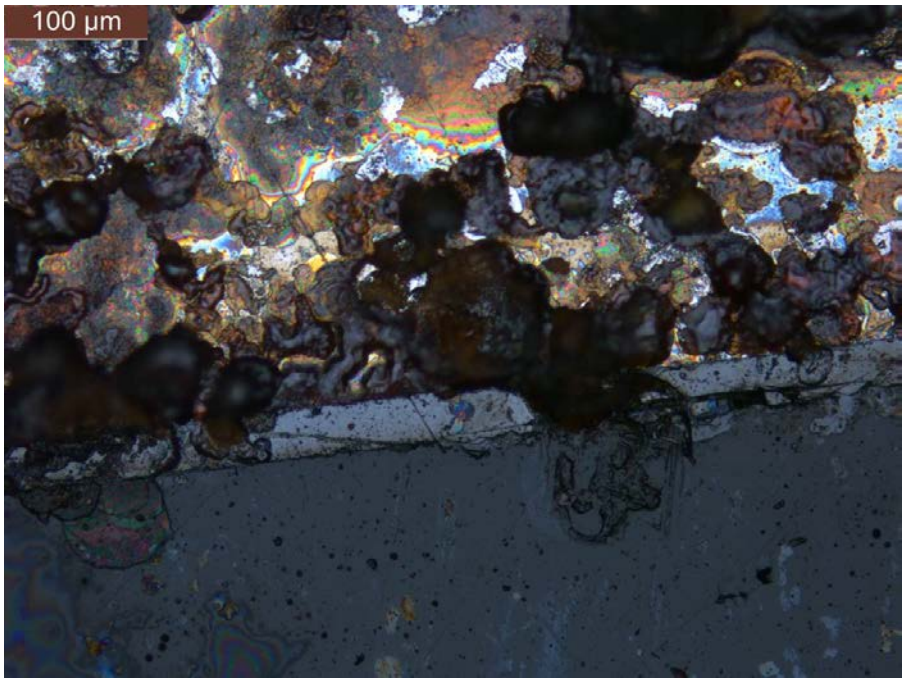

Figure 34: Optical microscope image at 200× magnification of Section "A" of Capsule 2 (Image MM2B2-0200X-014).

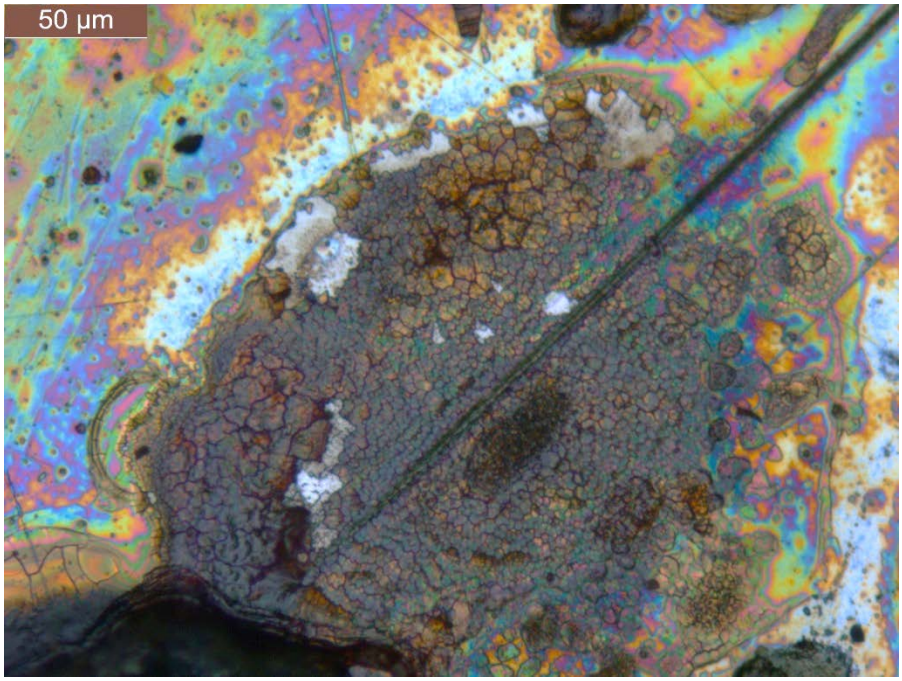

Figure 35: Detail optical microscope image at 400× magnification of Section "A" of Capsule 2 at higher magnification(Image MM2B2-400X-021).

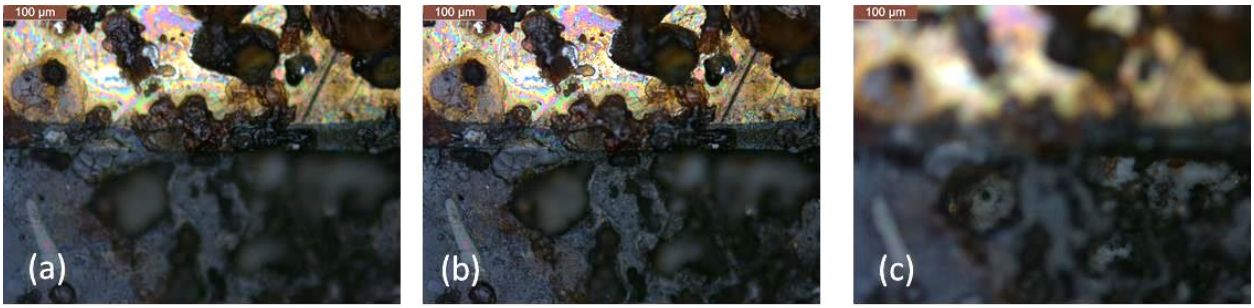

Figure 36: Optical microscope image series with focus plane above the polish surface (a), on surface (b), and below surface (c) for Section the "A" of Capsule 2 (images MM2B2-200x-016-18).

5.2 SEM Analysis

Figure 37 provides a guide to the locations of the capsule section that were examined by SEM. Figure 38 shows the cross section of the capsule wall at 50× and a 200× image of the interior surface to the capsule wall. These images appear to show what appear to be two film layers (this is very visible in the upper right corner of the lower left image and will be examined by EDS) and extensive pitting. There is also a bubble just above the sample that is an artifact of the mounting process. The BEC image shows the contrast between base metal of the capsule and the pitted areas. Figure 39 show the EDS elemental map for the higher resolution image. Figure 40 is the annotated EDS layered image of the same location showing the areas at which individual elemental spectra were produced. These individual spectra are shown in Figure 41. The spectra in Figure 41A shows only iron and oxygen present in addition to the carbon used to coat the sample. The absence of Cr and Ni would indicate that the capsule wall is likely to have been carbon steel. The spectra in Figure 41B again only shows iron and oxygen present in addition to the carbon used to coat the sample. There appears to be an iron oxide film on the inner surface of the capsule. The spectra in Figure 41C show the presence of Ci, Al, Ca and Na in the layer next to the iron oxide layer. The ratios of these four elements are consistent with 5A MS.

Figure 42 shows the cross section of the capsule wall and a potential weld site at 30× and at 150× magnification. Two areas shown in the upper images were selected for further examination at higher magnification. The BEC image shows the contrast between base metal of the capsule and the pitted areas. Figure 43 show the EDS elemental map for the higher resolution image associated with Figure 42B. Figure 44 is the annotated EDS layered image of the same location showing the areas at which individual elemental spectra were produced. These individual spectra are shown in Figure 45. The spectra in Figure 45A show only iron and oxygen present in addition to the carbon used to coat the sample. The absence of chromium and nickel would indicate that the capsule wall is likely to have been carbon steel. The spectra in Figure 45B show chromium and nickel in addition to the iron and oxygen present. This would appear to indicate that stainless steel welding wire was used to weld the bottom of the capsule to the walls.

Figure 37: Annotated optical microscope image of Section "A" of Capsule 2 showing locations that were examined by SEM (Image MM2B2-0MS-001).

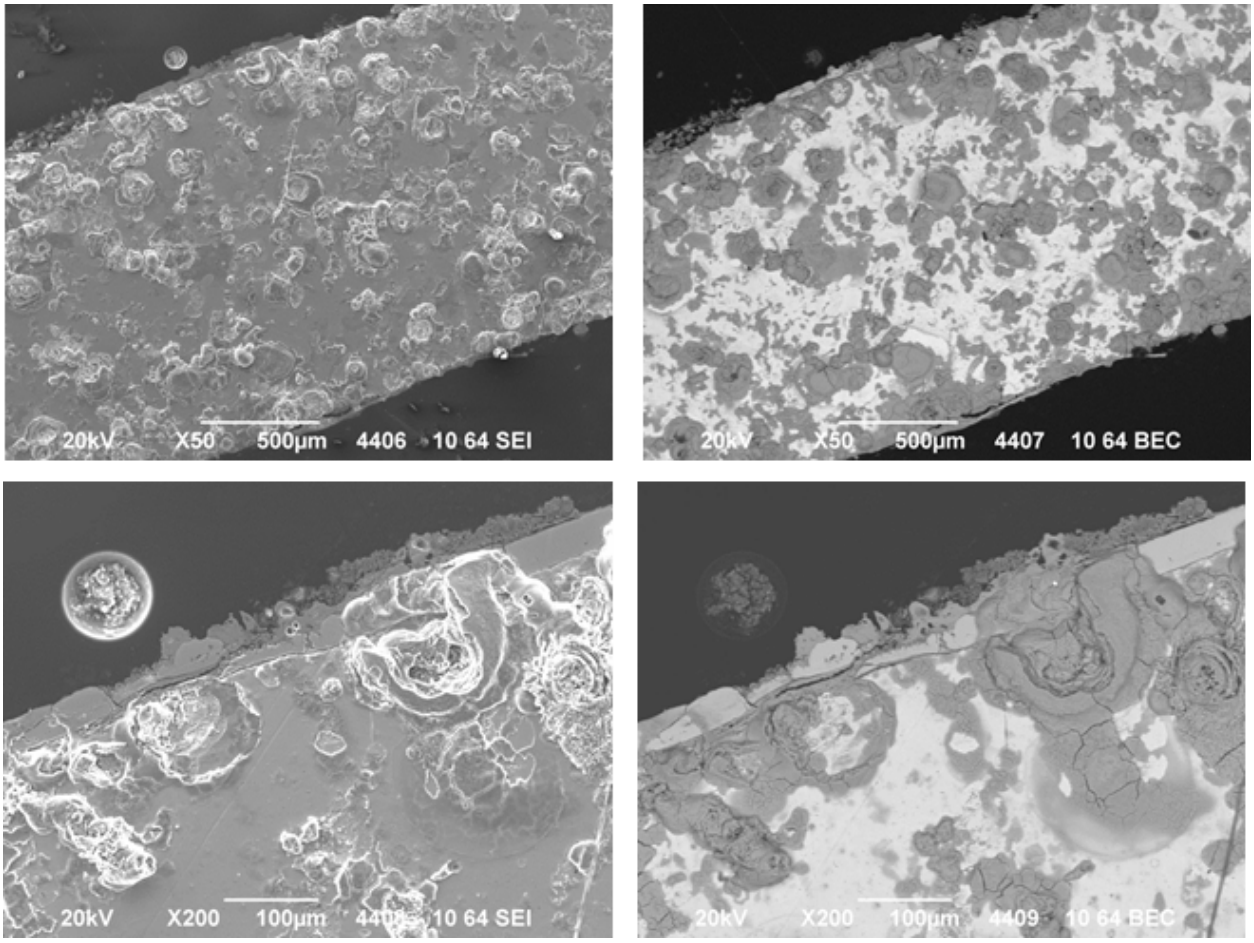

Figure 38: Detailed images of the wall of Capsule 2 at 50× to 200× magnification at Location 1. SEI images on the left and BEC images on the right (Images 4406 – 4409) [Sample 2B2].

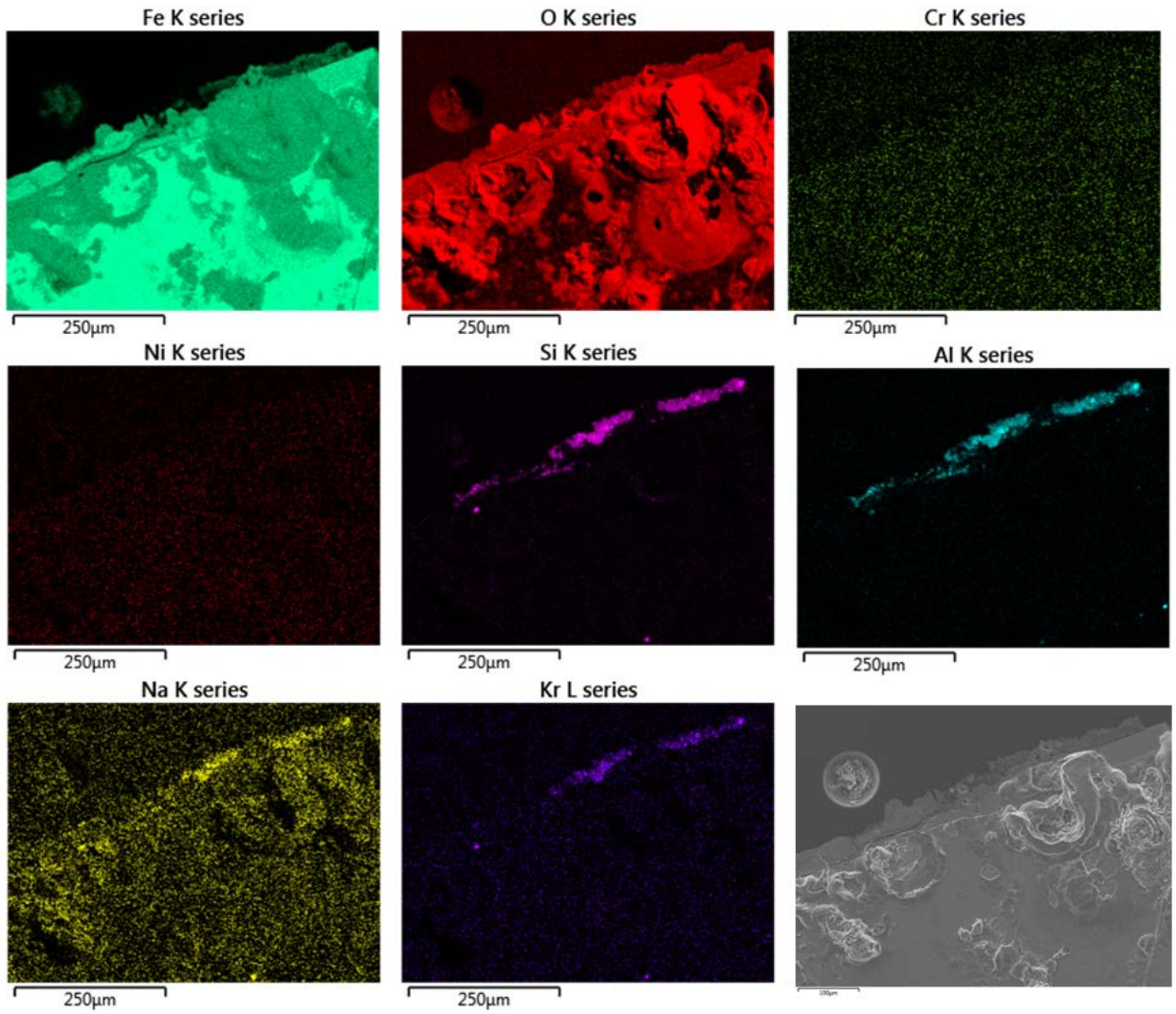

Figure 39: Elemental maps of area shown in bottom images of Figure 38 for Area 1 of the wall segment from Capsule 2 [Sample 2B2].

Figure 40: EDS layer image for bottom images of Figure 38 for Area 1 of the wall segment from Capsule 2. Sub-areas for localized spectral analysis are annotated [Sample 2B2].

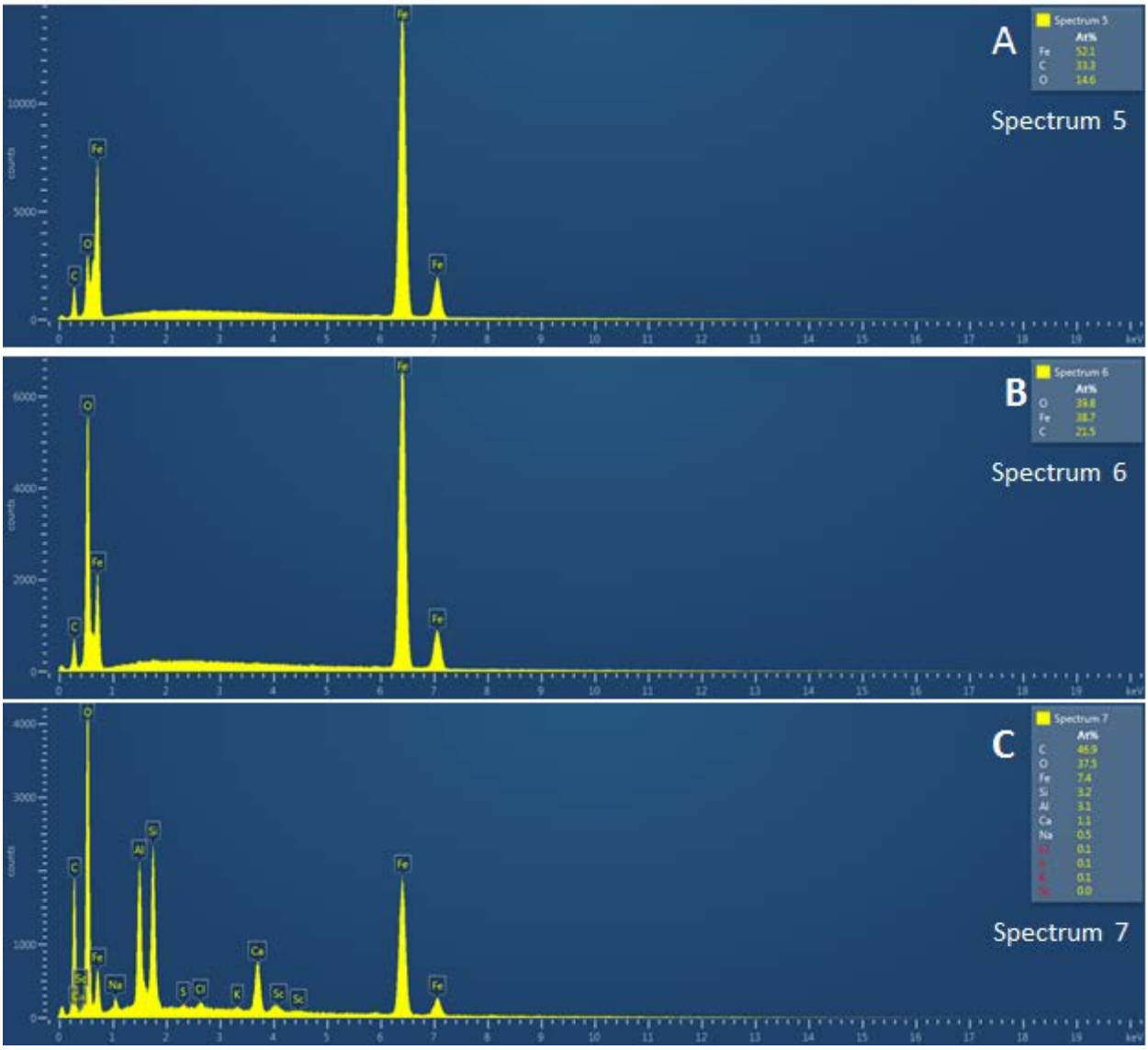

Figure 41: SEM-EDS spectra for the three sub-areas of the Capsule 2 wall segment shown in Figure 40 [Sample 2B2].

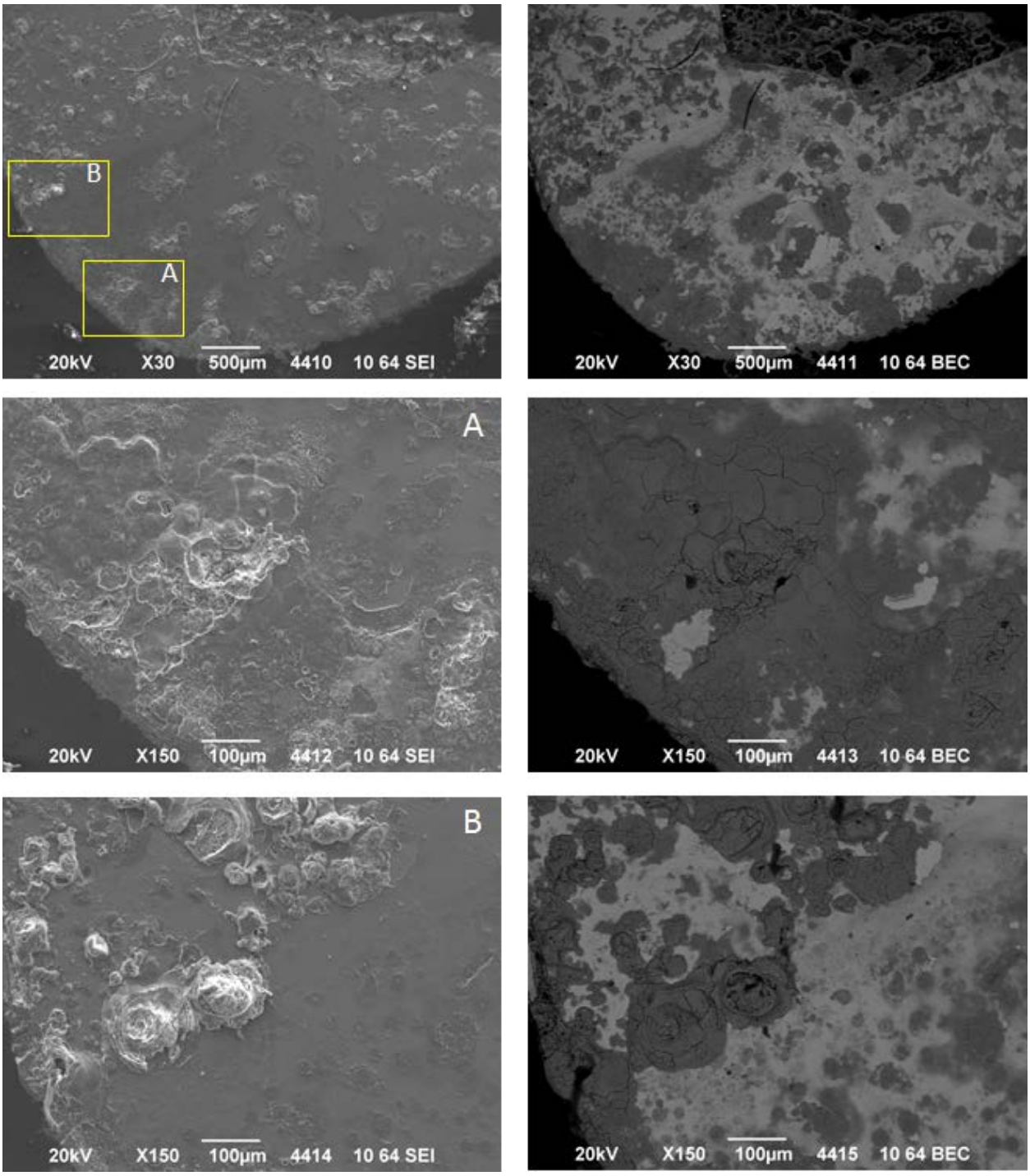

Figure 42: Detailed images of the wall of Capsule 2 at 30× to 150× magnification at Location 2. SEI images on the left and BEC images on the right (Images 4410 – 4415) [Sample 2B2].

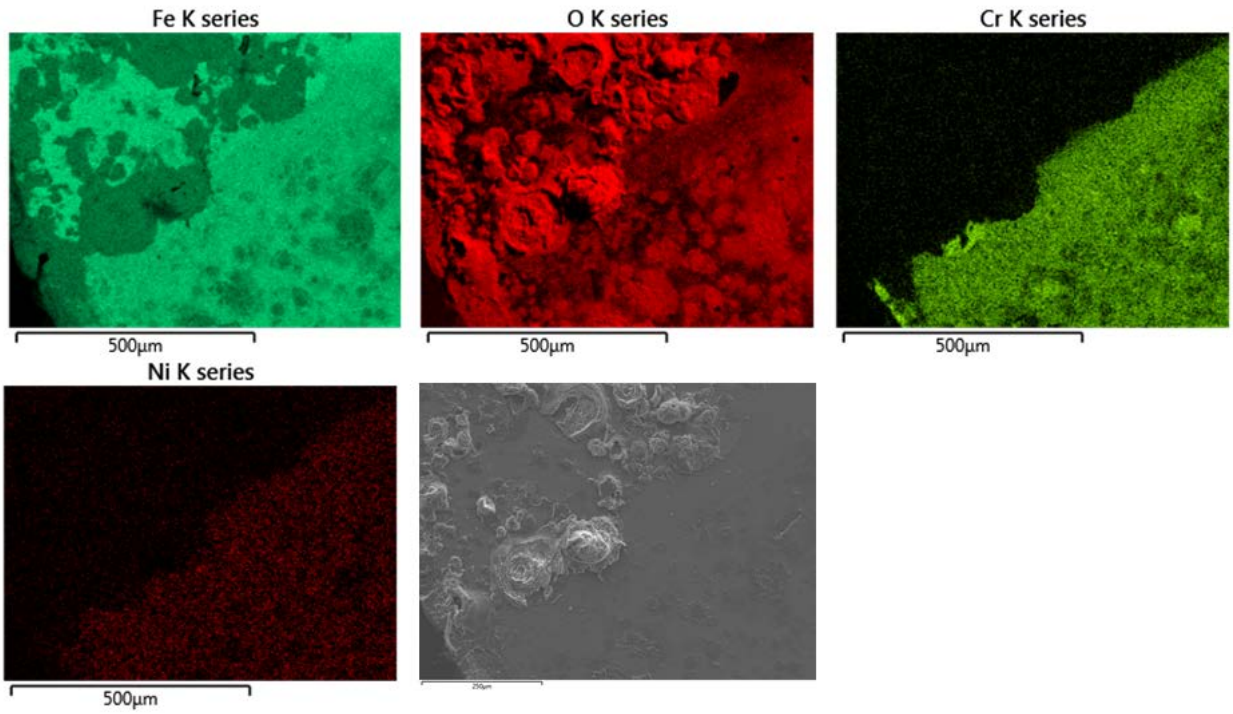

Figure 43: Elemental maps of area shown in bottom images of Figure 42B for Area 2 of the wall segment from Capsule 2 [Sample 2B2].

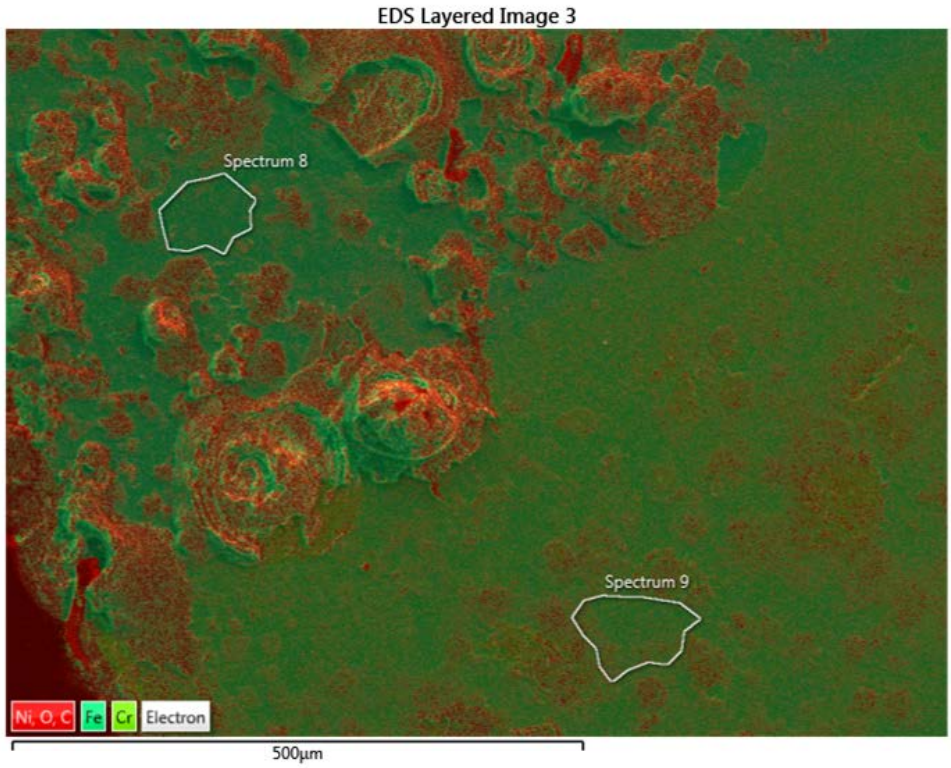

Figure 44: EDS layer image for bottom images of Figure 42B for Area 2 of the wall segment from Capsule 2. Sub-areas for localized spectral analysis are annotated [Sample 2B2].

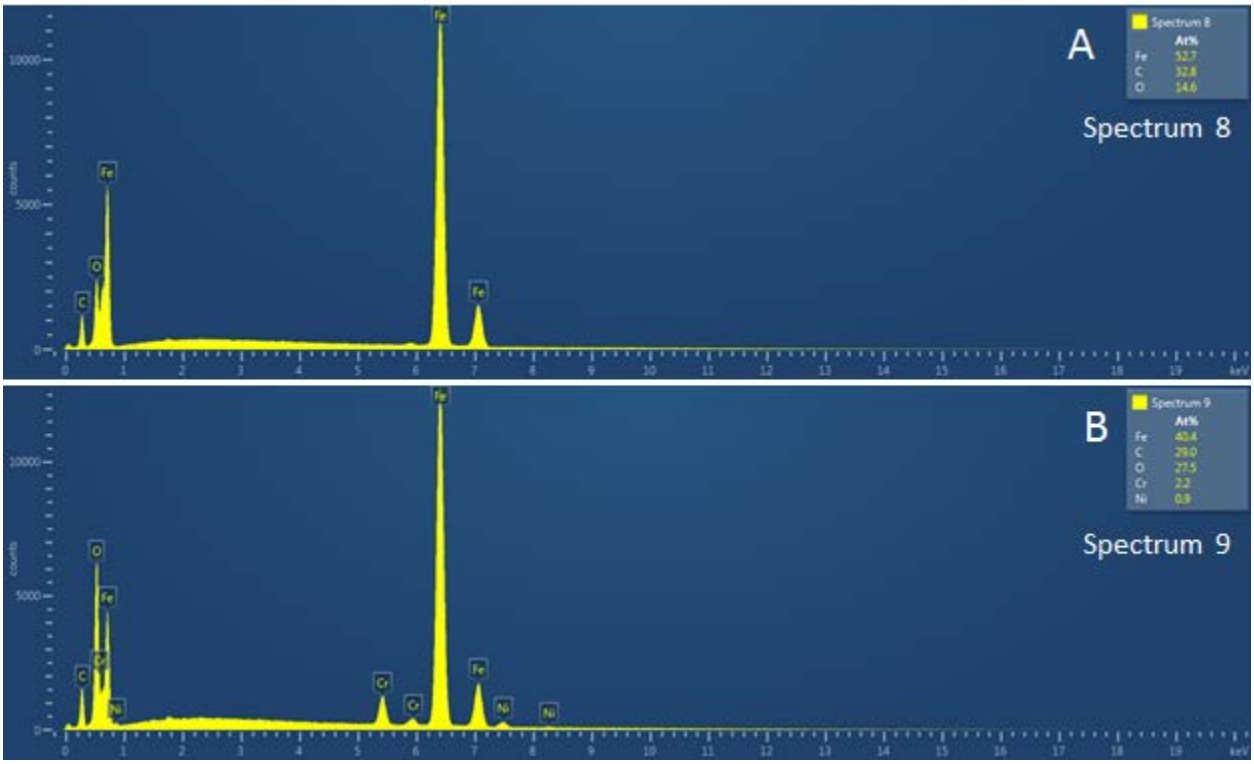

Figure 45. SEM-EDS spectra for the two sub-areas of the Capsule 2 wall segment shown in Figure 44 [Sample 2B2].

Figure 46 shows an interior corner of the weld site at 75× and at 150× magnification. Figure 47 shows the EDS elemental map for the higher resolution image associated with Figure 46. Note that only a portion of the area showing the presence of iron also shows the presence of Cr and Ni. It was also noted that elements associated with the zeolite material are located in a corner formed by the metal walls. Figure 48 is the annotated EDS layered image of the same location showing the areas at which individual elemental spectra were produced. These individual spectra are shown in Figure 49. The spectra in Figure 49A show a significant amount of Si but no Al. Manganese is present, but the origin is unknown at this time. Also the absence of Al is unexpected. It is possible that the Si and Mn are simply an impurity that was incorporated into the sample. The spectra in figure 49B show the presence of elements associated with the zeolite material and some Fe.

Figure 50 shows an interior corner the weld site at 50× and at 200× magnification. The middle images in Figure 50 are for area "A" noted in the top row of images. This is the exterior surface of the capsule. Figure 51 shows the EDS elemental map for the higher resolution image associated with middle row of images in Figure 50. Only Fe and O are observed in addition to the carbon used to coat the sample. This is consistent with the previous observations for area 1. Figure 52 shows the EDS elemental map for the higher resolution image associated with bottom row of images in Figure 50. These appear to show a number of individual layers on the interior surface of the capsule wall. Figure 53 is the annotated EDS layered image of the same location showing the areas at which individual elemental spectra were produced. These individual spectra are shown in Figure 54. The spectra in Figure 54A show iron oxide associated a pit within the wall. The spectra in Figure 54B show iron metal within the wall. The spectra in Figure 54C show an iron oxide layer with an O:Fe ratio of ~1. The spectra in figure 54D show an iron oxide layer with a higher O:Fe ratio of ~2. The spectra in Figure 54E show an iron oxide layer with an O:Fe ratio of ~1.

Table 2 provides a summary of the compositional data derived from the EDS spectra for the Capsule 2 wall samples.

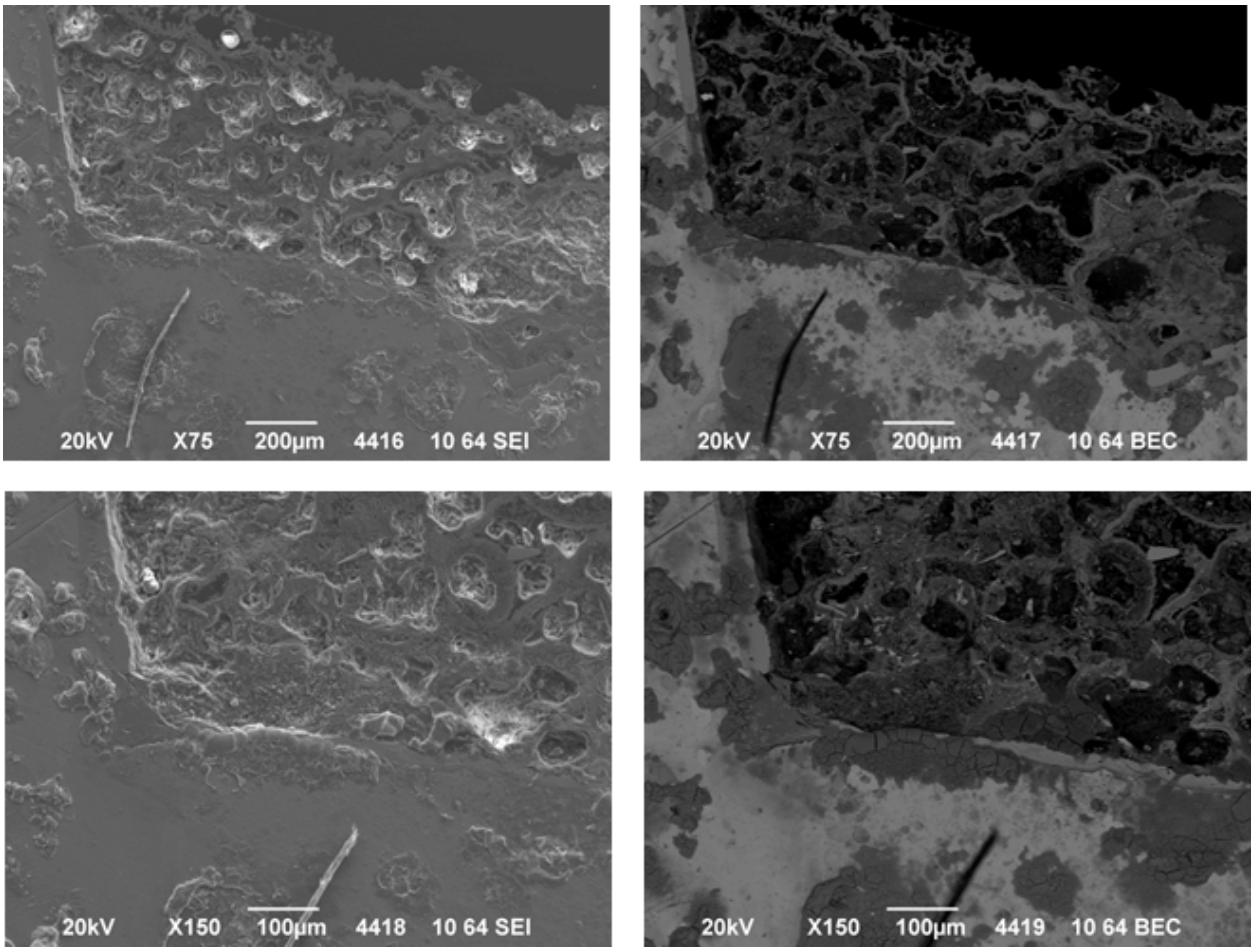

Figure 46: Detailed images of the wall of Capsule 2 at 75× to 150× magnification at Location 3. SEI images on the left and BEC images on the right (Images 4416 – 4419) [Sample 2B2].

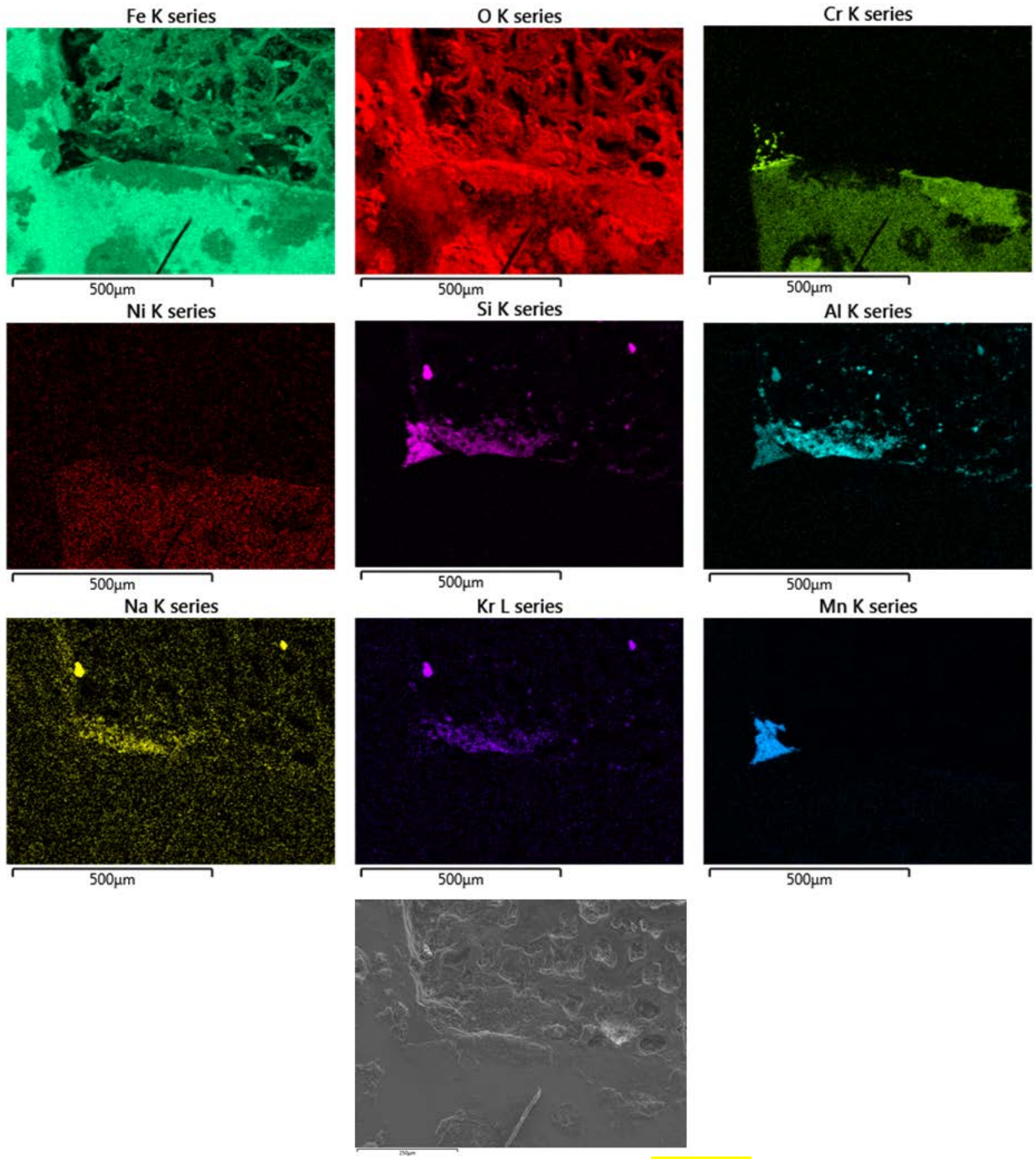

Figure 47: Elemental maps of area shown in bottom images of Figure 46 for Area 3 of the wall segment from Capsule 2 [Sample 2B2].

Figure 48: EDS layer image for bottom images of Figure 46 for Area 3 of the wall segment from Capsule 2. Sub-areas for localized spectral analysis are annotated [Sample 2B2].

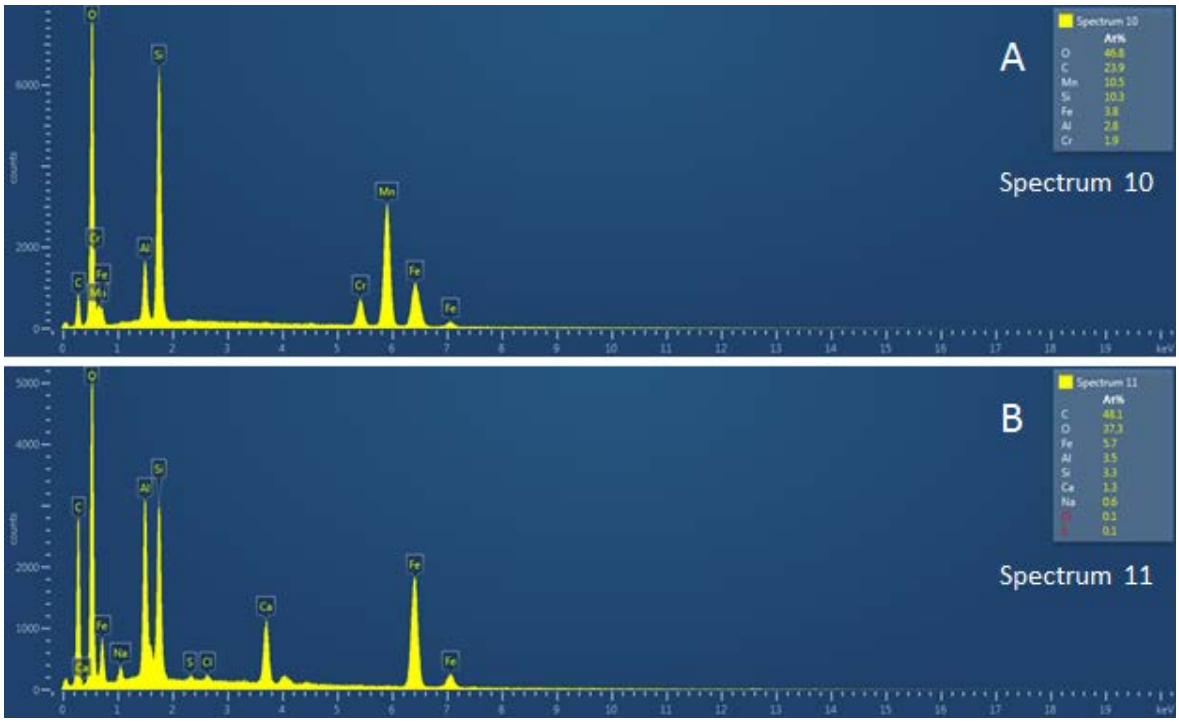

Figure 49: SEM-EDS spectra for the two sub-areas of the Capsule 2 wall segment shown in Figure 48 [Sample 2B2].

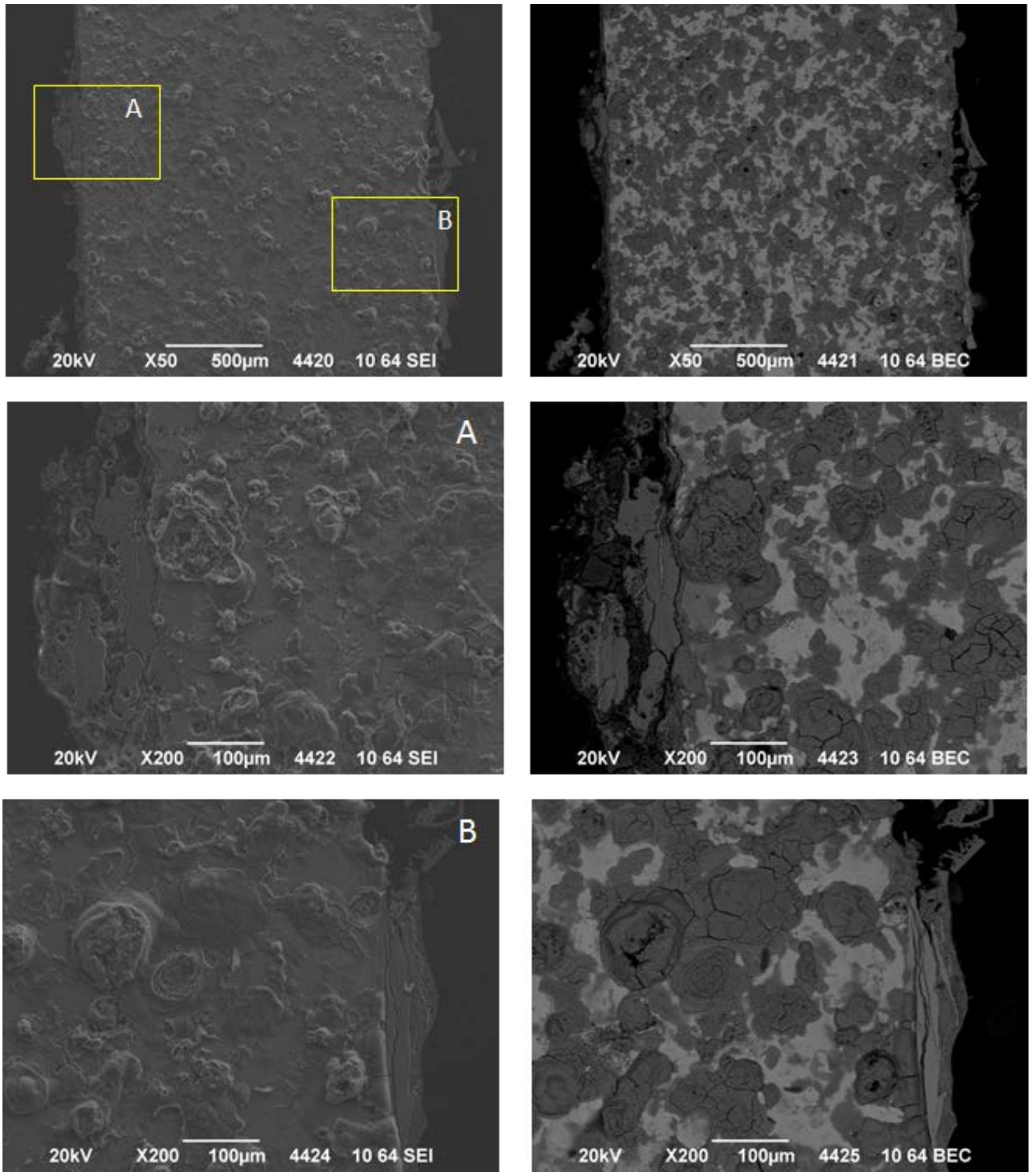

Figure 50: Detailed images of the wall of Capsule 2 at 50× to 200× magnification at Location 4. SEI images on the left and BEC images on the right (Images 4420 – 4425) [Sample 2B2].

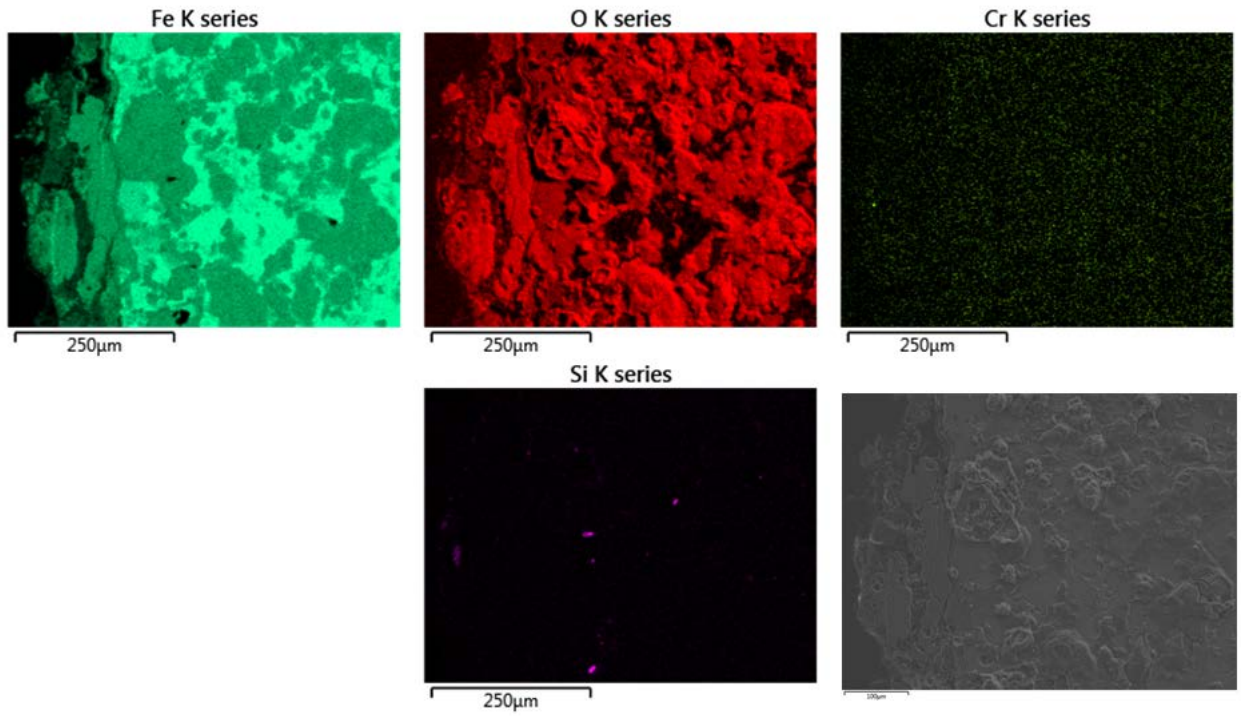

Figure 51: Elemental maps of area shown in middle images of Figure 50A for Area 4 of the exterior surface of the wall segment from Capsule 2 [Sample 2B2].

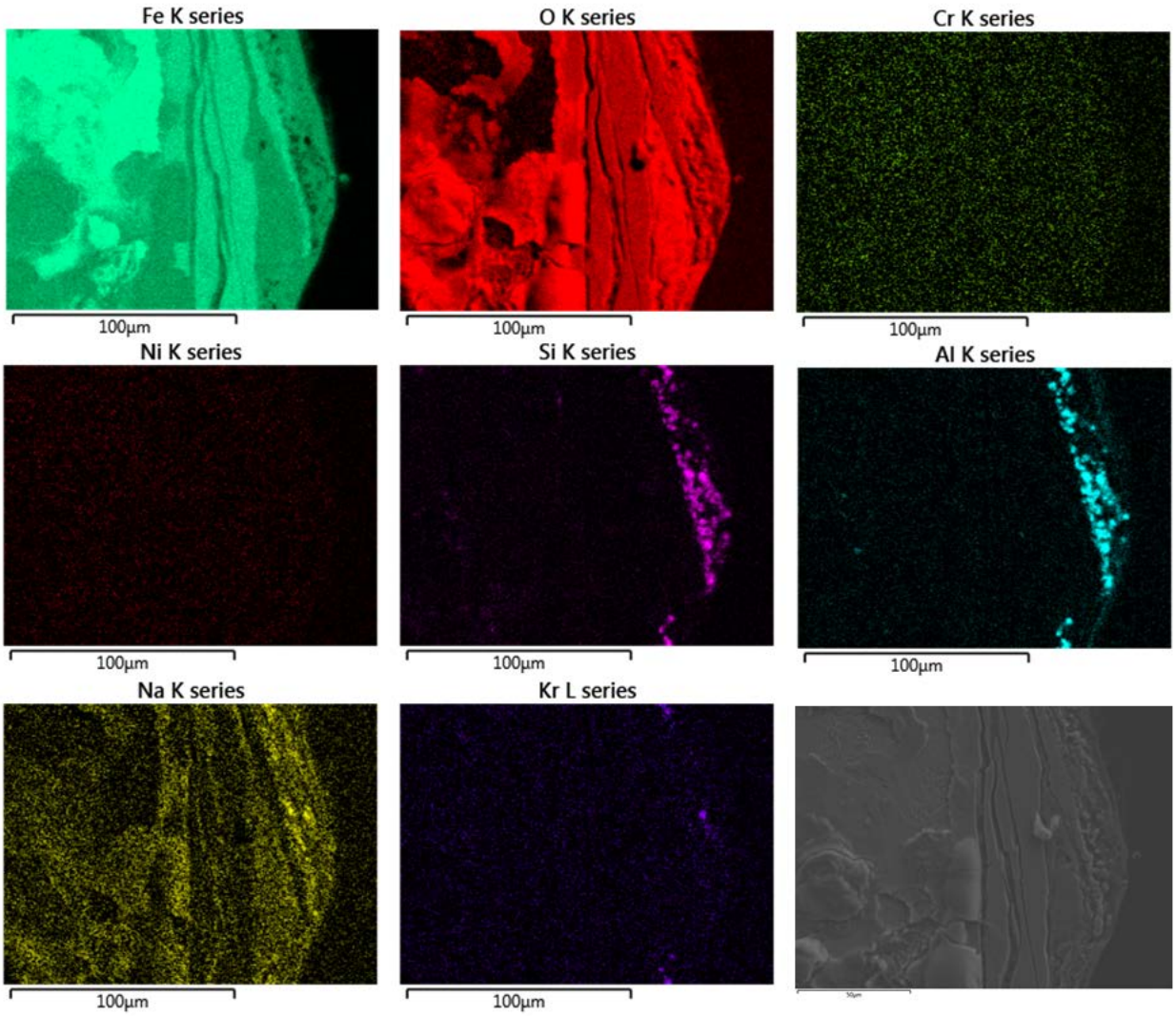

Figure 52: Elemental maps of area shown in bottom images of Figure 50B for Area 4 of the interior of the wall segment from Capsule 2 [Sample 2B2].

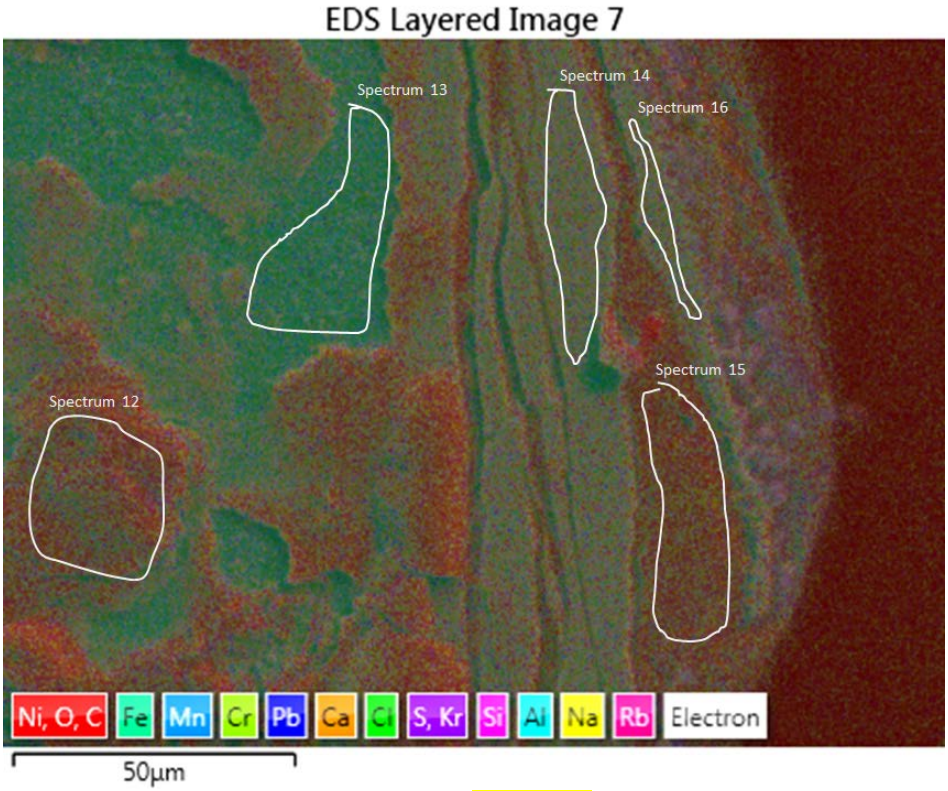

Figure 53: EDS layer image for bottom images of Figure 50B for Area 4 of the wall segment from Capsule 2. Sub-areas for localized spectral analysis are annotated [Sample 2B2].

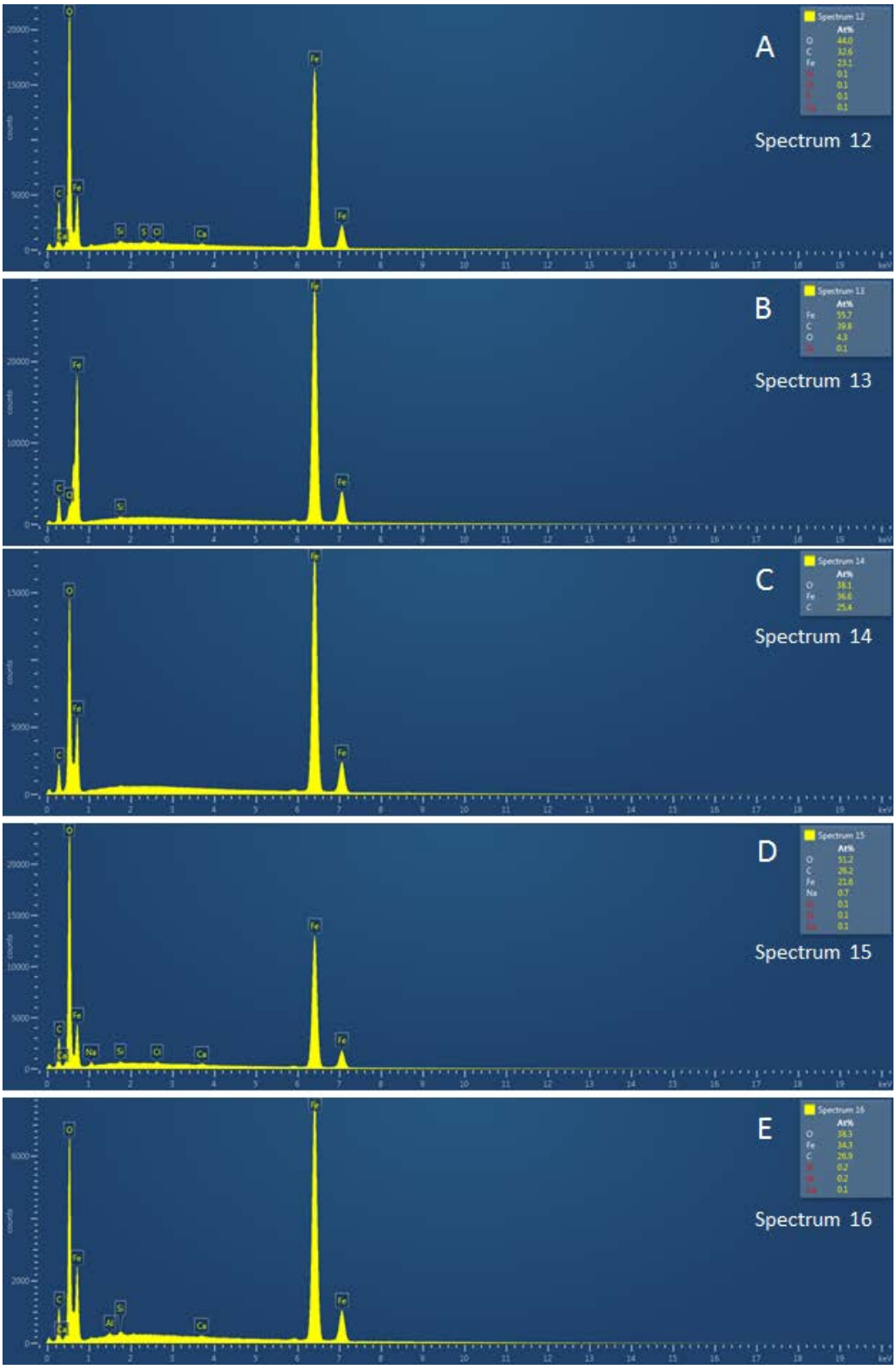

Figure 54: SEM-EDS spectra for the five sub-areas of the Capsule 2 wall segment shown in Figure 53 [Sample 2B2].

Table 2: Compositional analyis of selected area of the Capsule 2 wall sample based on EDS data

			Primary elements identified in EDS spectra														Elemental Ratios				
Image	Spectrum Area #	Feature	Fe	C	O	Cr	Ni	Mn	Si	Al	Ca	Na	Rb	Pb	Kr		Fe:O	Cr:Fe	Cr:Ni		Si:Al
Area 1																					
4408	5	Base metal	52.1	33.3	14.6												3.57				
4408	6	Oxide layer	38.7	21.5	39.8												0.97				
4408	7	Film	7.4	46.9	37.5				3.2	3.1	1.1	0.5					0.20				1.03
Area 2																					
4414	8	Base metal	52.7	32.8	14.6												3.61				
4414	9	Weld	40.4	29	27.5	2.2	0.9										1.47	0.05	2.44		
Area 3																					
4418	10	Unknown feature	3.8	23.9	46.8	1.9		10.5	10.3	2.8							0.08	0.50			3.68
4418	11	Unknown feature	5.7	48.1	37.3				3.3	3.5	1.3	0.6					0.15				0.94
Area 4																					
4424	12	Pit	23.1	32.6	44				0.1		0.1						0.53				
4424	13	Base metal	55.7	39.8	4.3				0.1								12.95				
4424	14	Layer	36.6	25.4	38.1												0.96				
4424	15	Film	21.6	26.2	51.2				0.1		0.1	0.7					0.42				
4424	16	Film	34.3	26.9	38.3				0.2	0.2	0.1						0.90				

6. ANALYSIS OF CAPSULE 5

6.1 Optical Analysis

Capsule 5 was sectioned vertically by cutting down the vertical sides of what had been the right circular cylinder using a diamond rotary saw. Water was used to cool the blade during cutting. The sectioned capsule (Figure 55) was examined visually with the aid of an optical microscope within the hot cell. Composite images from the optical microscope showing the interior of a halved Capsule 5 are shown in Figures 56 and 57. These figures show a mass of spherical pellets that appear to be bound together but still retain their shape. Figure 58 is a magnification of the lower portion of Section A of the capsule that shows pitting and corrosion at multiple points on the capsule wall. Note that both this capsule and Capsule 2 have been open to the atmosphere for extended periods of time, and any observations must be interpreted within that context. Figures 56 through 58 appear to show discoloration or potential corrosion on the capsule wall cross section.

Several of the pellets were removed from one of the sectioned halves prior to sub-sectioning one of the halves for SEM examination. The examination of these recovered pellets will be discussed in Sect. 6.2. The SEM examination of the sub-sectioned capsule wall will be discussed in Sect. 7

One half of this capsule was then cut in to smaller sections that would allow it to be mounted for SEM analysis. The mounted sample from Capsule 5 is identified as MM5A2 and is shown in Figure 59. This section is from the lower left portion of the section shown in Figure 56. The mount was polished to a 1-µm finish. Results from the optical analysis of the capsule are striking. Again, the extensive corrosion that had been observed in the macro images taken through the stereo-microscope appears to extend through the entire wall thickness. The large dark area is a bubble in the epoxy used to pot the wall segment. Several of the zeolite beads remain attached to the wall and can be seen at several locations. A detail of the attachment point is shown at 50× magnification in Figure 60. Figure 61 shows a suspected weld location in the corner of the capsule. The extent and behavior of the corrosion appears quite different from the corrosion observed on the walls. In the image taken at 200× magnification (Figure 62), multiple phases appear to be present. These will be further examined with the SEM. Figure 63 shows at 400× magnification what appears to be some type of “grain” structure. This structural feature is very similar to that observed on Capsule 2 (Figure 35).

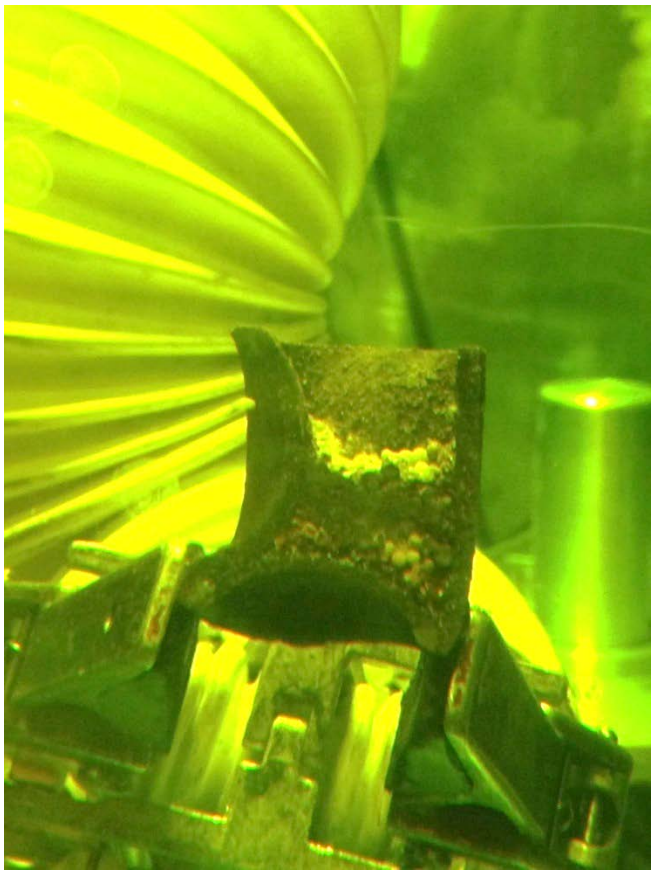

Figure 55: Section "A" of Capsule 5 looking through cell window.

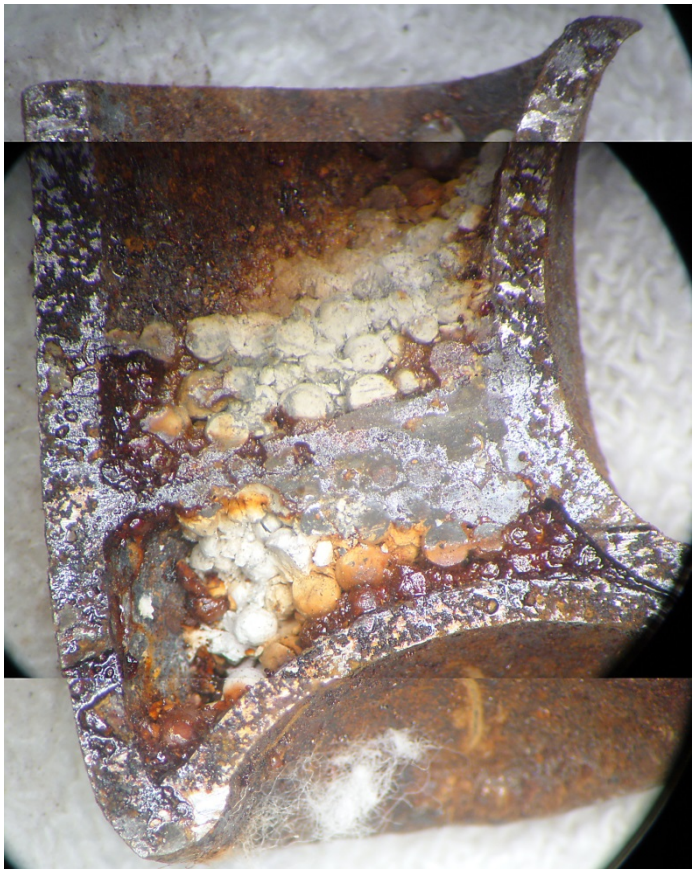

Figure 56: Composite optical microscope image of Section "A" of Capsule 5.

Figure 57: Composite optical microscope image of Section "B" of Capsule 5.

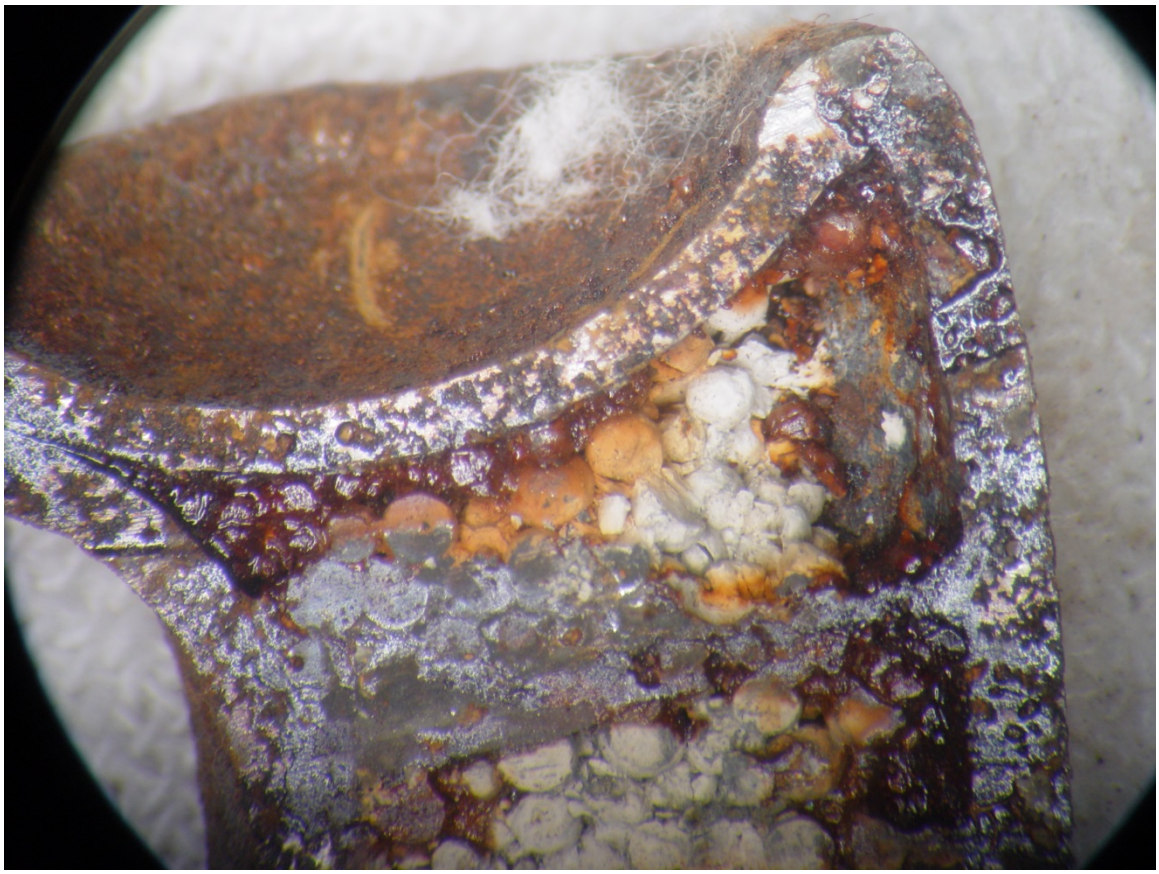

Figure 58: Detail optical microscope image of Section "A" of Capsule 5.

Figure 59: Optical microscope image of Section "A" of Capsule 5 (Image MM5A2-0MS-001).

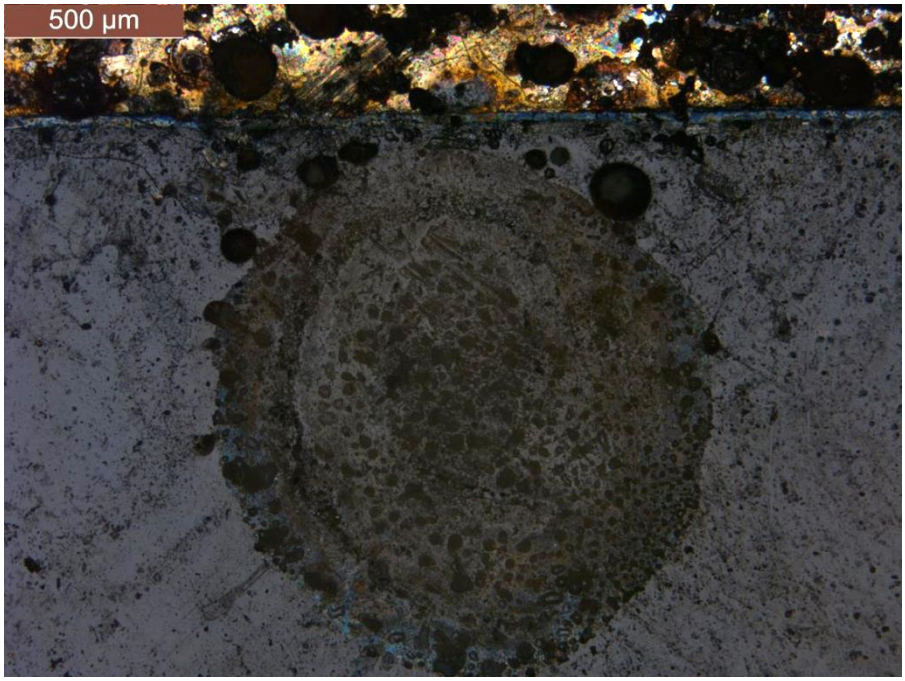

Figure 60: Optical microscope image at 50× magnification of section "A" of Capsule 5 with possible zeolite material attached to wall (Image MM5A2-050X-004).

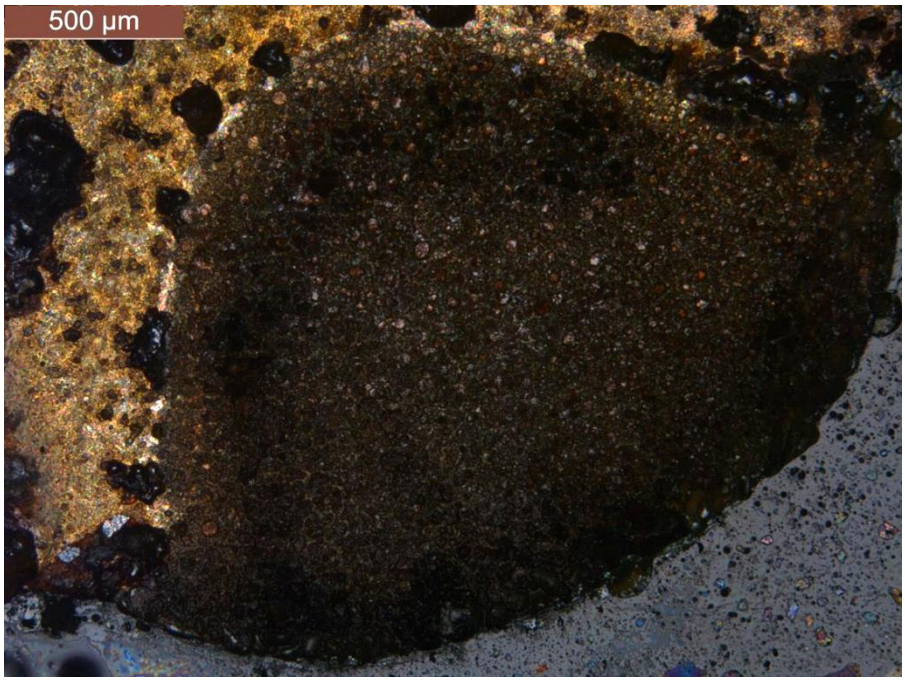

Figure 61: Optical microscope image at 50× magnification of Section "A" of Capsule 5 showing suspected weld area (Image MM5A2-050X-010).

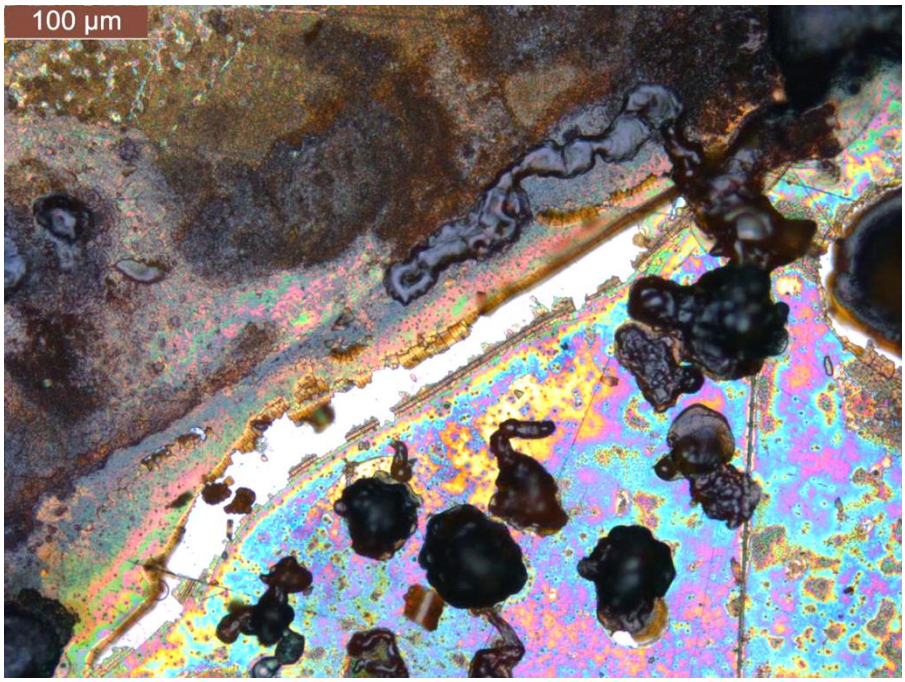

Figure 62: Optical microscope image at 200× magnification of Section "A" of Capsule 5 (Image MM5A2-0200X-011).

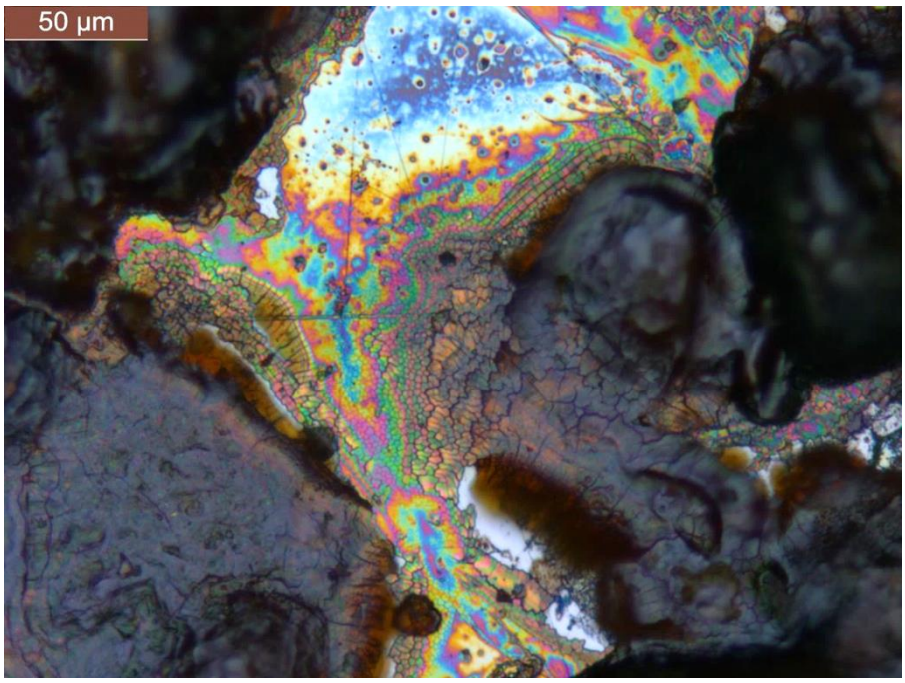

Figure 63: Detail optical microscope image at 400× magnification of Section "A" of Capsule 5 at higher magnification(Image MM5A2-400X-013).

6.2 SEM Analysis of Zeolite Material Recovered from Capsule 5

As with the pellets recovered from Capsule 2, the zeolite material recovered from the capsule was mounted and ground to the midpoint of the pellet. The surface was coated with a layer of carbon ~7 µm thick. This sample was designated K5. A second sample was also recovered and mounted but was not carbon coated. This sample is designated K4. Both K4 and K5 samples appeared to retain much of their original spherical shape.

The surface of K5 was then examined by SEM. First, the sample was examined at low magnification. The SEI revealed the presence of some surface pitting (Figure 64). The BEC of the same area is shown in Figure 65. The BEC indicates several bright areas which are typically high-Z materials. As with the pellet from Capsule 2, three areas across the diameter of the pellet were selected for further examination at higher magnifications. A fourth area associated with the bright spot in Figure 65 was also examined. At each location, elemental maps were prepared using EDS, and a spectrum was collected to determine the approximate elemental composition. Finally, an EDS line analysis was completed from the center point to the outer edge of the pellet. The SEM images taken near the center of the pellet are shown in Figure 66. The elemental mapping of the selected point near the center of the pellet is shown in Figure 67, and the EDS spectrum is presented in Figure 68. The SEM images taken near the midpoint between the center and the edge of the pellet are shown in Figure 69. The corresponding elemental mapping of the selected point is shown in Figure 70, and the EDS spectrum is presented in Figure 71. The SEM images taken near the outer edge of the pellet are shown in Figure 72. The corresponding elemental mapping of the selected point is shown in Figure 73, and the EDS spectrum is presented in Figure 74. The SEM images taken to examine the apparent high-Z area near the center of the pellet are shown in Figure 75. The corresponding elemental mapping of the selected point is shown in Figure 76, and the EDS spectrum is presented in Figure 77.

The SEM images do not appear to indicate an area of lower density material near the center of the pellet as was observed for the pellets from the unHIPed Capsule 2. In all cases, the elemental mapping of the three points across the pellets showed that the Al, Si, and Ca were coincident with each other. The approximate atom % numbers obtained from the EDS analysis are consistent with the composition of 5A molecular sieves. The Na is also consistent the production of 5A molecular sieve (MS) from 4A with the ~67% exchange of Ca for Na in the 4A molecular sieve[4]. The Kr and Xe elemental maps are also coincident with the Al, Si, and Ca which is indicative of the Kr being trapped in the zeolite structure. The Kr:Xe atom % numbers would indicate that the Kr that was loaded into the zeolite had some Xe impurities, ~20% Xe. These results are completely consistent with those from the material recovered from Capsule 2.

With regard to the presences and distribution of the Rb, the EDS spectra clearly show it is present based on the peak at ~13.4 KeV, and the elemental maps also show that it is widely dispersed and also appears to be coincident with the Kr.

The examination of the bright spot noted on Figure 65 using EDS (Figures 76 and 77) revealed the presence of lead at about 1 at. %. The origin of the lead is currently unknown. This may have been used as a sintering aid during the HIPing process or for internal shielding. However, neither use has been noted in the literature found thus far regarding the origin of these samples.

The EDS line scan (Figure 78) covering the area between the center of the pellet and the outer edge also shows significant correlation between the 5A MS structural elements and the Kr, Xe, and to a slightly lesser degree the Rb. The spike in Cl at ~300 µm is from the epoxy mounting material.

Figures 79 and 80 are SEM images of the interface between what appears to be two pellets. Four locations were examined using EDS point scans. The locations of the scans are shown in Figure 81. The EDS spectra are shown in Figures 82 to 85.

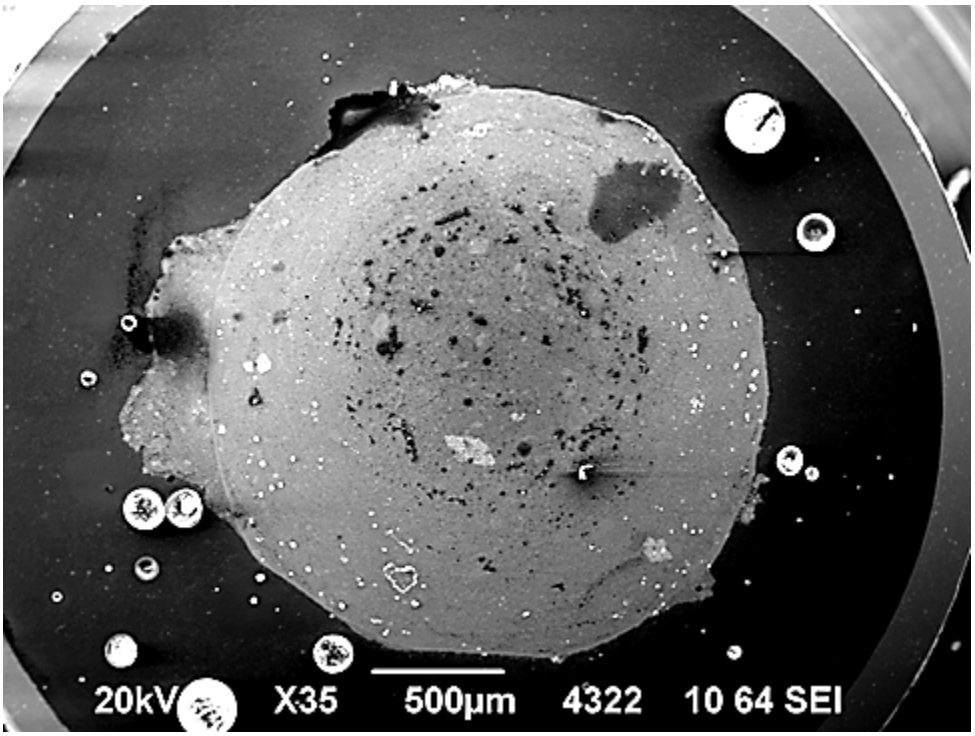

Figure 64: Secondary electron image of cross section of pellet recovered from Capsule 5 at 35× magnification (Image 4322) [Sample K5].

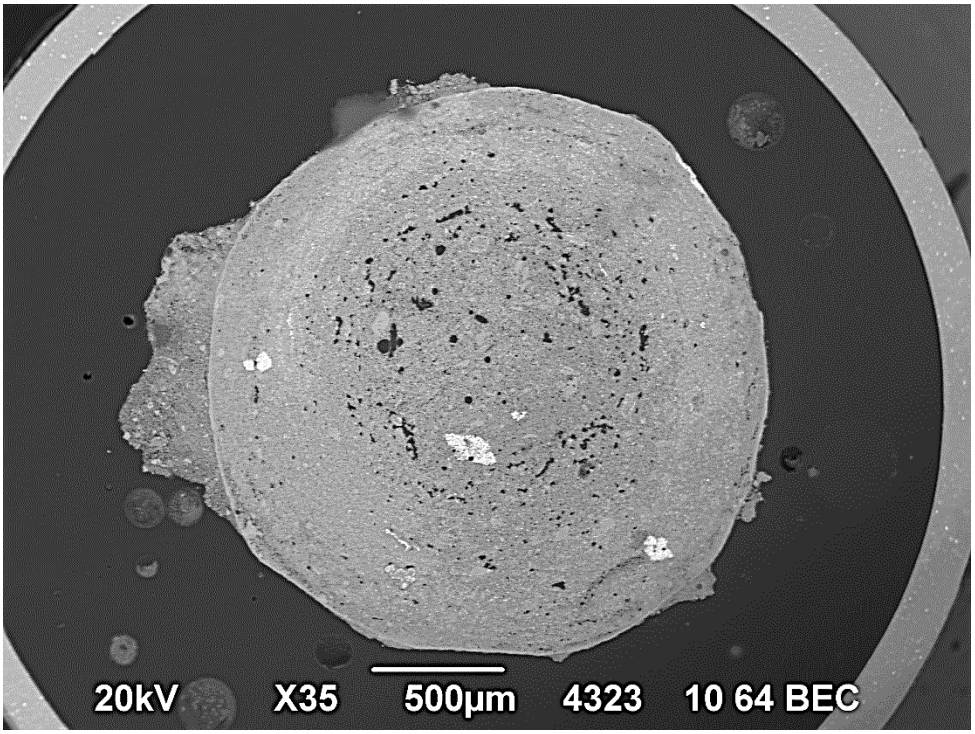

Figure 65: Backscatter electron image of cross section of pellet recovered from Capsule 5 at 35× magnification (Image 4323) [Sample K5].

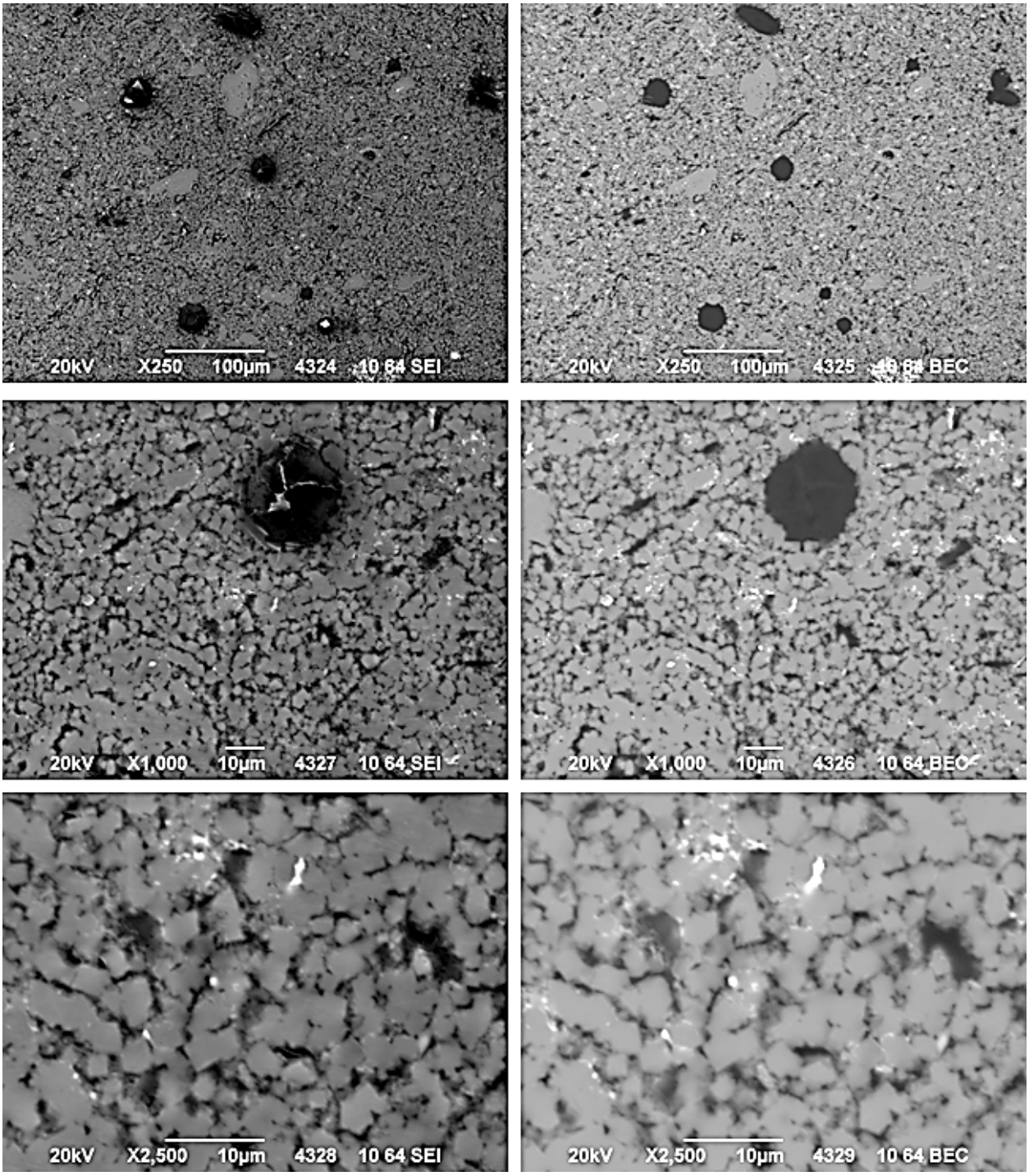

Figure 66: Detailed images of area near center of pellet recovered from Capsule 5 at 250× to 2500× magnification. SEI images on the left and backscatter images on the right (Images 4324–4329) [Sample K5].

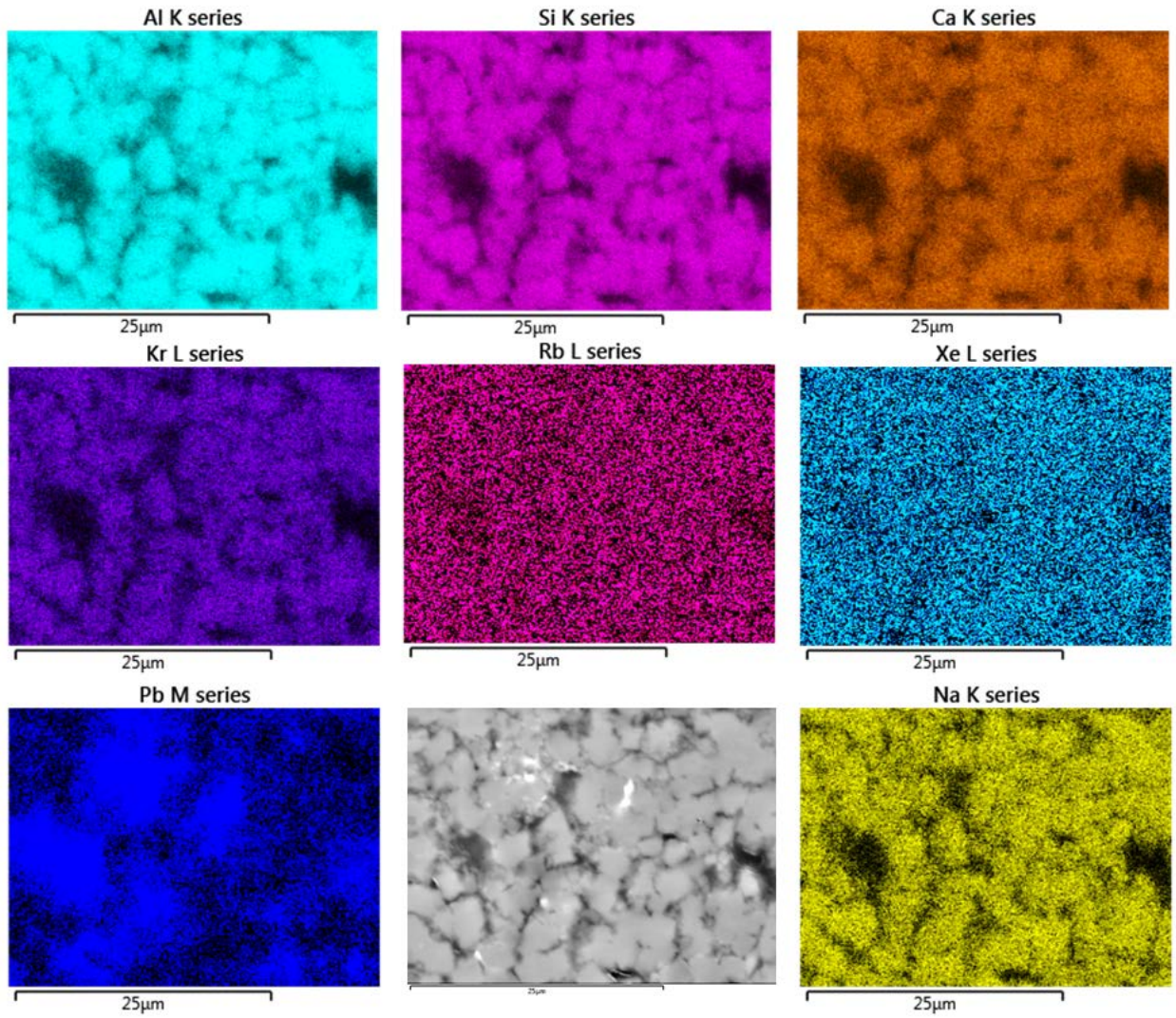

Figure 67: Elemental maps of area shown in bottom images of Figure 66 for pellet recovered from Capsule 5 [Sample K5].

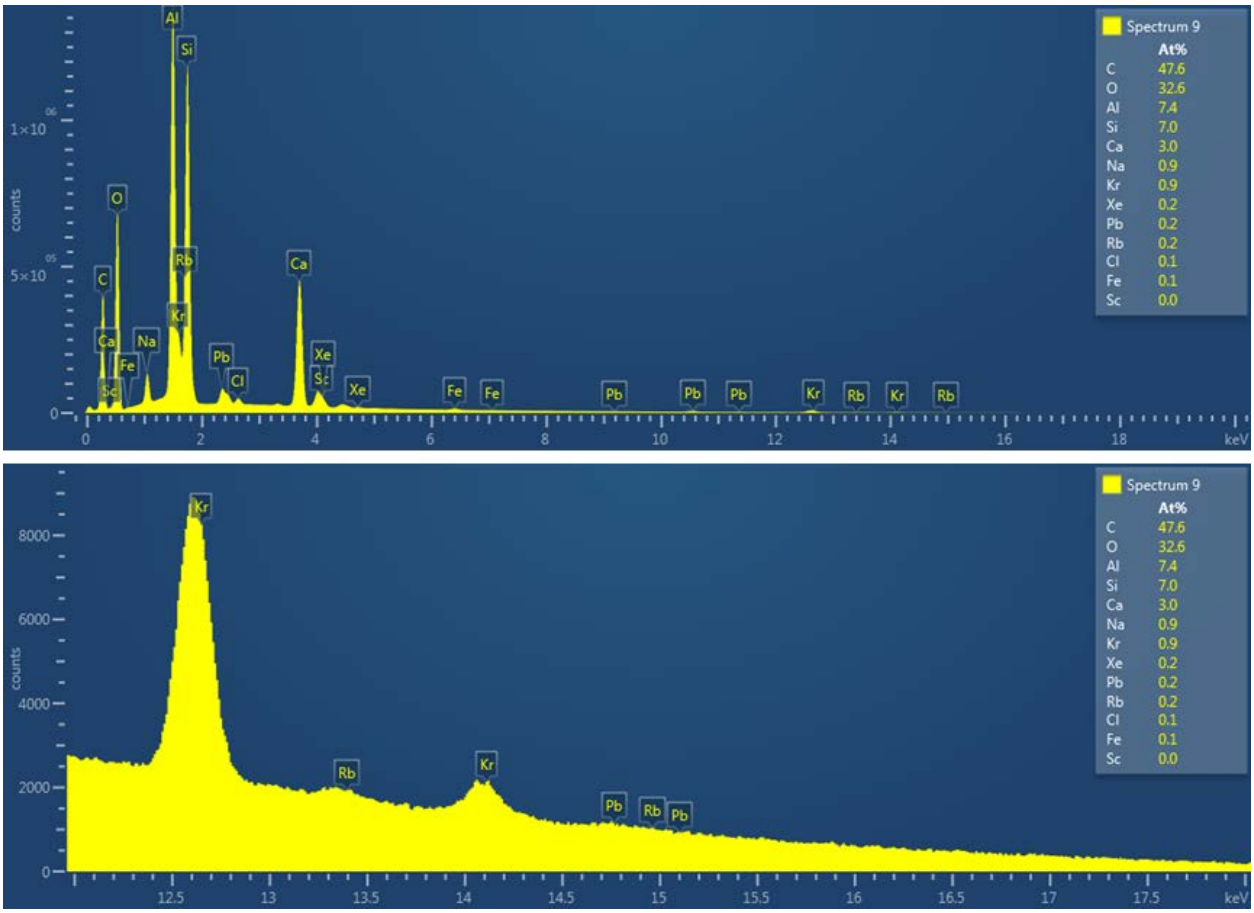

Figure 68: SEM-EDS of the area shown in the elemental maps for Image 4329 near center of pellet recovered from Capsule 5 [Sample K5].

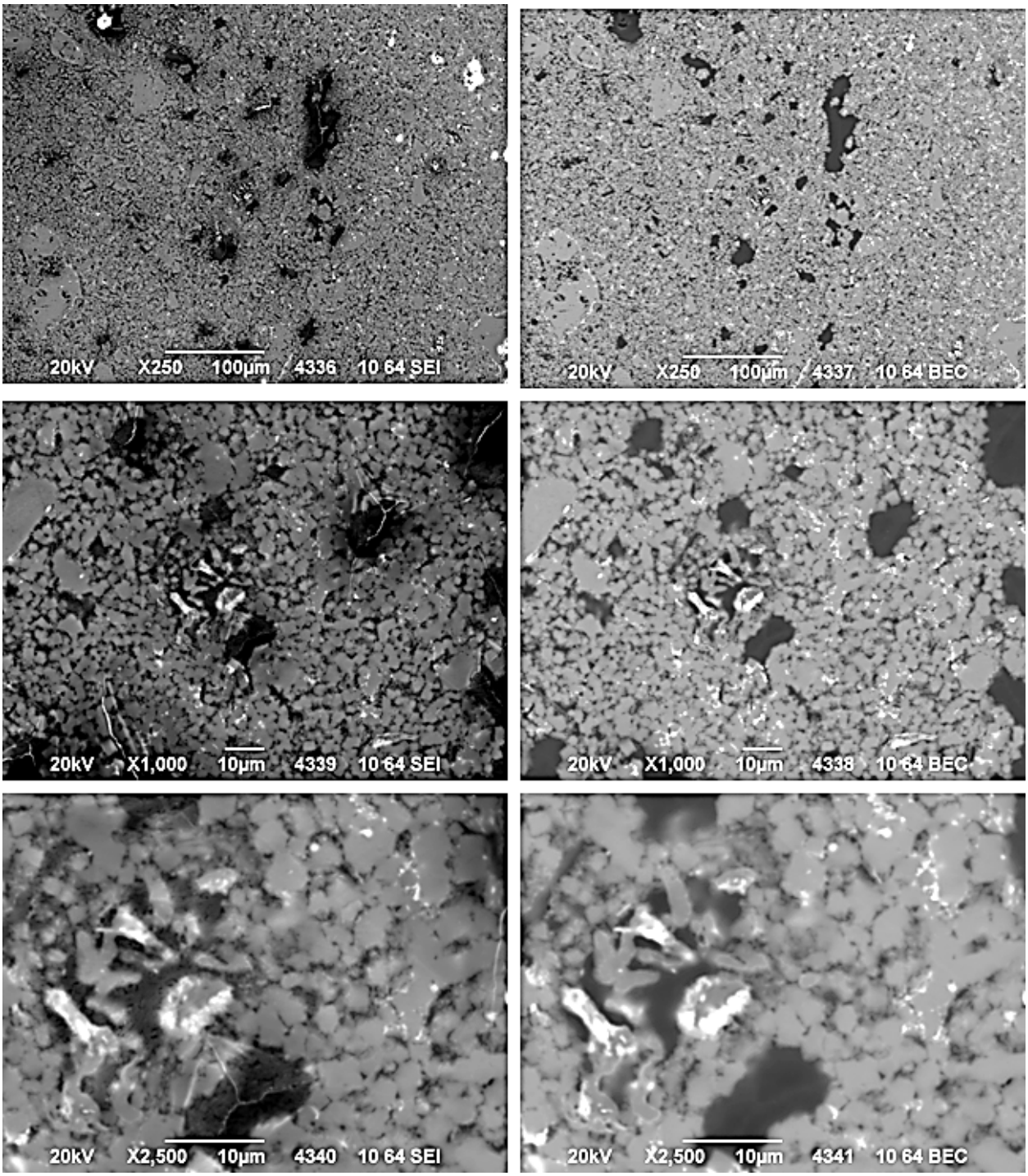

Figure 69: Detailed images of area near midpoint between center and edge of pellet recovered from Capsule 5 at 250× to 2500× magnification. SEI images on the left and backscatter images on the right (Images 4336–4341) [Sample K5].

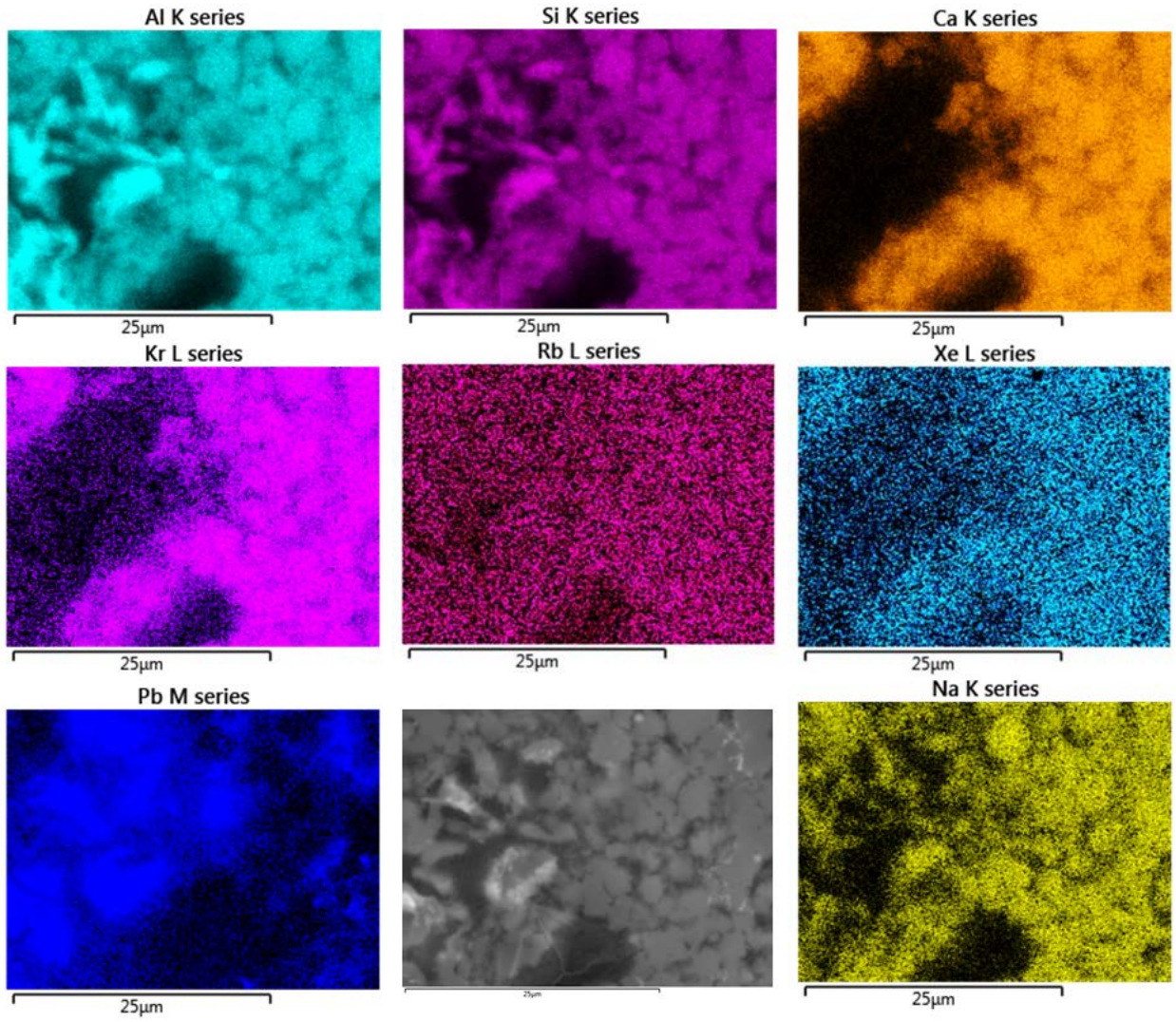

Figure 70: Elemental maps of area shown in bottom images of Figure 69 for pellet recovered from Capsule 5 [Sample K5].

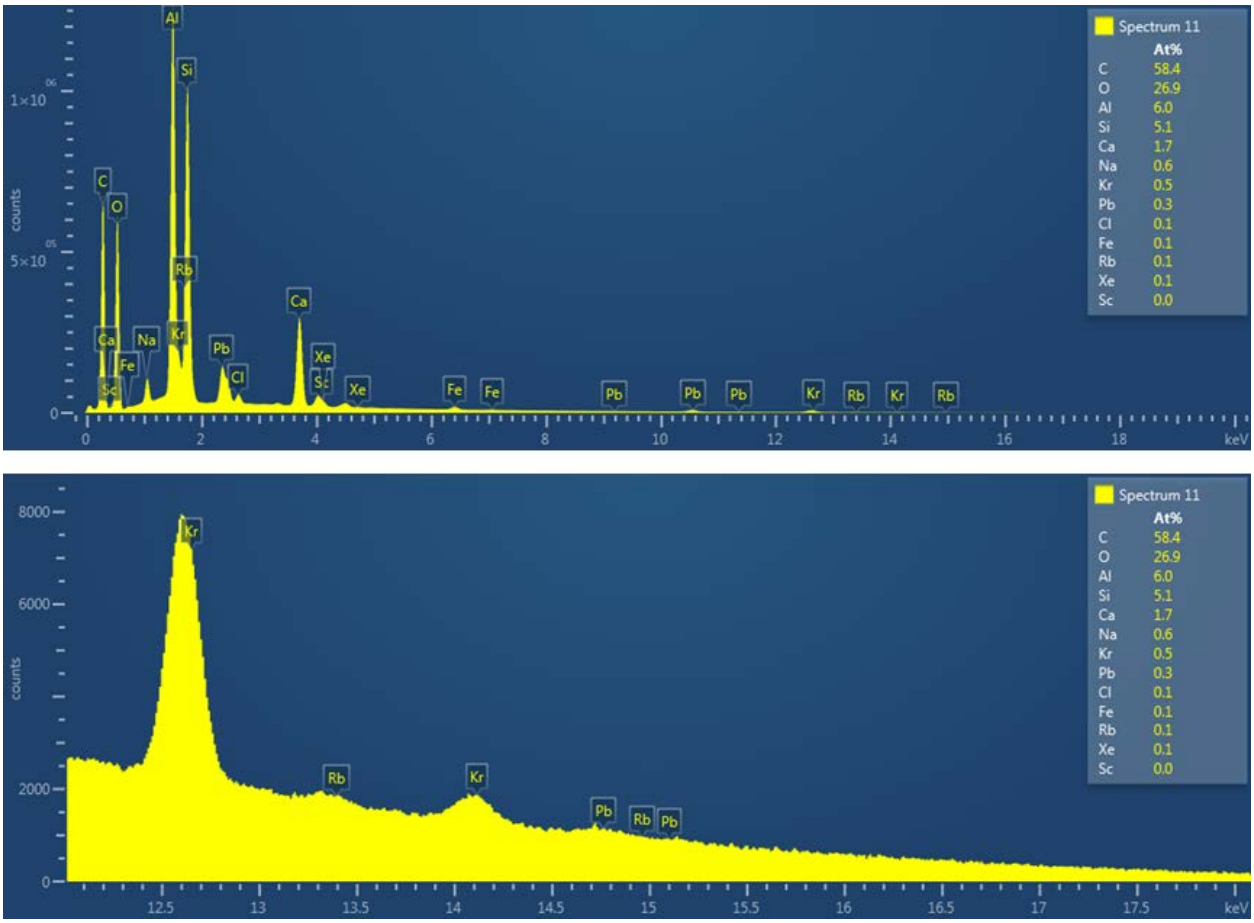

Figure 71: SEM-EDS of the area shown in the elemental maps for Image 4341 near midpoint between center and edge of pellet recovered from Capsule 5 [Sample K5].

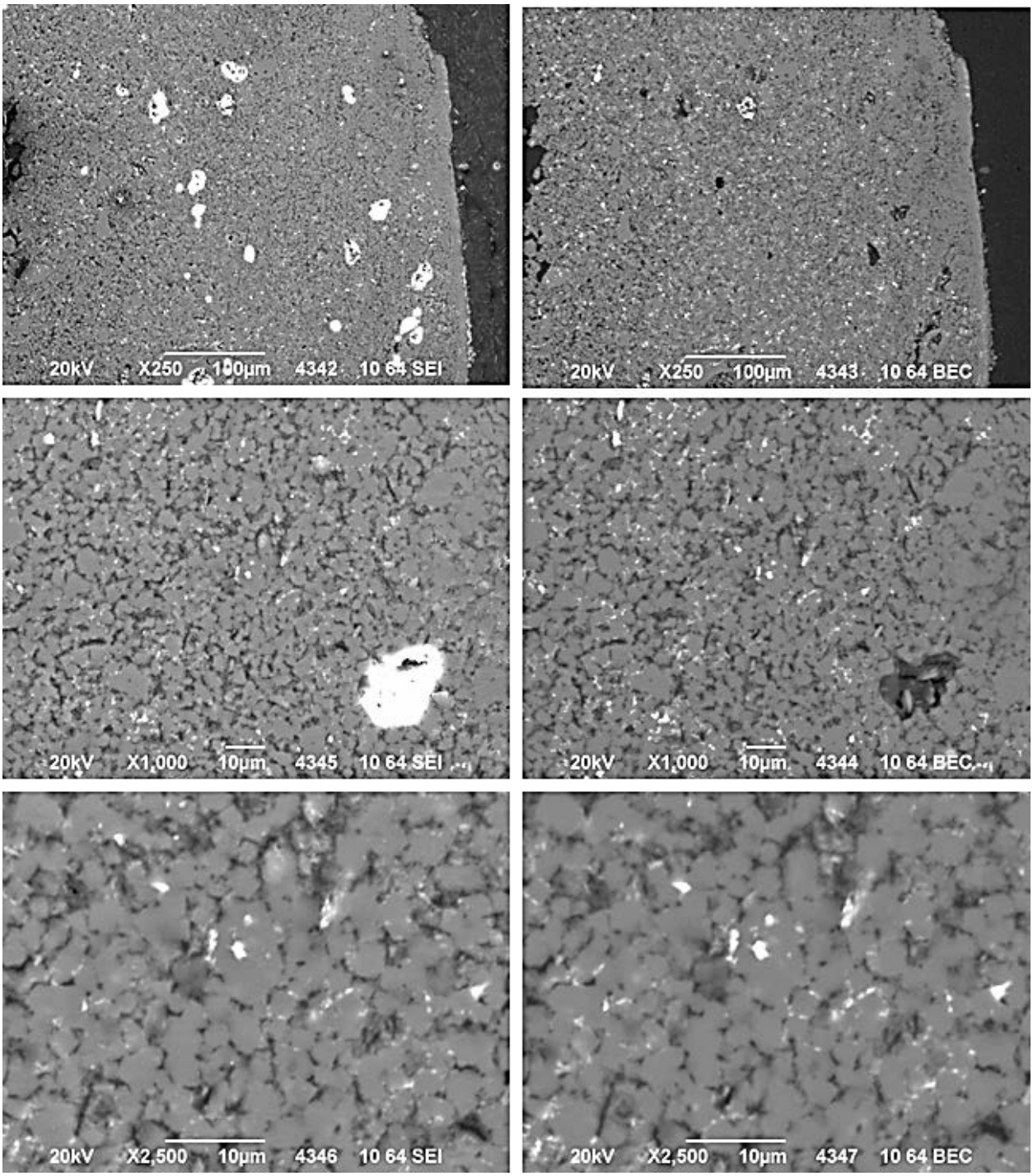

Figure 72: Detailed images of area near outer edge of pellet recovered from Capsule 5 at 250× to 2500× magnification. SEI images on the left and backscatter images on the right (Images 4342–4347) [Sample K5].

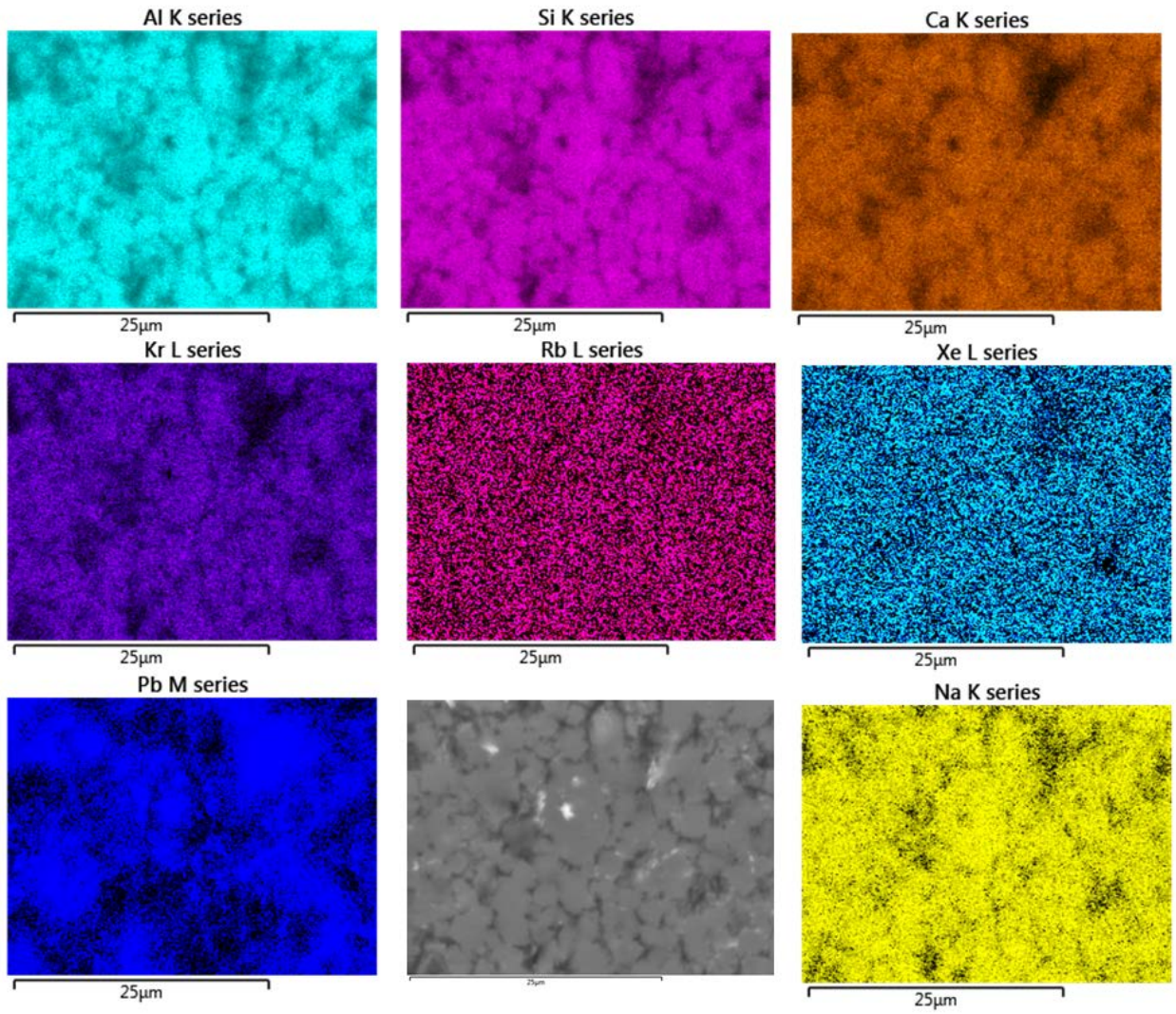

Figure 73: Elemental maps of area shown in bottom images of Figure 72 for pellet recovered from Capsule 5 [Sample K5].

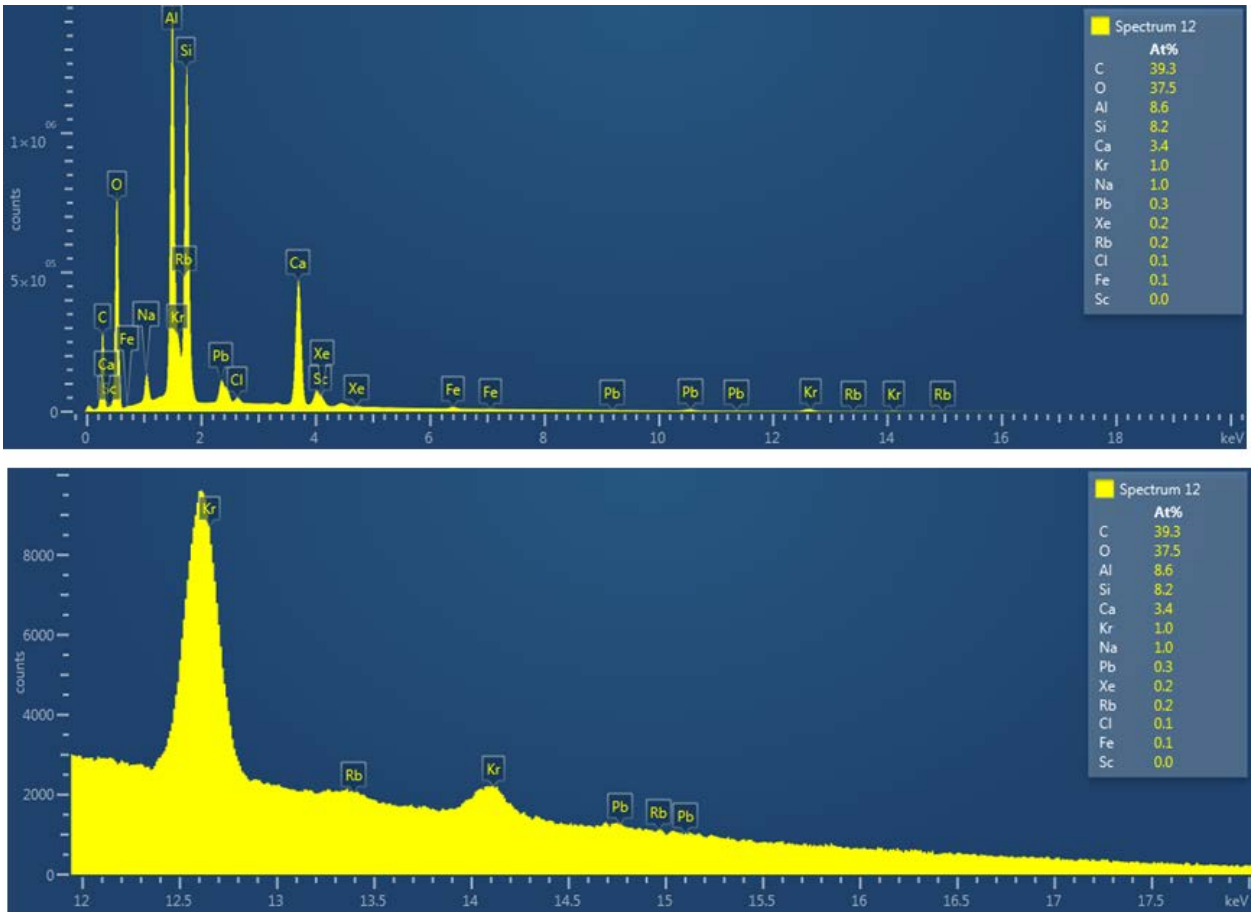

Figure 74: SEM-EDS of the area shown in the elemental maps for Image 4347 near the outer edge of pellet recovered from Capsule 5 [Sample K5].

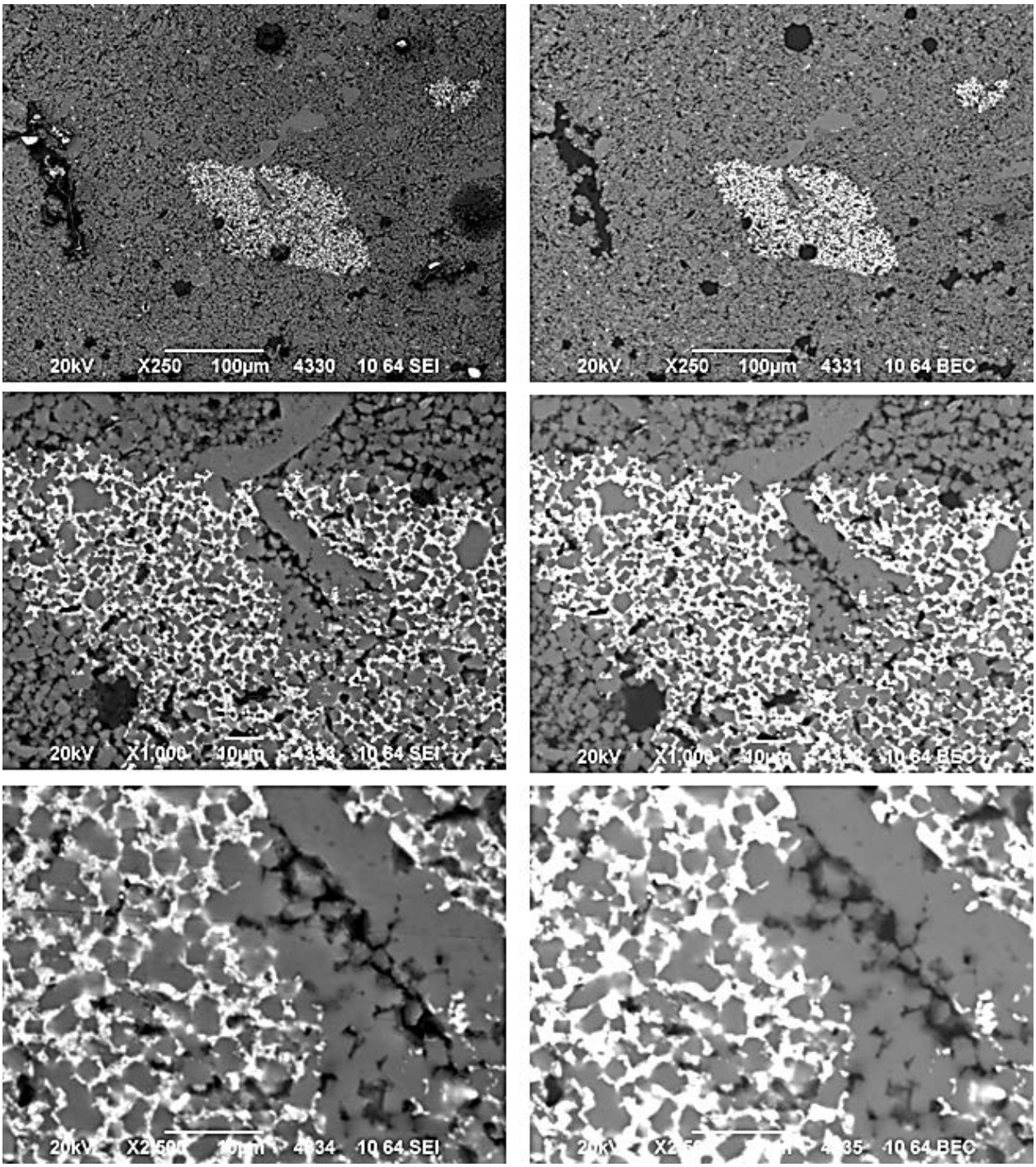

Figure 75: Detailed images of high-Z area near center of pellet recovered from Capsule 5 at 250× to 2500× magnification. SEI images on the left and backscatter images on the right (Images 4330–4335) [Sample K5].

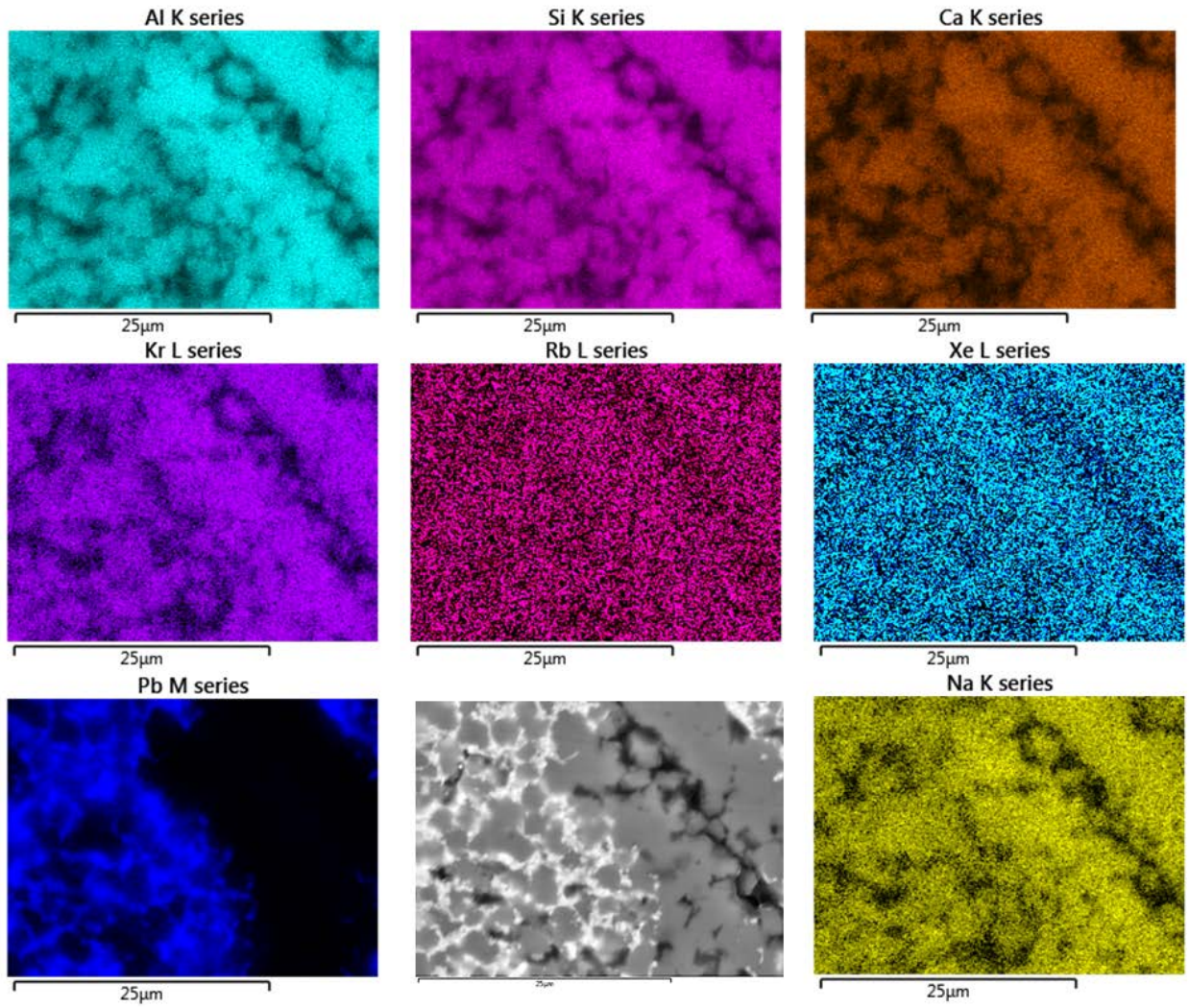

Figure 76: Elemental maps of area shown in bottom images of Figure 75 for pellet recovered from Capsule 5 [Sample K5].

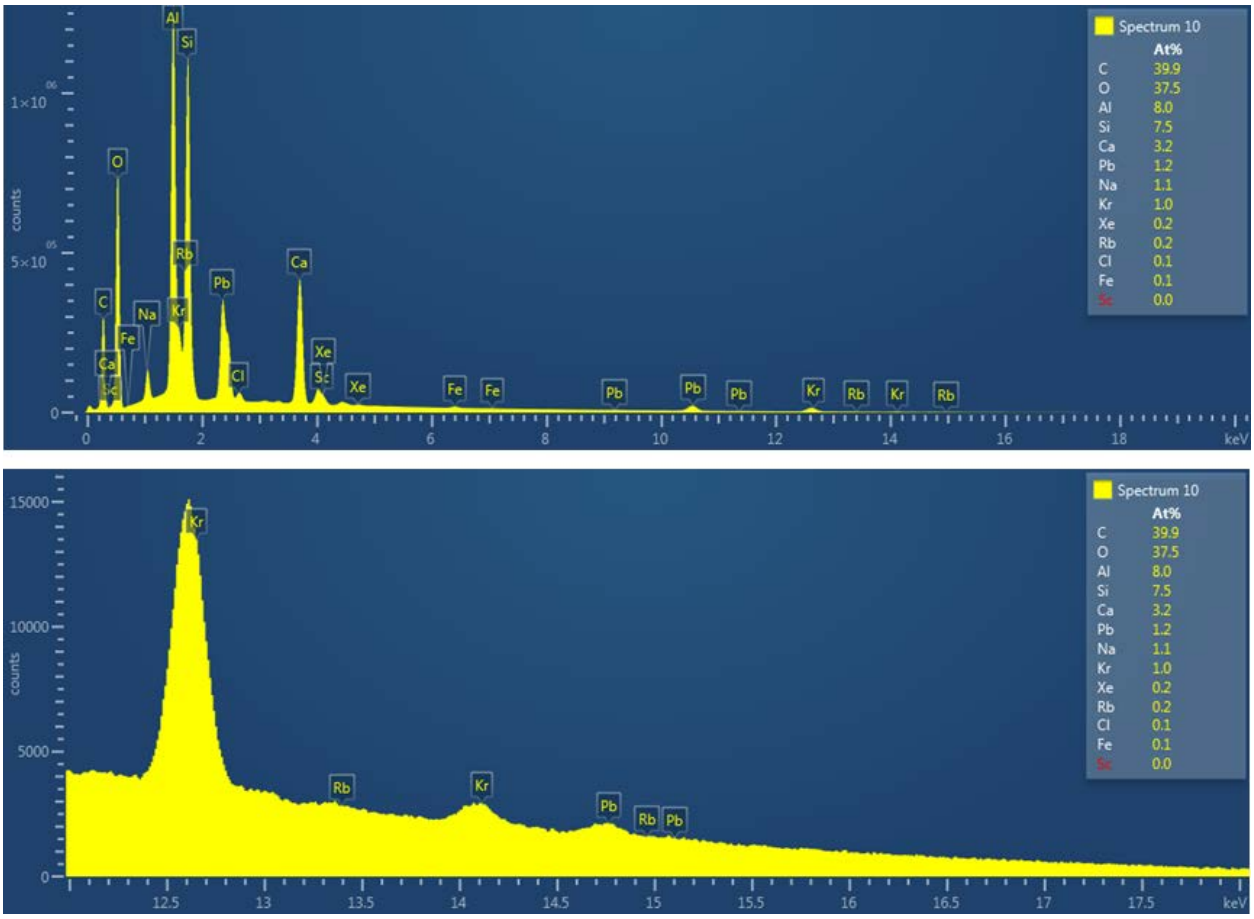

Figure 77: SEM-EDS of the high-Z area shown in the elemental maps for Image 4335 near center and edge of pellet recovered from Capsule 5 [Sample K5].

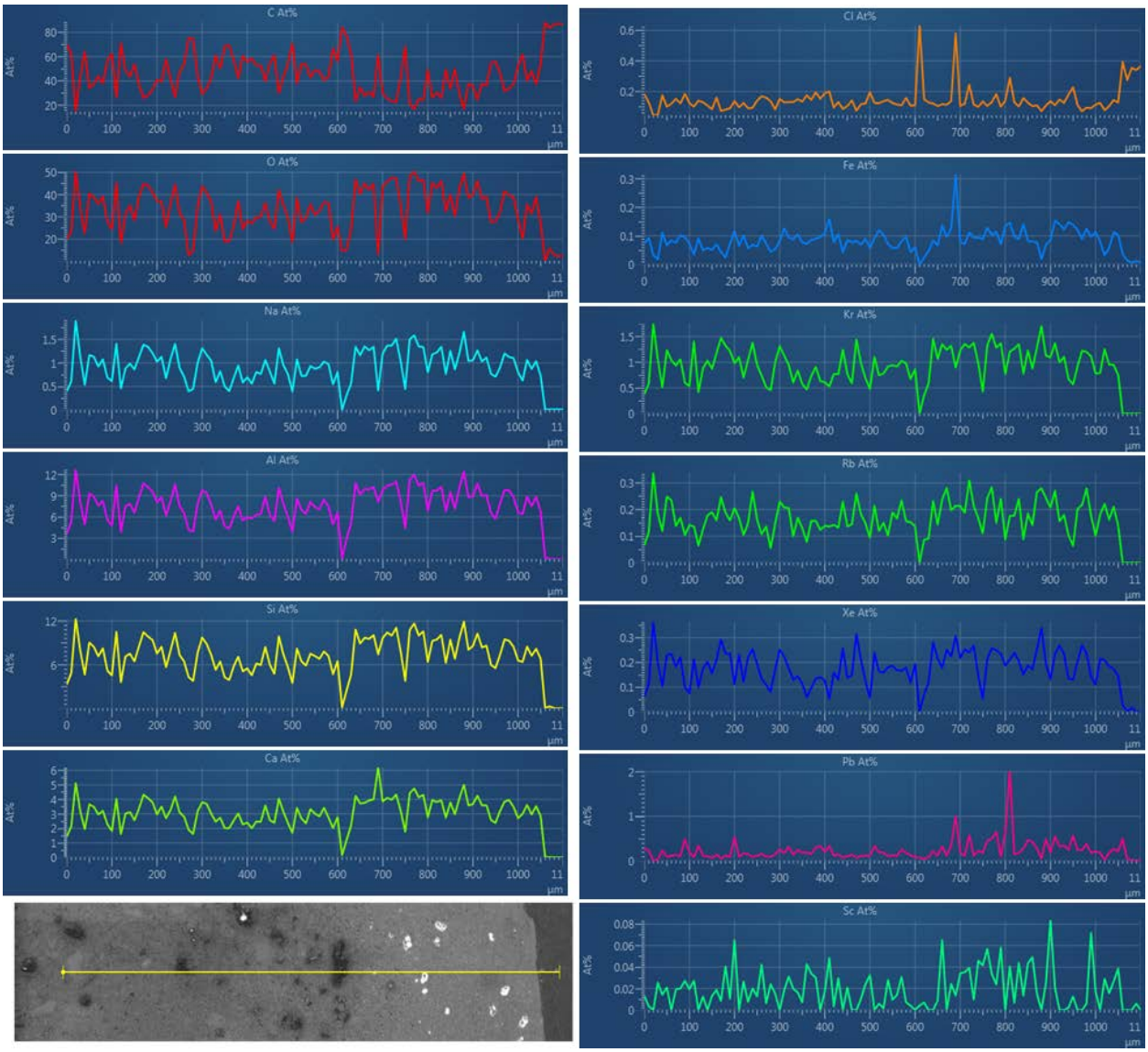

Figure 78: SEM-EDS line data for pellet recovered from Capsule 5 [Sample K5].

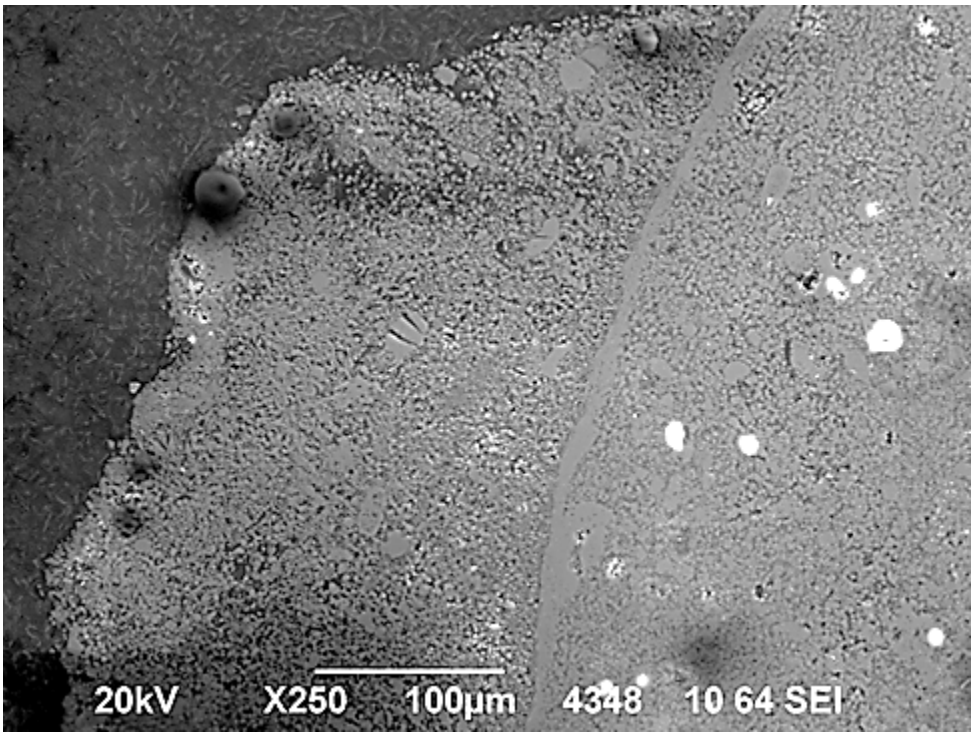

Figure 79: Secondary electron image of surface showing interface between two HIPed pellets recovered from Capsule 5 at 250× magnification (Image 4348) [Sample K5].

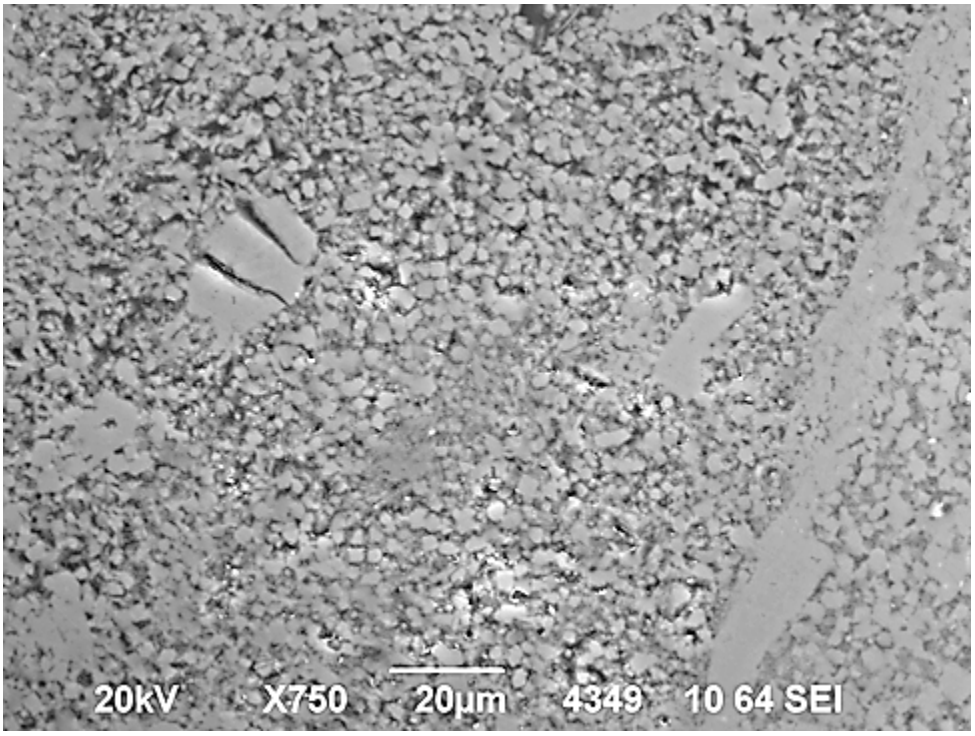

Figure 80: Secondary electron image of surface showing interface between two HIPed pellets recovered from Capsule 5 at 750× magnification (Image 4349) [Sample K5].

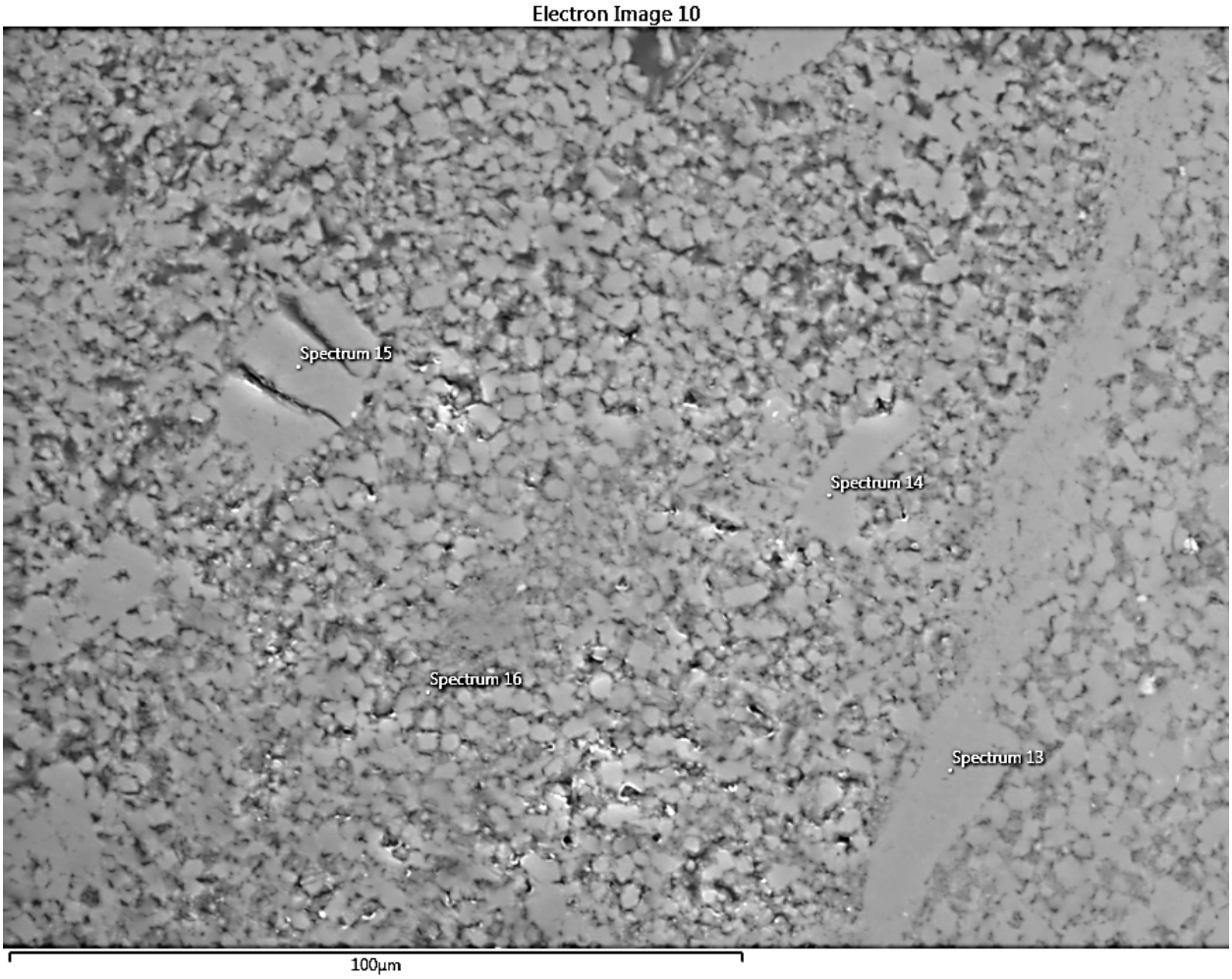

Figure 81: Backscatter electron image of interface area for HIPed pellet recovered from Capsule 5 at 750× magnification showing location for EDS point scans shown in Figures 82-85 (Image 4349) [Sample K5].

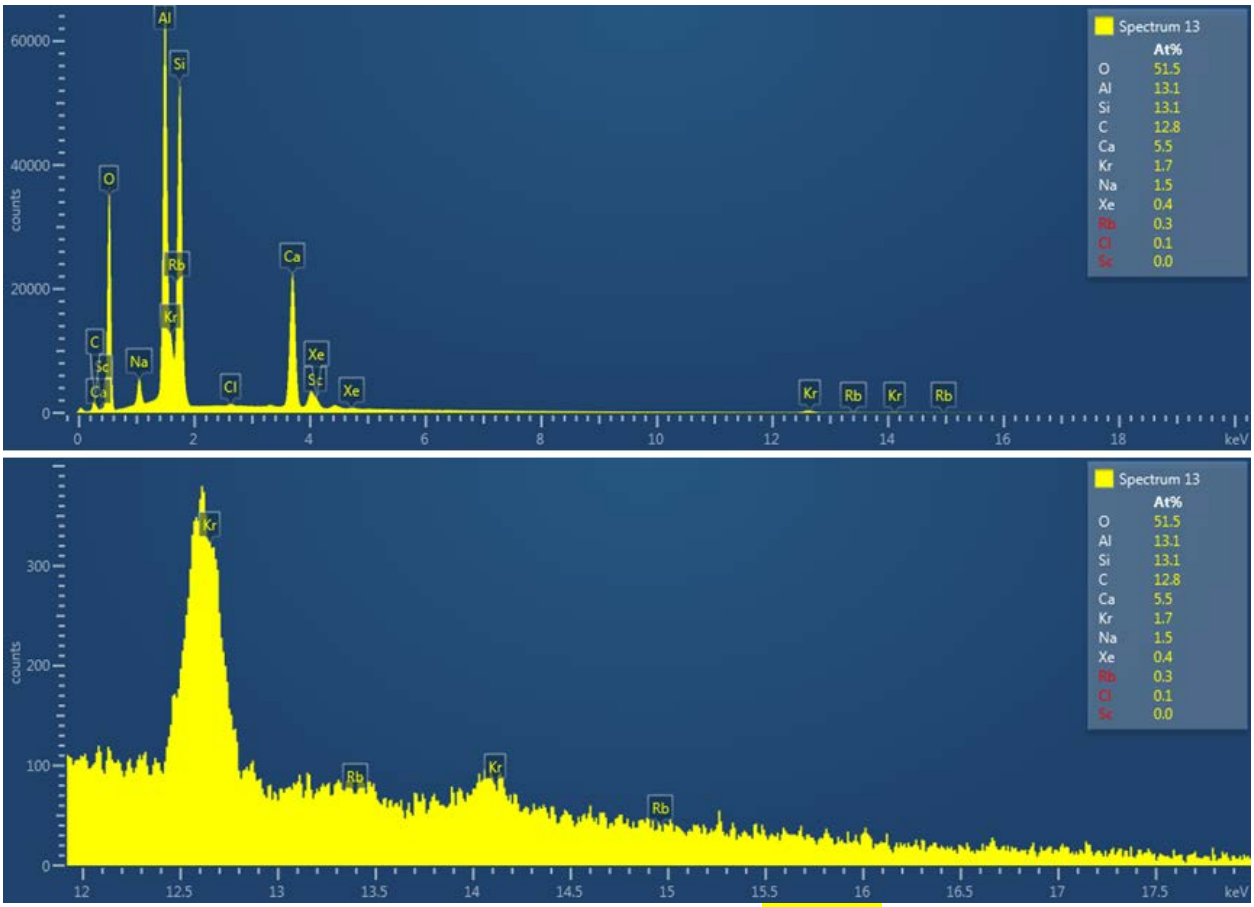

Figure 82: EDS point scan spectrum 13 for location noted in Figure 81 (Image 4349) [Sample K5].

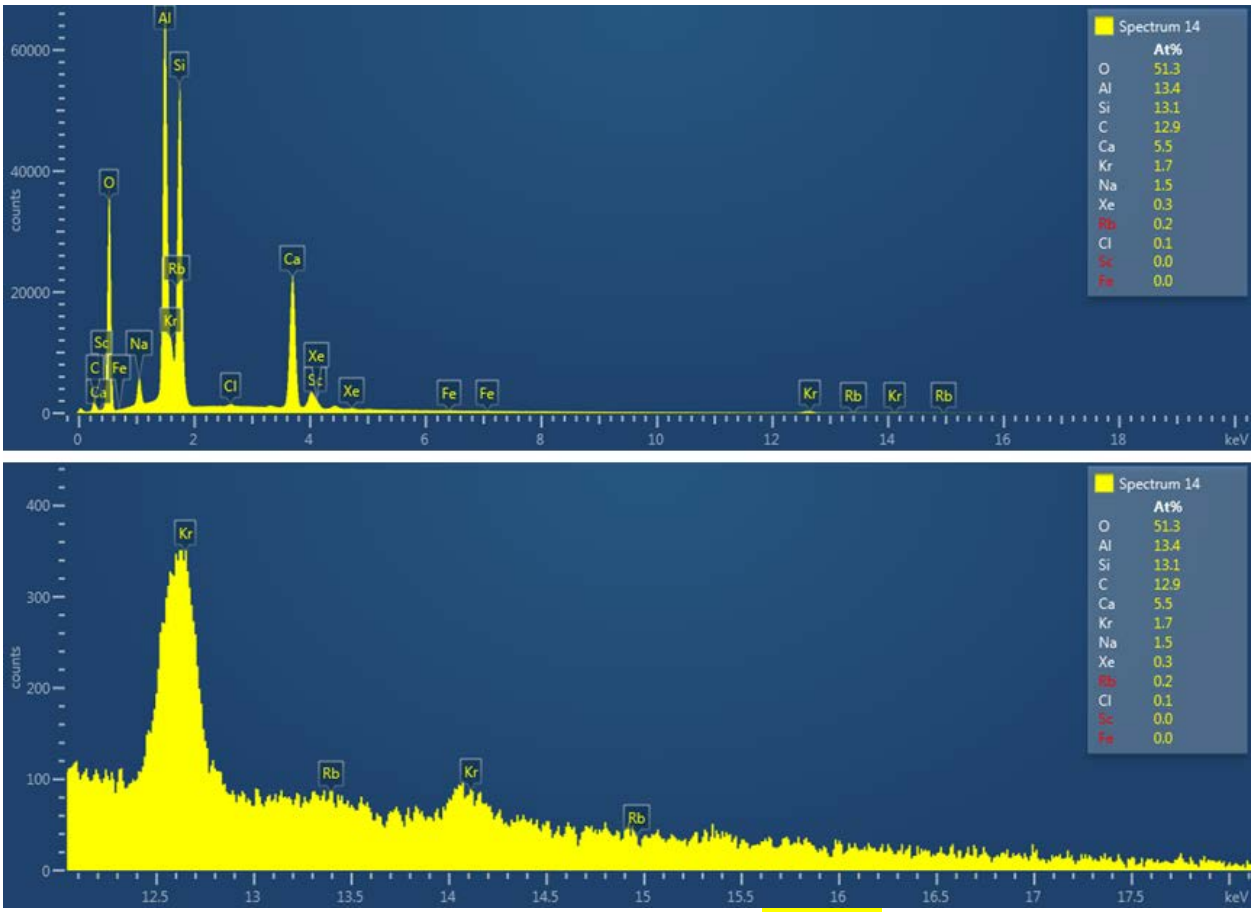

Figure 83: EDS point scan spectrum 14 for location noted in Figure 81 (Image 4349) [Sample K5].

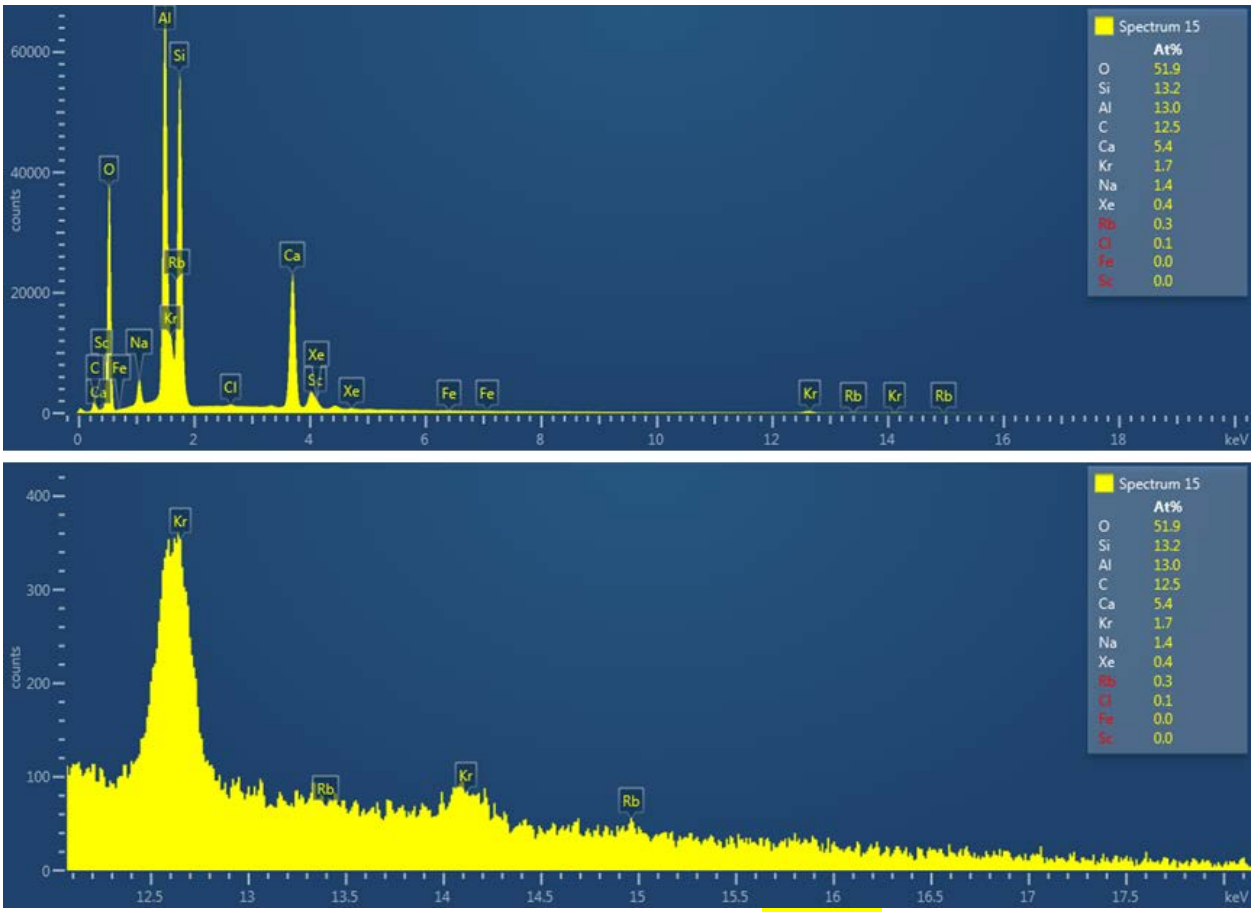

Figure 84: EDS point scan spectrum 15 for location noted in Figure 81 (Image 4349) [Sample K5].

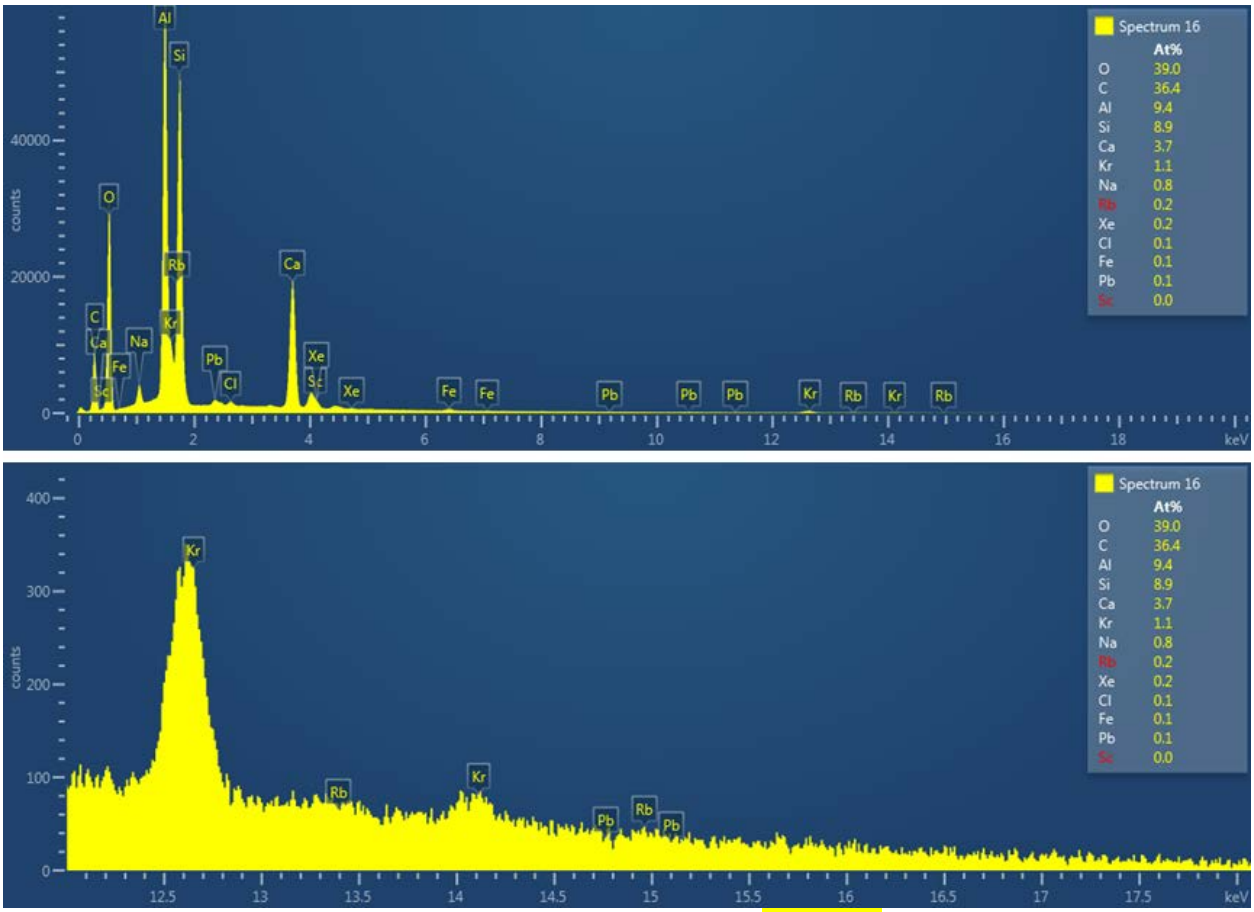

Figure 85: EDS point scan spectrum 16 for location noted in Figure 81 (Image 4349) [Sample K5].

6.3 Chemical Analysis

Chemical analysis of the zeolite material recovered from Capsule 5 was based on EDS data (see Table 3). Starting with the Ca, Na, Si, and Al data from the four positions that were examined within the pellet, several points can be made. First the average ratio of Si to Al is 0.92. The average ratio of Ca to Na is 3.12. Christensen et al.,[5] indicated that one of the starting materials was a 5A zeolite obtained from W. R. Grace Company in the form of 2-mm spheres which was produced by a 67% exchange of calcium for sodium in zeolite 4A. The typical formula for A-type zeolites is $Na_2O \cdot Al_2O_3 \cdot 2SiO_2 \cdot 4.5H_2O$. From this formula, it is clear that the ratio of Si to Al should be 1, and the ratio of Na to either Al or Si should also be 1. However, if Ca^{+2} is exchanged for Na^{+1} then the ratio of (2Ca + Na) to either Al to Si should also be 1. For this sample, the ratio of (2Ca + Na) to Al was 0.86 and to Si was 0.93. This supports the initial assumption that these samples were formed using a 5A zeolite. It does appear that the Ca for Na exchange was significantly greater than 67%, with closer to 88% of the sodium removed.

The average Kr atom % for these same four points is 0.85. The molecular weight for the 5A zeolite with the Ca exchange based on the EDS data and no waters of hydration is 278.8. Christensen et al.,[5] indicated that the 5A material used contained 0.8% water. This would increase the effective molecular weight to 281 g/mol. Since there are 2 mol of Si or Al per mole of zeolite, the molar ratio of Kr to 5A could be determined. For this pellet, the average atom % values for Kr and (Si+Al)/4 yield 0.85/3.61. Back calculation then from the 1.03 atom % Kr + Xe would indicate a loading of 23 cm^3 STP/g solid. Reported data indicated that loading of 30 to 50 cm^3 STP Kr/g could be achieved.

The observed Rb content is close to 20% of the Kr, which is significantly higher than the anticipated 4.6%. However, the Rb value from EDS has only one significant figure. This value could have 50 to 75% error.

All of areas examined for sample K5 also showed some amount of lead present, typically about 0.2 to 0.3 at. %. However, in one of the areas selected for examination due to the presence of a suspected high-Z material, the Pb concentration was ~1.7 at. %. This concentration is significant when compared to the Kr at 1 at. %, Na at 1.1 at. % and Ca at 3.2 at. %. The origin of the lead is unknown at this time.

Table 3: Compositional analyis of zeolite material, noble gases and Rb from Capsule 5 based on EDS data

	Atom %								*Atom % ratios*						
Sample Point (Image No.)	Ca	Na	Si	Al	Kr	Xe	Rb	Pb	Ca:Na	Si:Al	Ca:Al	(2Ca+Na):Al	(2Ca+Na):Si	Kr:Xe	Kr:Rb
4329	3	0.9	7	7.4	0.9	0.2	0.2	0.2	3.33	0.95	0.41	0.93	0.99	4.5	4.5
4341	1.7	0.6	5.1	6	0.5	0.1	0.1	0.3	2.83	0.85	0.28	0.67	0.78	5.0	5.0
4347	3.4	1	8.2	8.6	1	0.2	0.2	0.3	3.40	0.95	0.40	0.91	0.95	5.0	5.0
4335	3.2	1.1	7.5	8	1	0.2	0.2	1.7	2.91	0.94	0.40	0.94	1.00	5.0	5.0
Ave	2.83	0.90	6.95	7.50	0.85	0.18	0.18	0.63	3.12	0.92	0.37	0.86	0.93	4.9	4.9

7. ANALYSIS OF CAPSULE 5 CONTAINER

7.1 Optical Analysis

One half of Capsule 5 was then cut in to smaller sections that would allow it to be mounted for SEM analysis. The mounted sample from Capsule 5 is identified as MM5A2. The mount was polished to a 1-µm finish. As with the sample of the Capsule 2 wall material, the results are striking. The extensive corrosion that had been observed in the macro images taken through the stereo-microscope appears to be real and extends through the entire wall thickness. Representative high-magnification images (Figures 86 and 87) show the base material around representative pits in the material. Again, there is a potential concern that the capsule may be reacting with the water that was used while polishing and with air, but the dispersion of the pitting within the capsule wall indicates that these pits may be integral to the sample. This sample was further analyzed using SEM techniques as discussed in the following section.

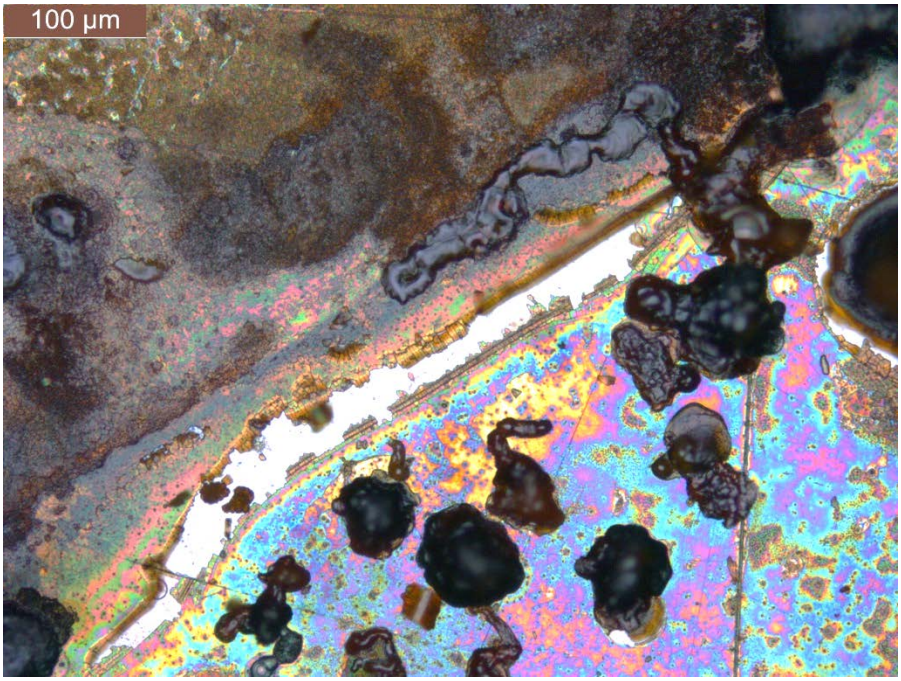

Figure 86: Detail optical microscope image of Section "A" of Capsule 5.

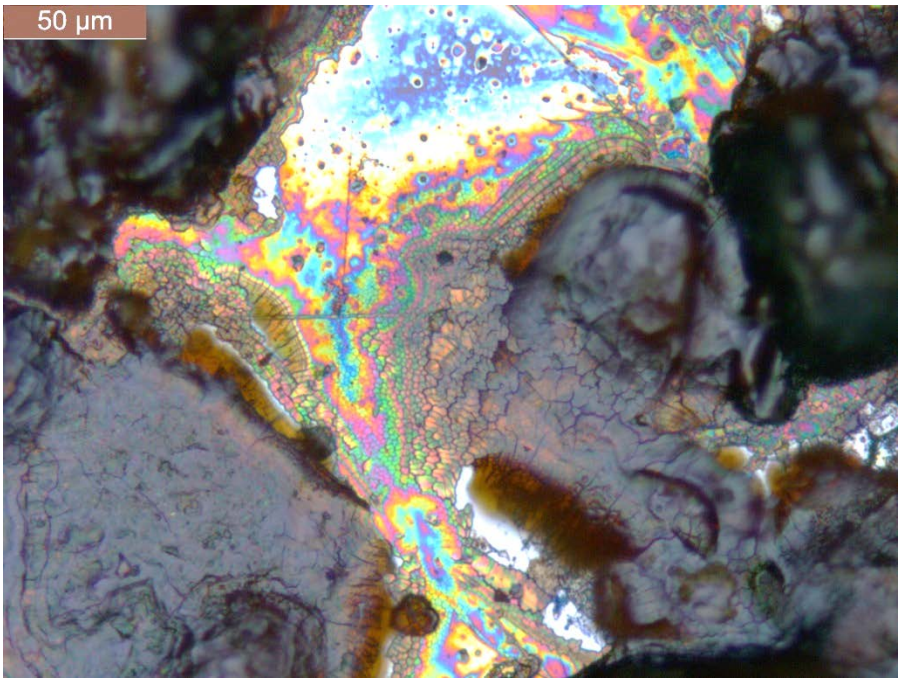

Figure 87: Detail optical microscope image of Section "A" of Capsule 5.

7.2 SEM Analysis

Figure 88 provides a guide to the locations of the Capsule 5 section that were examined by SEM. Figure 89 shows the cross section of the capsule wall at 50× and at 150× image of the interior surface to the capsule wall. This image appears to show what is suspected to be film layers and extensive pitting. Figure 90 show the EDS elemental map for the higher resolution image. There appears to be some iron oxide extending well beyond the surface of the capsule wall. There are also areas that show the coincident presence of Si, Al, Na, Ca (not shown in figure) and Kr. A small localized area containing Pb is also noted. Figure 91 is the annotated EDS layered image of the same location showing the areas at which individual elemental spectra were produced. These individual spectra are shown in Figure 92. The spectra in Figure 92A shows an iron oxide layer. The O:Fe ratio is ~2. Next to this layer is an interface layer (Figure 92B) with an O:Fe ratio of ~1. Figure 92C also contains iron oxide with an O:Fe ratio ~2. Figure 92D has spectra that show the coincident presence of Si, Al, Na, Ca (not shown in figure) and Kr. Figures 92E and 92F show the base metal in the wall. The absence of Cr and Ni would indicate that the capsule wall is likely to have been carbon steel as was the case for Capsule 2.

Figure 93 shows the cross section of the capsule wall in area 6 at 50× and at 150×. This area also appears to have portions of the zeolite material still attached. Figure 94 show the EDS elemental map for the higher resolution image associated with Figure 93. Of interest here was the interface and what appears to be an oxide film layer that have both detached from the surface of the wall, and a second oxide layer below. Figure 95 is the annotated EDS layered image of the same location showing the areas at which individual elemental spectra were produced. These individual spectra are shown in Figure 96. The spectra in Figures 96A and 96B show mainly iron and oxygen present with an O:Fe ratio of ~2. There may be traces of Al and Si in Figure 96A, but these are in the 0.1 at. % levels. Figure 96C shows the EDS spectra for what appears to be a detached oxide layer. This layer has an O:Fe ratio of ~1. The spectra in Figure 96D is consistent with the 5A MS composition.

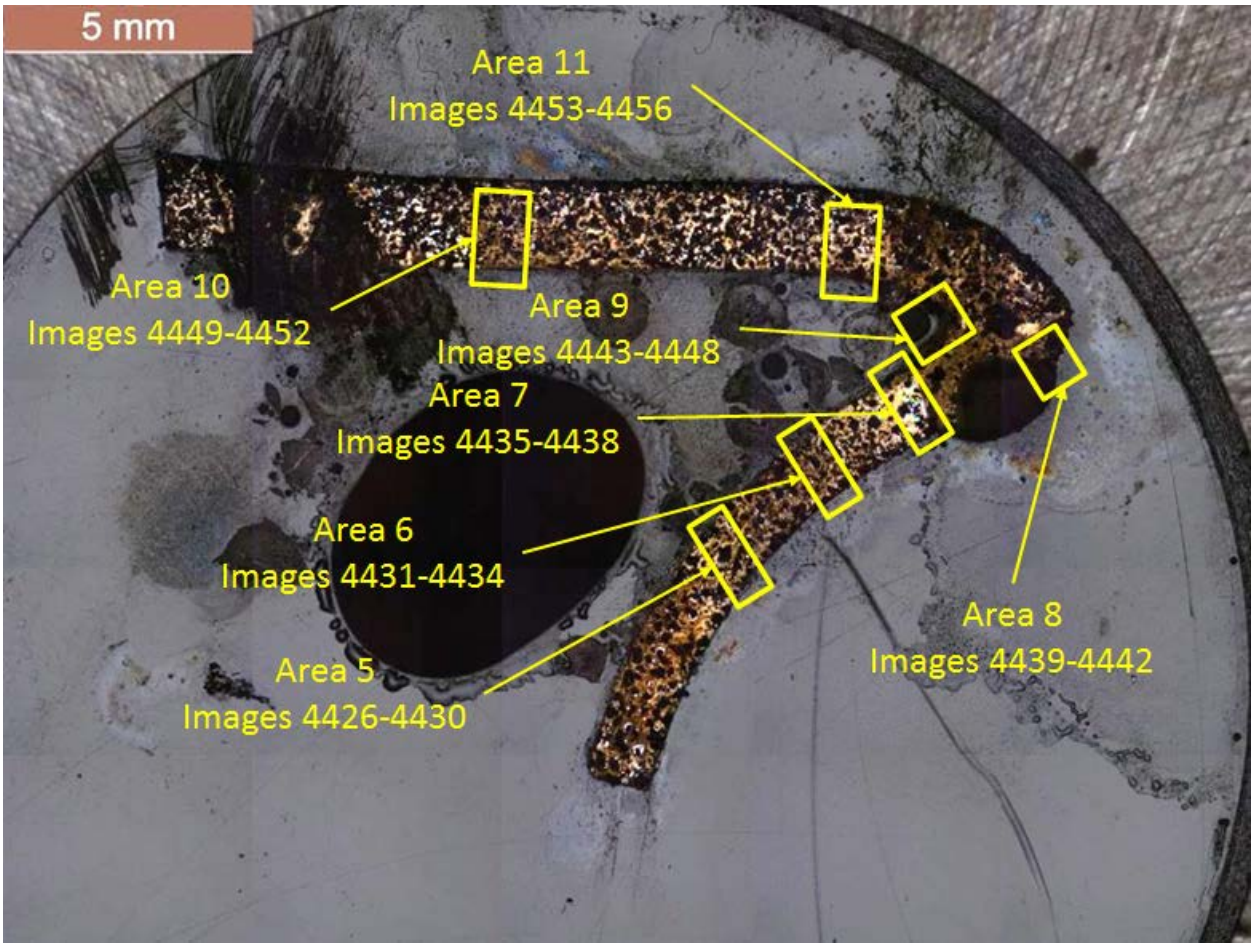

Figure 88: Annotated optical microscope image of Section "A" of Capsule 5 showing locations that were examined by SEM (Image MM5A2-0MS-001).

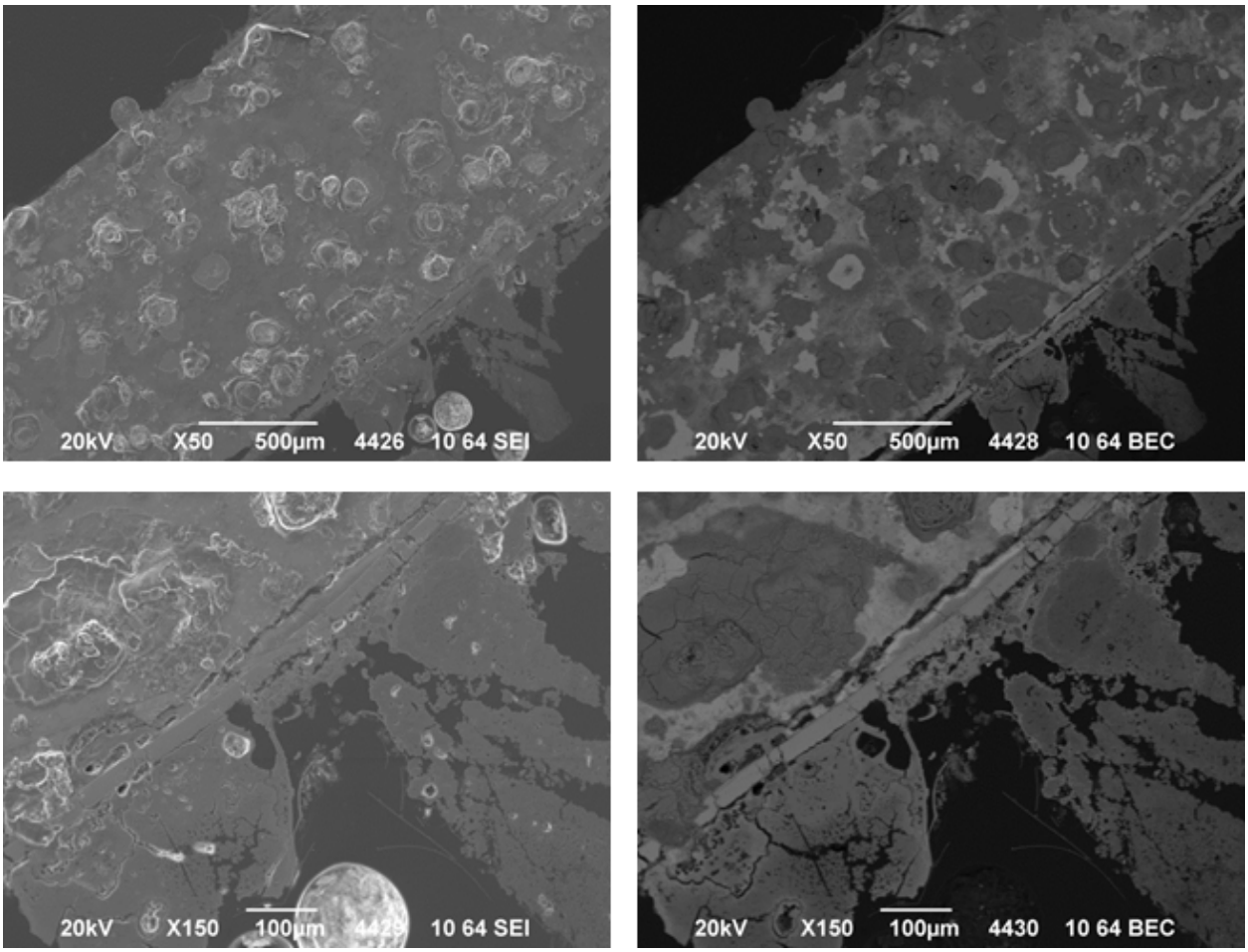

Figure 89: Detailed images of the wall of Capsule 5 at 50× to 200× magnification at location 5. SEI images on the left and BEC images on the right (Images 4426–4429) [Sample 5AB2].

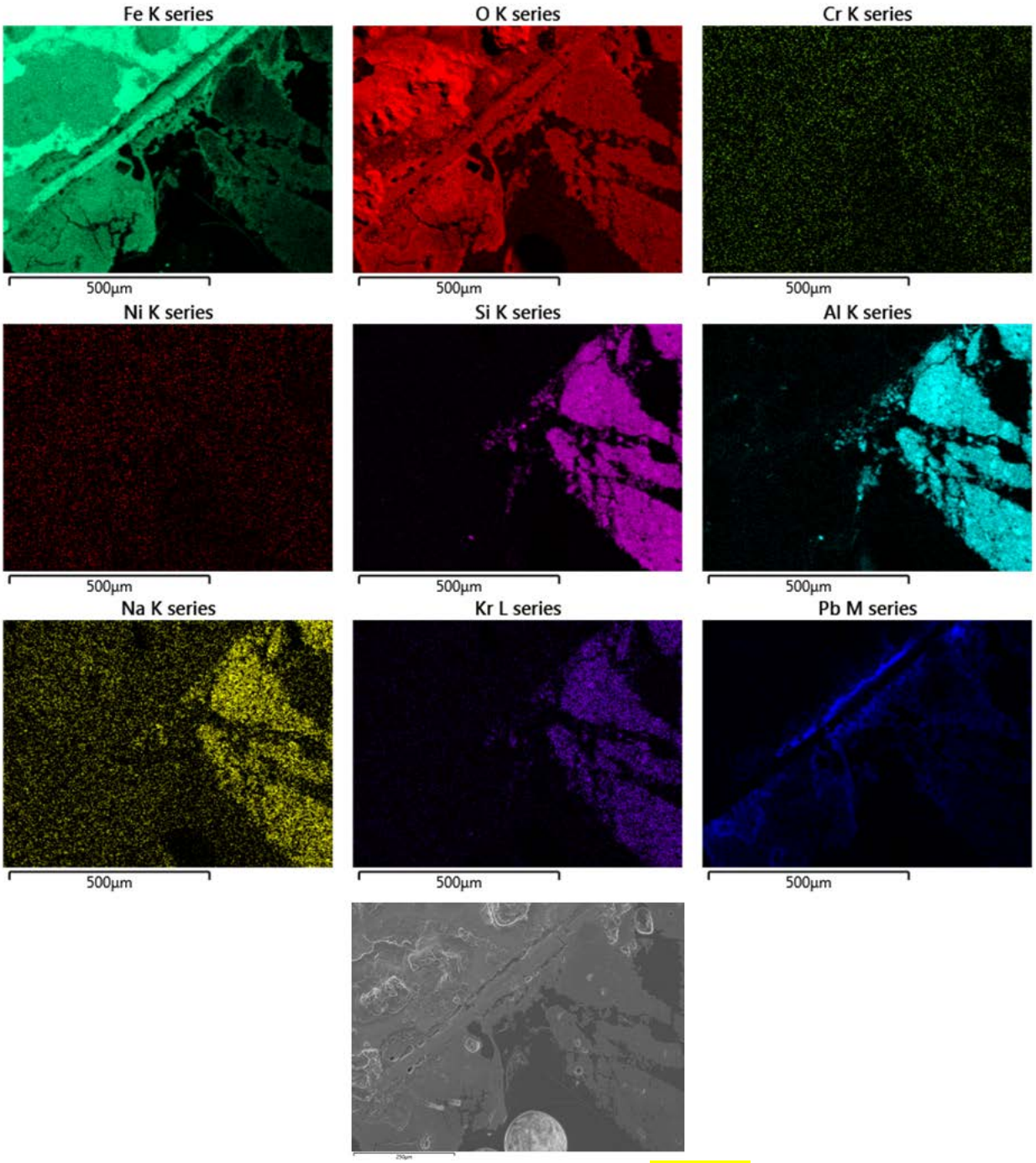

Figure 90: Elemental maps of area shown in bottom images of Figure 89 for area 5 of the wall segment from Capsule 5 [Sample 5A2].

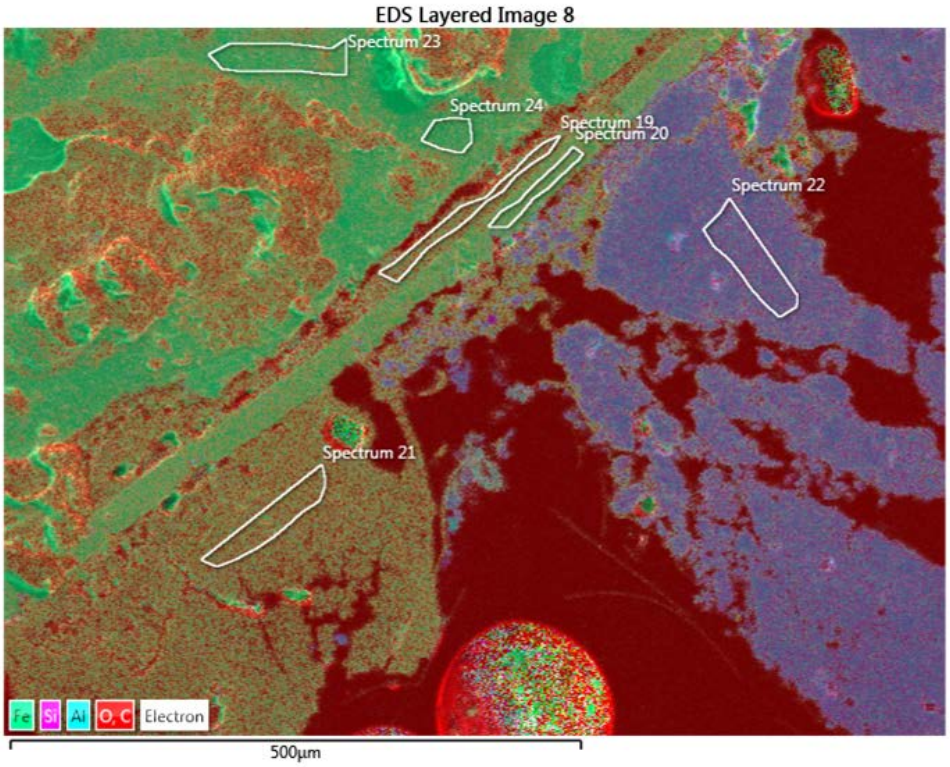

Figure 91: EDS layer image for bottom images of Figure 89 for area 5 of the wall segment from Capsule 5. Sub-areas for localized spectral analysis are annotated [Sample 5A2].

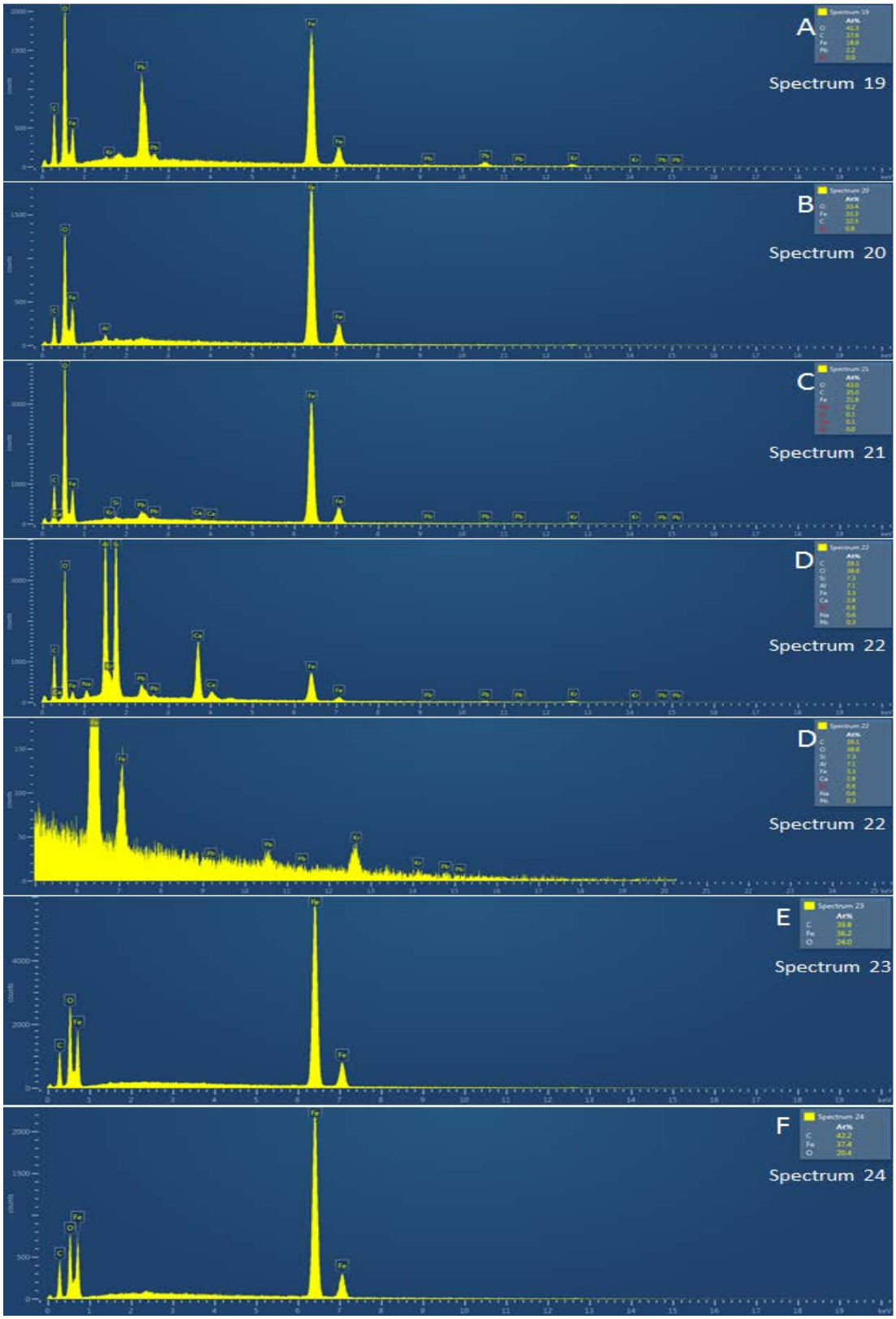

Figure 92: SEM-EDS spectra for the six sub-areas of the Capsule 5 wall segment shown in Figure 91 [Sample 5A2].

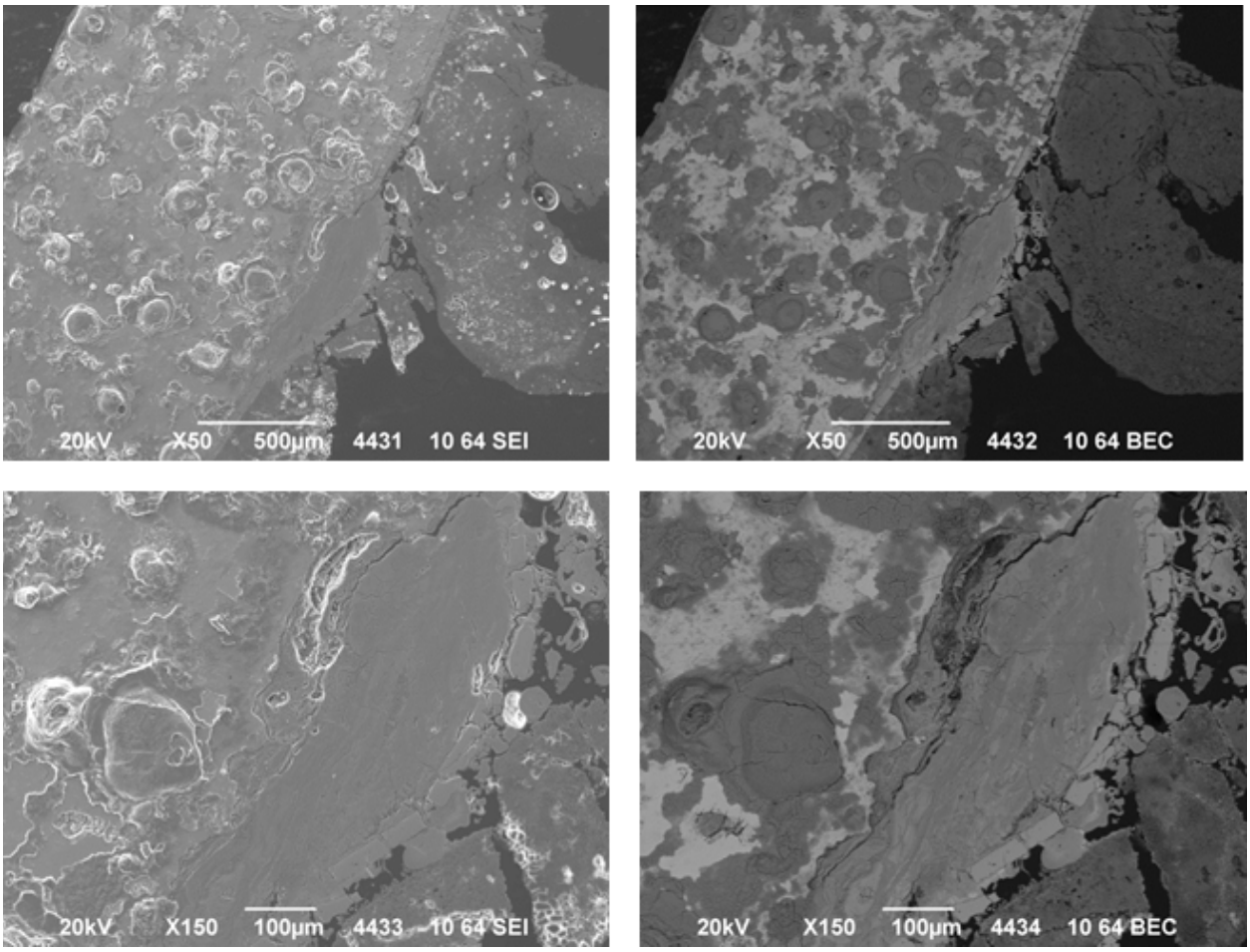

Figure 93: Detailed images of the wall of Capsule 5 at 50× to 150× magnification at location 6. SEI images on the left and BEC images on the right (Images 4431–4434) [Sample 5A2].

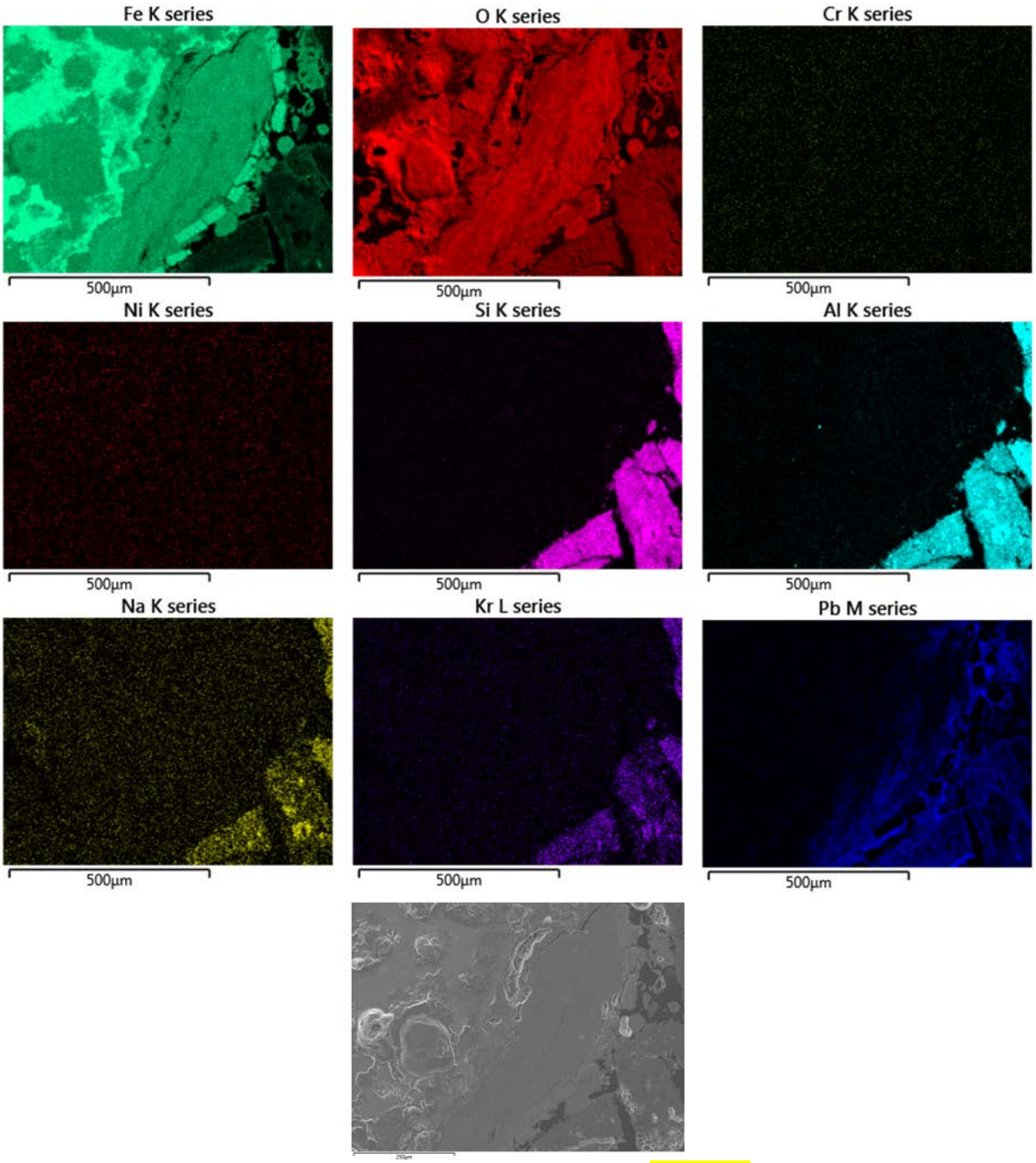

Figure 94: Elemental maps of area shown in bottom images of Figure 93 for area 6 of the wall segment from Capsule 5 [Sample 5A2].

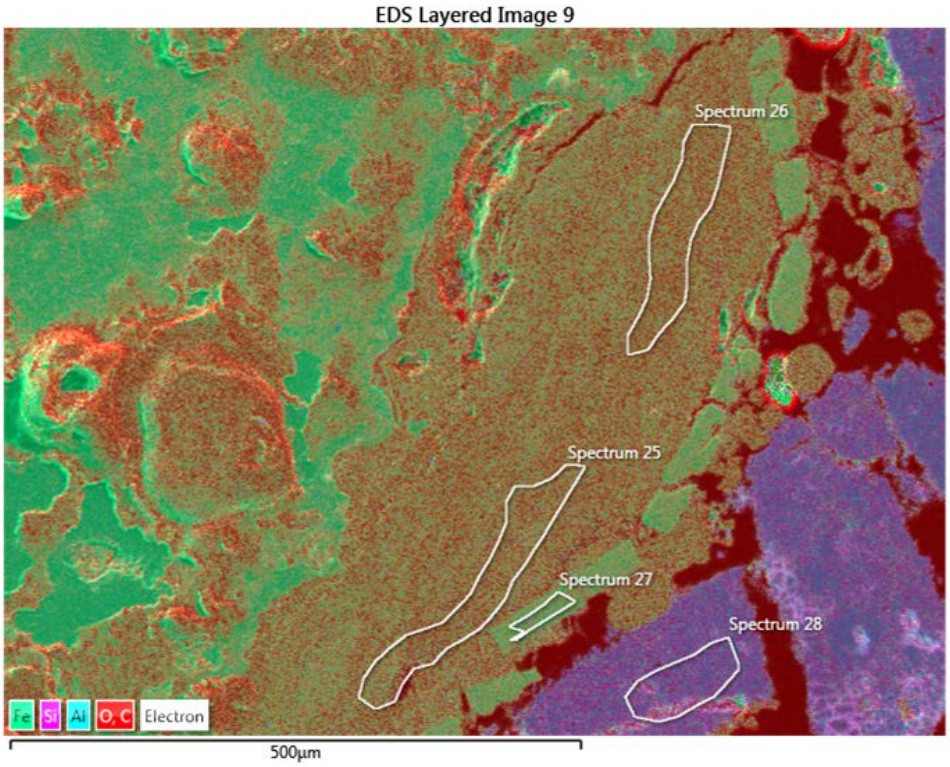

Figure 95: EDS layer image for bottom images of Figure 93 for area 6 of the wall segment from Capsule 5. Sub-areas for localized spectral analysis are annotated [Sample 5A2].

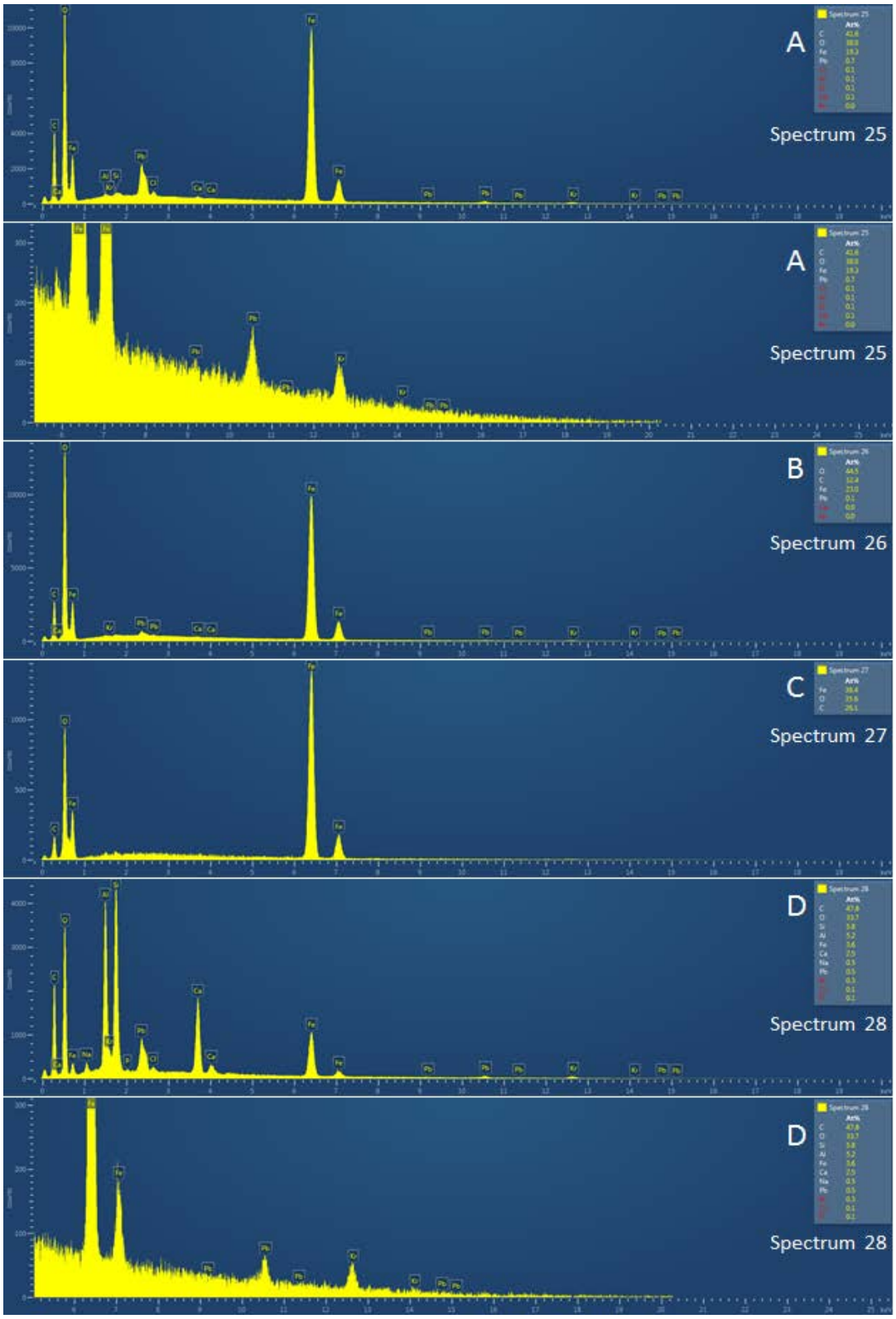

Figure 96. SEM-EDS spectra for the four sub-areas of the Capsule 5 wall segment shown in Figure 95 [Sample 5A2].

Figure 97 shows the cross section of the capsule wall in area 7 at 50× and a 150×. This area appears to be a weld. Figure 98 show the EDS elemental map for the higher resolution image associated with Figure 97. Of note is the clear line separating the region containing Cr and, to a lesser degree, Ni from the carbon steel areas. Figure 99 is the annotated EDS layered image of the same location showing the areas at which individual elemental spectra were produced. These individual spectra are shown in Figure 100. The spectra for the weld metal, weld interface and base metal are shown in Figures 100A, 100B and 100C, respectively.

Figure 101 shows a large weld area on the corner of the sample (area 8) at 50× and at 200×. Figure 102 focuses on an area located in just about the area shown in the lower resolution images in Figure 101. This appears to be an interface area with some interesting features in the weld metal. Figure 103 shows the EDS elemental map of the same area shown in Figure 102. Note that only a portion of the area showing the presence of iron also shows the presence of Cr and Ni. Also note the area of very high Cr concentrations. Figure 104 is the annotated EDS layered image of the same location showing the areas at which individual elemental spectra were produced. These individual spectra are shown in Figure 105. All four spectra are fairly similar. The ratio of Cr:Ni in Figures 105A, 105C, and 105D is ~3. For Figure 105B, the ratio is ~5.

Figure 106 shows an interior corner the weld site (area 9) at 50× and at 150×. This area appears to contain some zeolite material, as well as several interesting material layers. The EDS elemental map for the higher resolution images associated with middle row of images in Figure 106A is shown in Figure 107. This shows a region on the upper left that contains Cr, which is associated with the weld metal. Figure 108 shows the annotated EDS layered image of the same location showing the areas at which individual elemental spectra were produced. Figure 108A shows an area near the wall that is composed of a small amount of Al and Fe. This is most likely a void area in the sample. The spectra in Figure 108B shows both Fe and the constituents of the zeolite material. The spectra shown in Figure 108C show Fe and O. The ratio of O:Fe is ~1.5. The spectra shown in Figure 108D also most likely associated with a void in the sample. The EDS elemental map for the higher resolution images associated with the bottom row of images in Figure 106B is shown in Figure 110. This shows a region in the center that contains Fe. The Fe appears to bridge over to what is thought to be a portion of zeolite material. The upper left portion of the image shows a region that contains Fe but no Cr. Figure 111 is the annotated EDS layered image of the same location showing the areas at which individual elemental spectra were produced. Figure 112A is the region that is thought to contain zeolite material. The spectra shown are consistent with the constituents in 5A MS. The spectra in Figure 112B show both Fe and a small amount of the constituents of the zeolite material. The spectra shown in Figures 112C and 112D are consistent with the constituents of the zeolite material. The spectra in Figure 112E show mainly Fe and O. The ratio of O:Fe is ~1. The spectra shown in Figure 112F also show mainly Fe and O, but the O:Fe ratio is >2.

Figure 113 shows an interior wall section of Capsule 5 with a zeolite layer attached (area 10) at 50× and at 150×. Figure 114 shows the EDS elemental map for the higher resolution image associated with Figure 113. Of note is the clear line separating the region containing Al and Si from the regions containing Fe. Figure 115 shows the annotated EDS layered image of the same location showing the areas at which individual elemental spectra were produced. These individual spectra are shown in Figure 116. Figure 116A shows the spectra for what appears to be a granular area on the cross section of the capsule wall. This area contains both Fe and the constituents of the zeolite material. These later elements may have been transported during the polishing operations. The O:Fe ratio is ~3 in this region. Figure 116B shows the wall base metal. Figure 116C shows of the small portion of oxide layer between the zeolite and the capsule wall. The O:Fe ratio is ~1. Figure 116D shows spectra consistent with the 5A MS material.

Figure 117 also shows an interior wall section of Capsule 5 with zeolite material attached (area 10) at 50× and at 150×. Figure 118 shows the EDS elemental map for the higher resolution image associated with

Figure 117. Of note is the clear line separating the region containing Al and Si from the regions containing Fe. Figure 119 shows the annotated EDS layered image of the same location showing the areas at which individual elemental spectra were produced. These individual spectra are shown in Figure 120. Figure 120A shows spectra consistent with the 5A MS material. Figure 120B shows the zeolite wall interface area. The spectra contain all of the elements expected to be present in 5A MS, as well as some Fe. These are the only spectra in which Rb was potentially identified. However, that is not to say that it is not present in other cases, but at levels below the EDS detection limits. If the Kr levels, when observed, are relatively accurate (~0.7 at. %) then the expected Rb levels for this length of decay would be <0.1 at. %. Figure 120C shows a region that appears to be an oxide layer between the zeolite and the capsule wall. The O:Fe ratio is ~1. Figure 120D shows the wall base metal. The O:Fe ratio is ~0.5. Figure 120E shows a pit-like region in the capsule wall cross section. The O:Fe ratio is ~2.0.

Table 4 provides a summary of the compositional data derived from the EDS spectra for selected locations of the wall sample from Capsule 5.

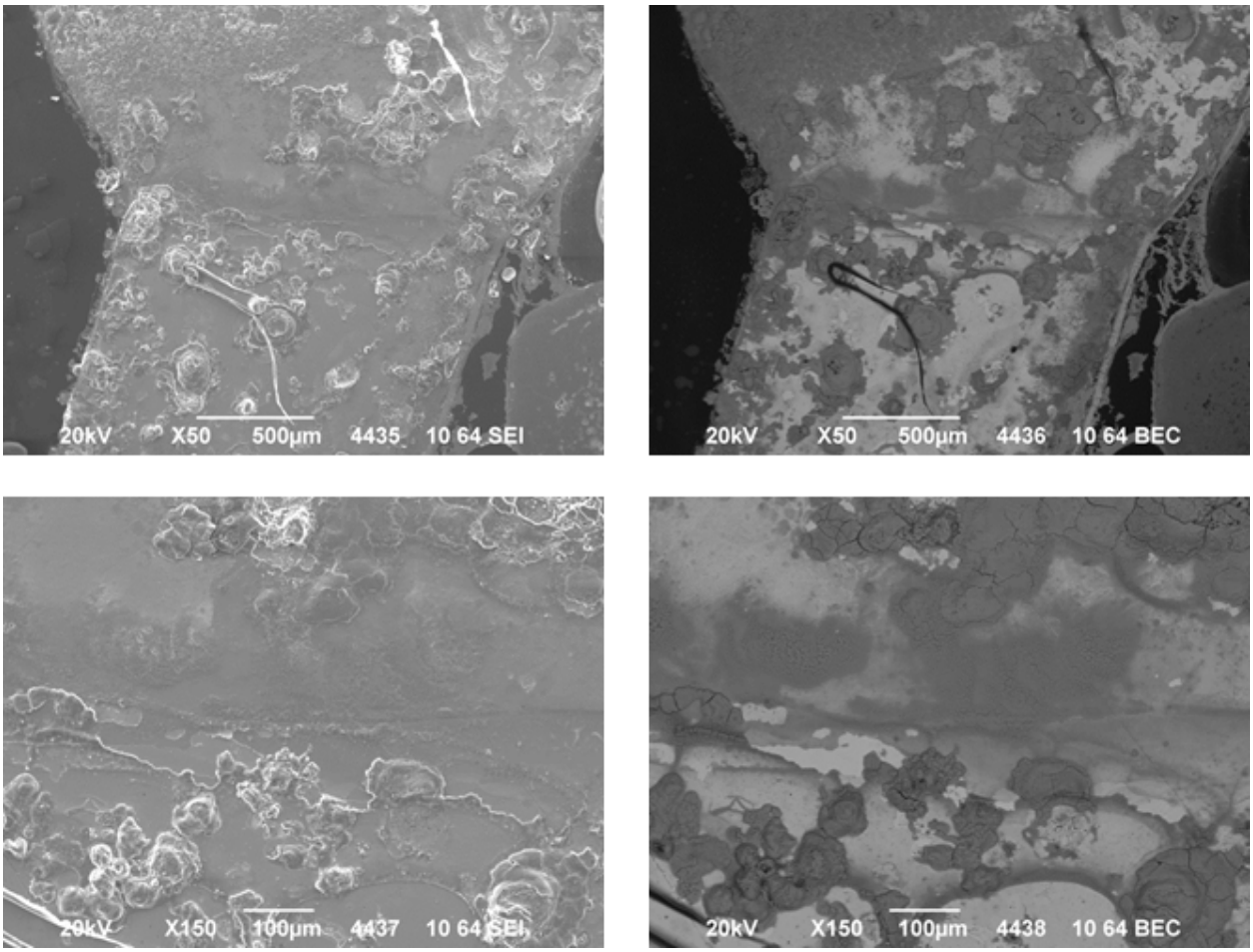

Figure 97: Detailed images of the wall of Capsule 5 at 50× to 150× magnification at location 7. SEI images on the left and BEC images on the right (Images 4435–4438) [Sample 5A2].

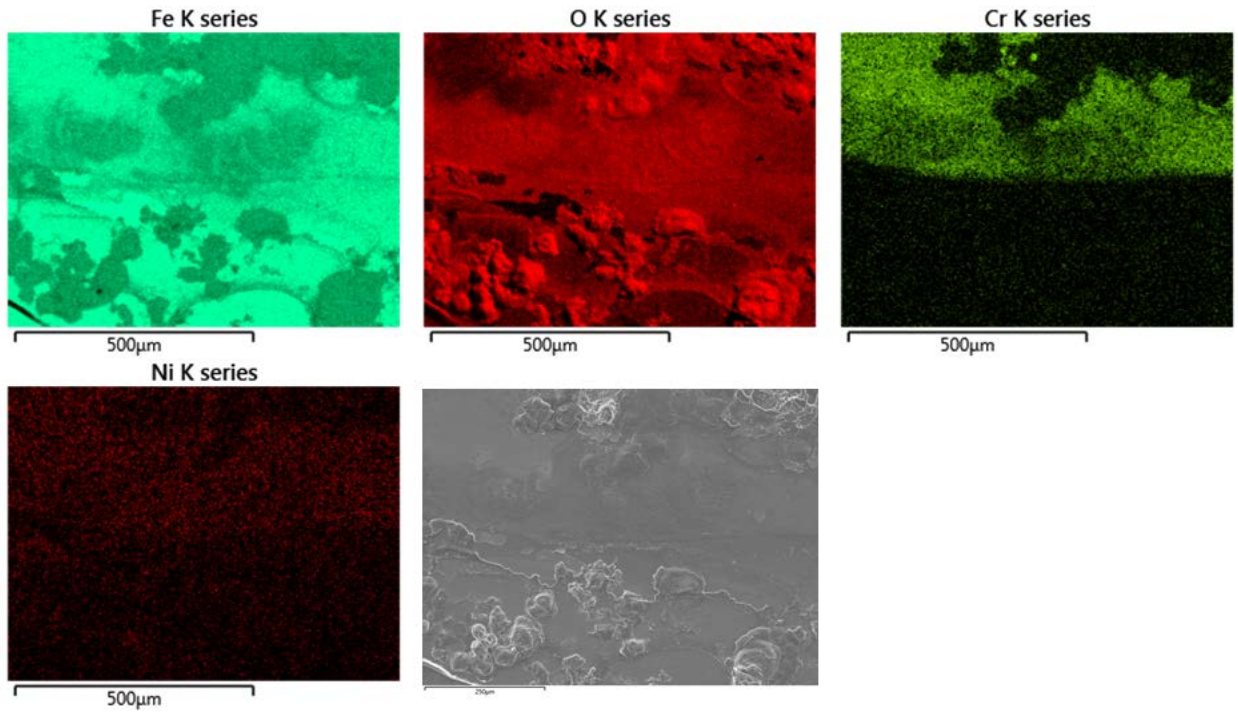

Figure 98: Elemental maps of area shown in bottom images of Figure 97 for area 7 of the wall segment from Capsule 7 [Sample 5A2].

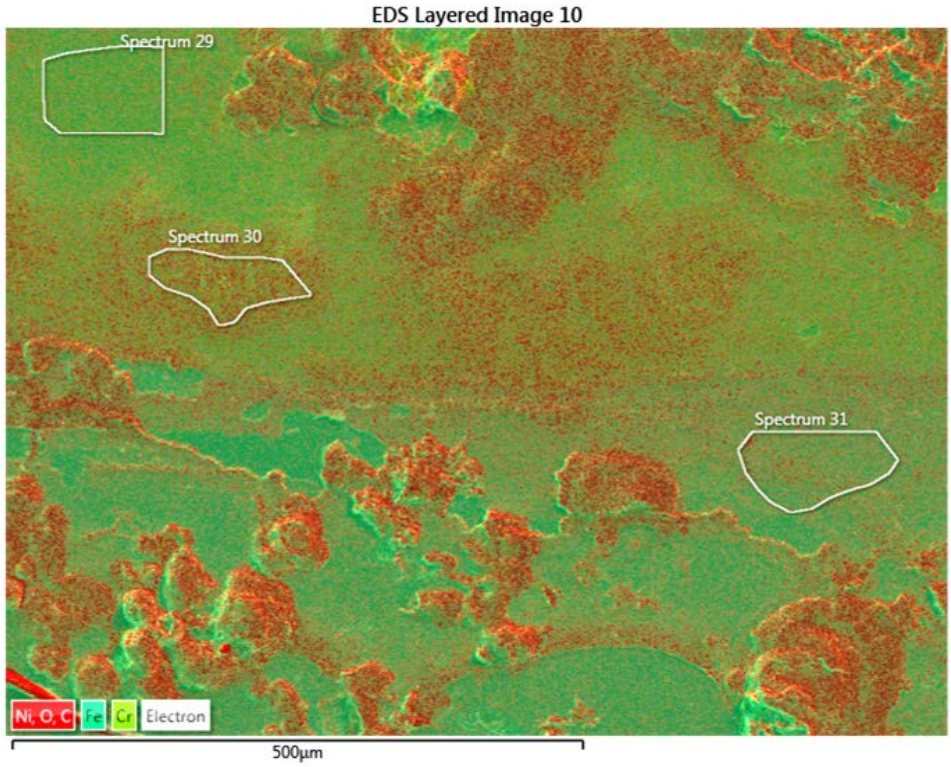

Figure 99: EDS layer image for bottom images of Figure 97 for area 7 of the wall segment from Capsule 5. Sub-areas for localized spectral analysis are annotated [Sample 5A2].

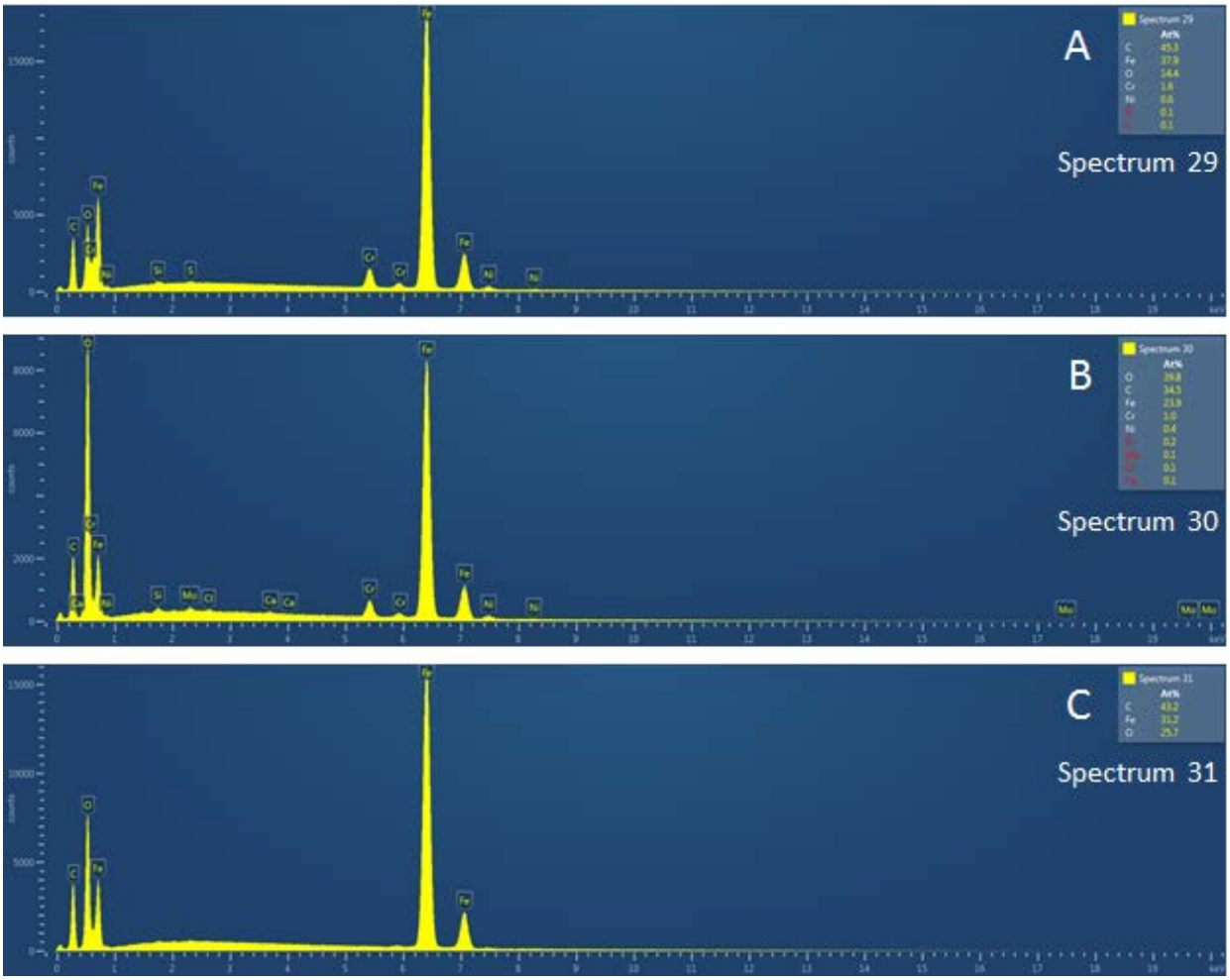

Figure 100: SEM-EDS spectra for the three sub-areas of the Capsule 5 wall segment shown in Figure 99 [Sample 5A2.].

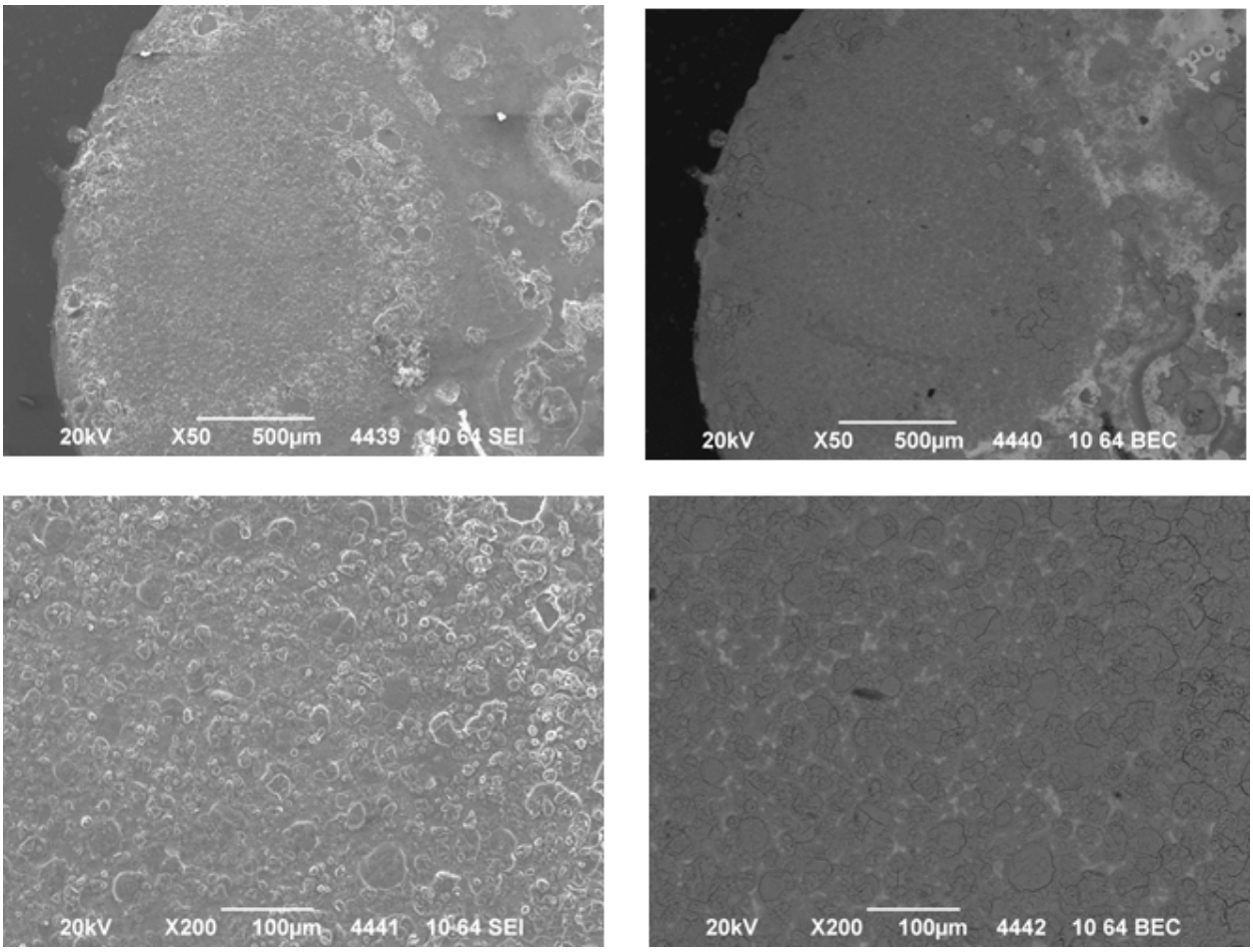

Figure 101: Detailed images of the wall of Capsule 5 at 50× to 200× magnification at location 8. SEI images on the left and BEC images on the right (Images 4439–4442) [Sample 5A2].

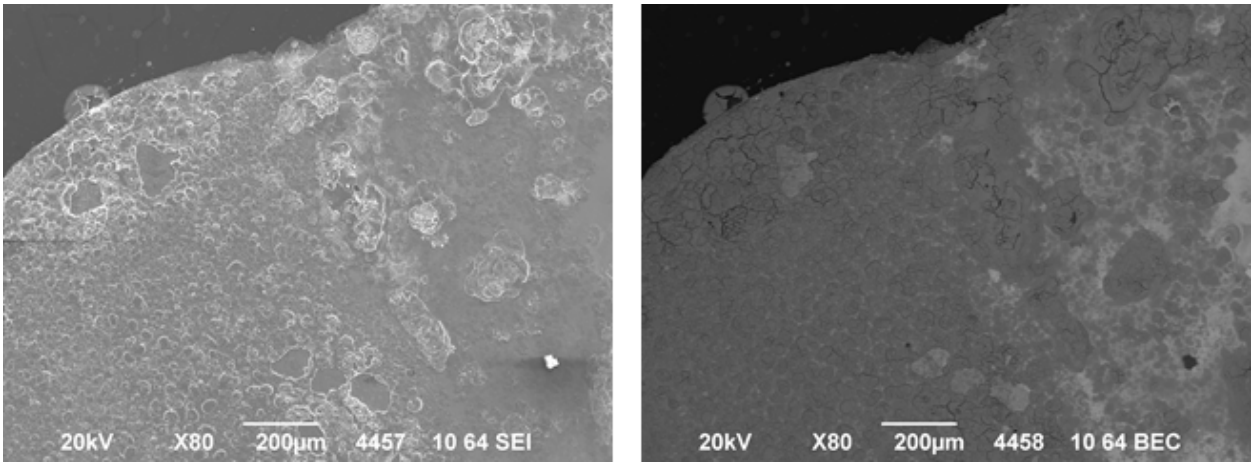

Figure 102: Detailed images of the wall of Capsule 5 at 50× to 200× magnification at location 8. SEI images on the left and BEC images on the right (Images 4457–4458) [Sample 5A2].

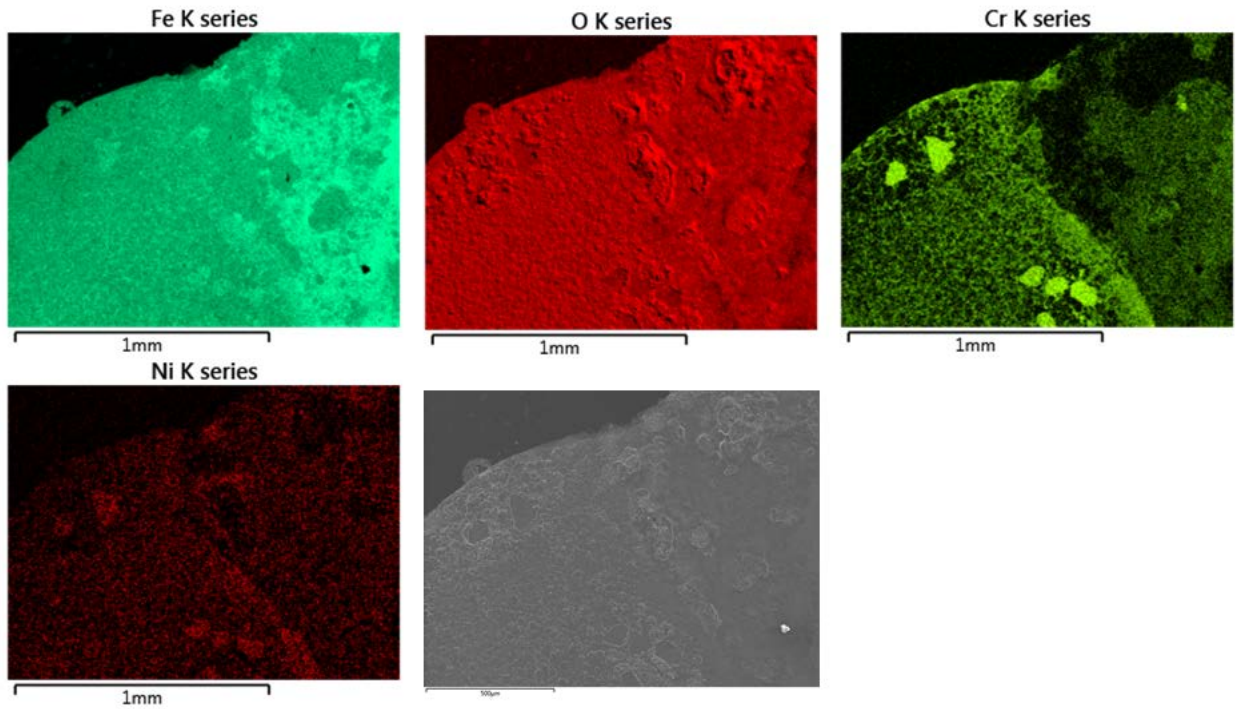

Figure 103: Elemental maps of area shown in middle images of Figure 102 for area 8 of the exterior surface of the wall segment from Capsule 5 [Sample 5A2].

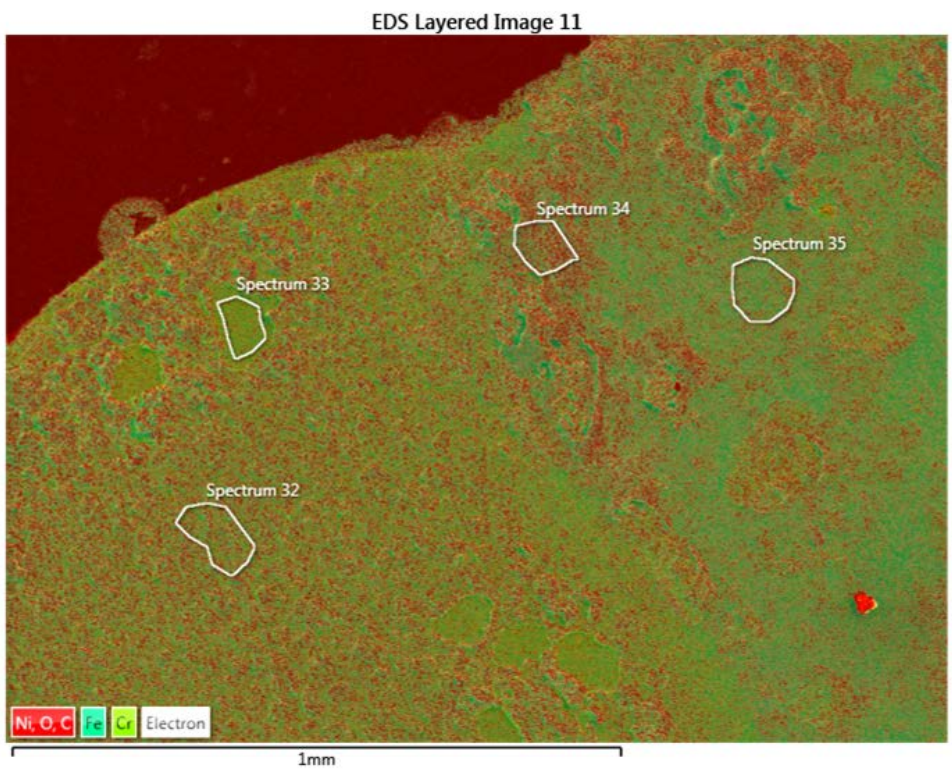

Figure 104: EDS layer image for bottom images of Figure 102 for area 8 of the wall segment from Capsule 5. Sub-areas for localized spectral analysis are annotated [Sample 5A2].

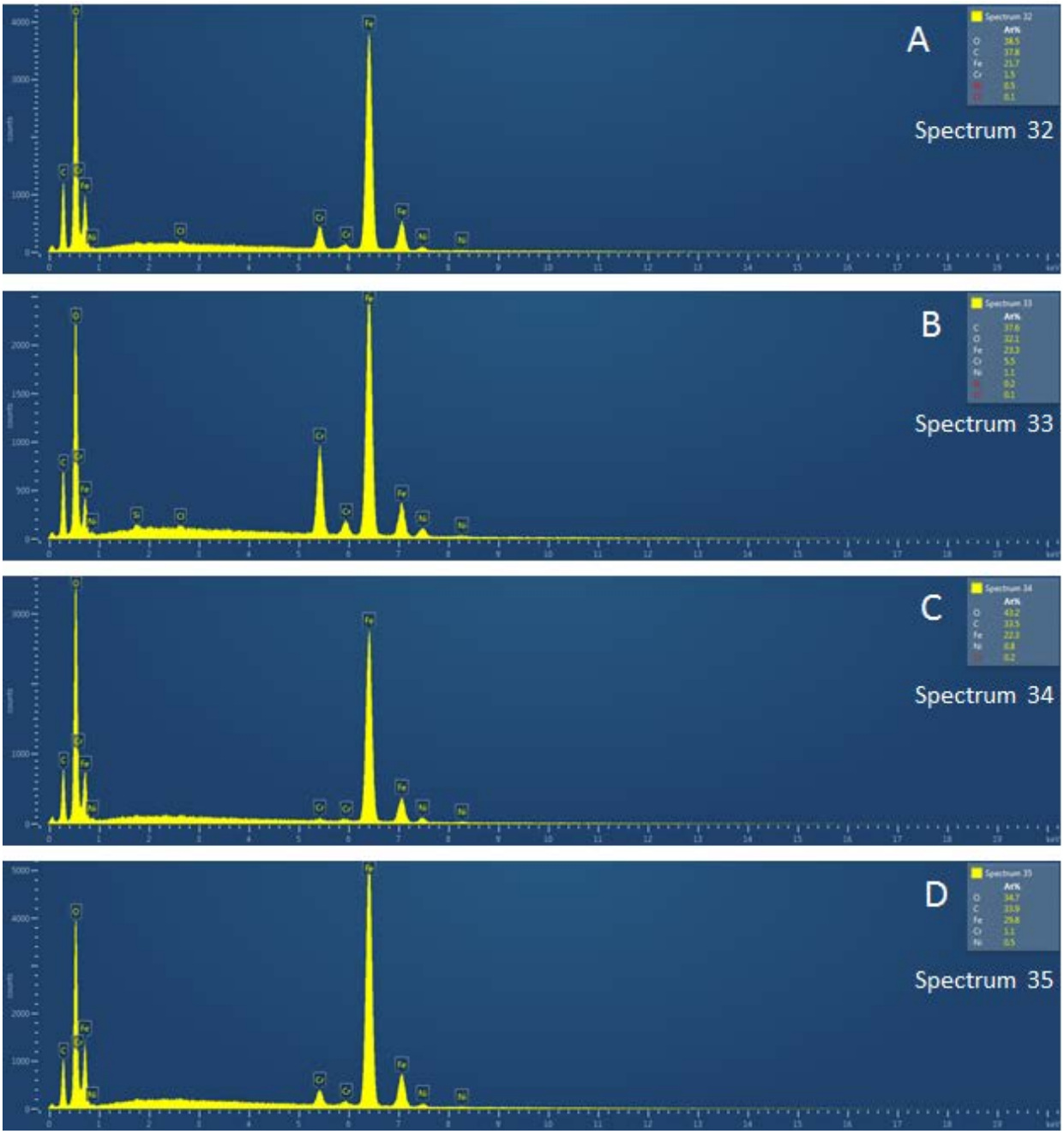

Figure 105: SEM-EDS spectra for the five sub-areas of the Capsule 5 wall segment shown in Figure 102 [Sample 5A2].

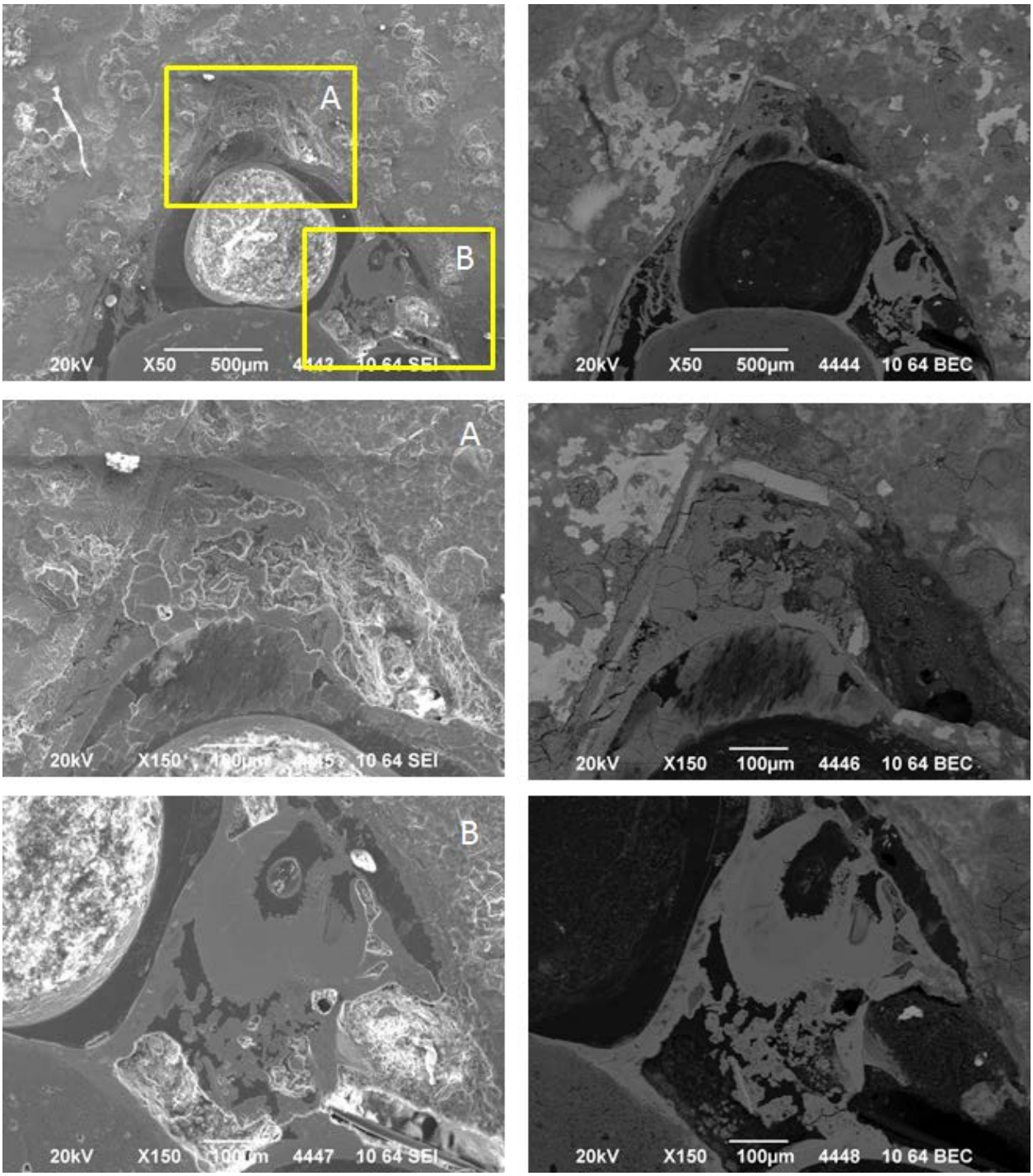

Figure 106: Detailed images of the wall of Capsule 5 at 50× to 150× magnification at location 9. SEI images on the left and BEC images on the right (Images 4443–4448) [Sample 5A2].

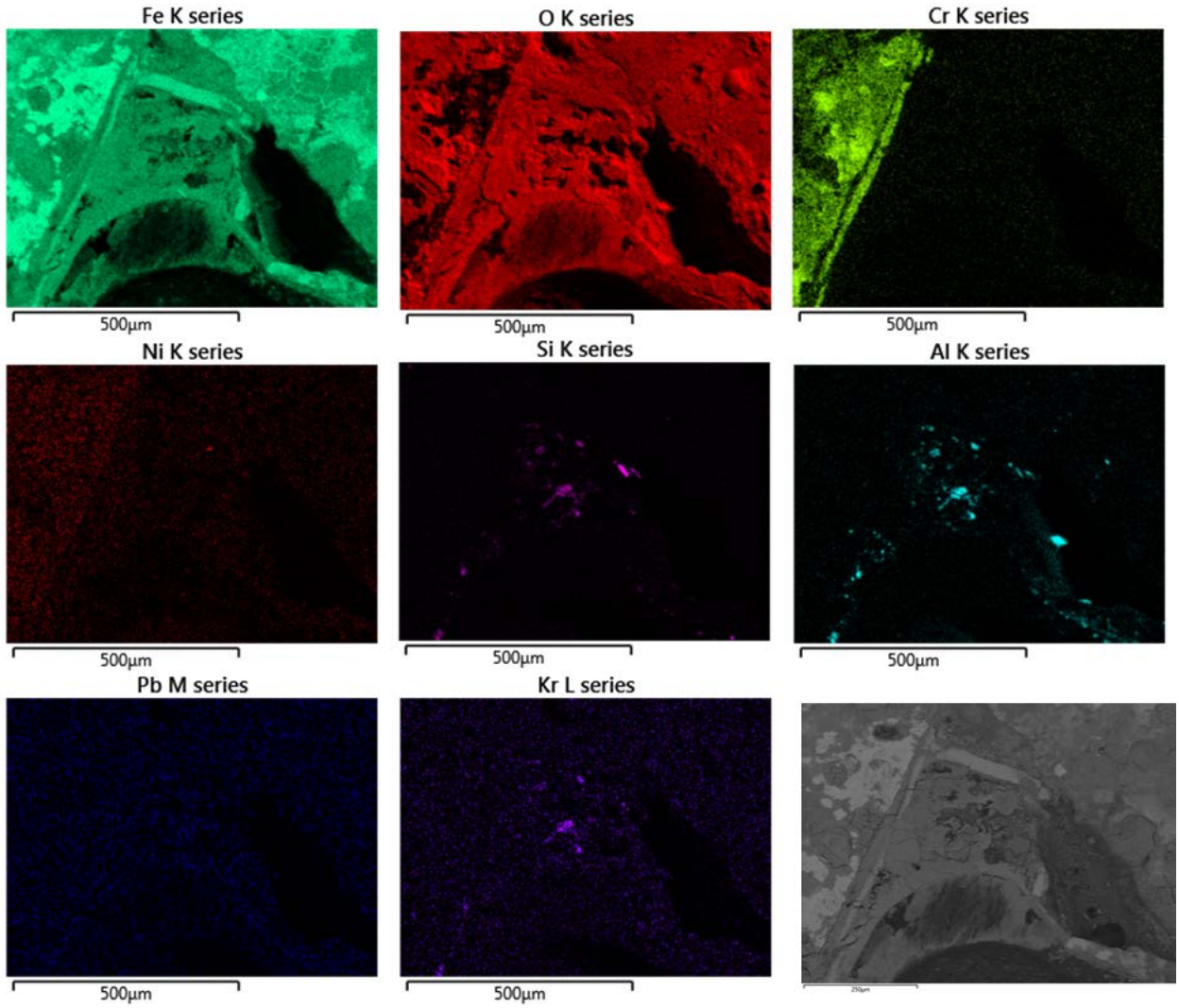

Figure 107: Elemental maps of area shown in middle images of Figure 106A for area 9 of the interior surface of the wall segment from Capsule 5 [Sample 5A2].

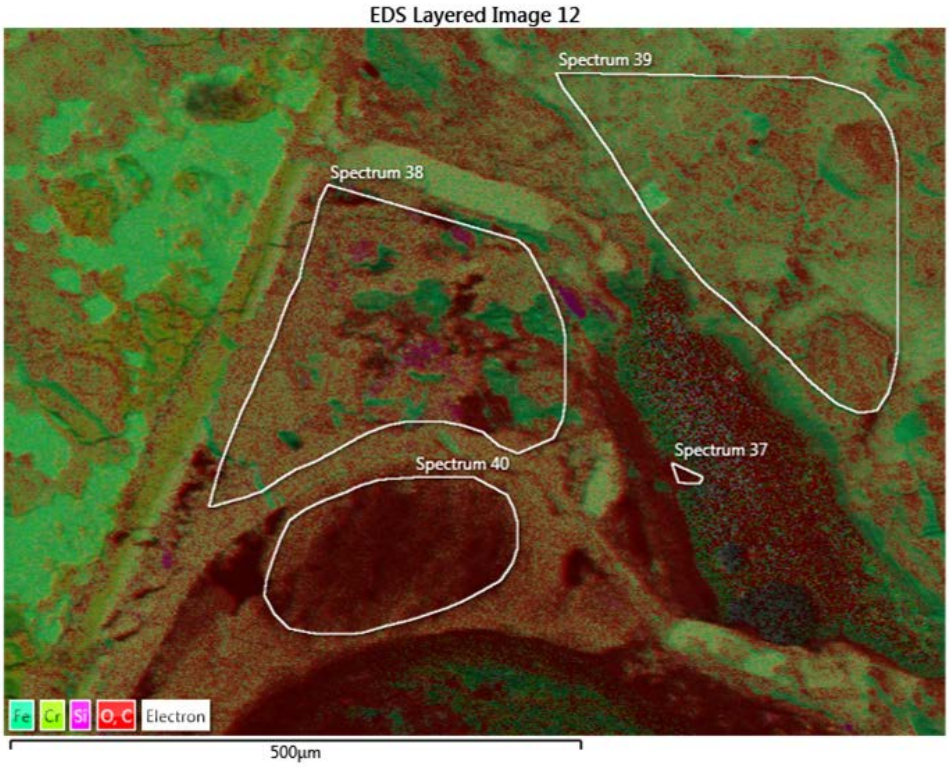

Figure 108: EDS layer image for middle images of Figure 106A for area 9 of the wall segment from Capsule 5. Sub-areas for localized spectral analysis are annotated [Sample 5A2].

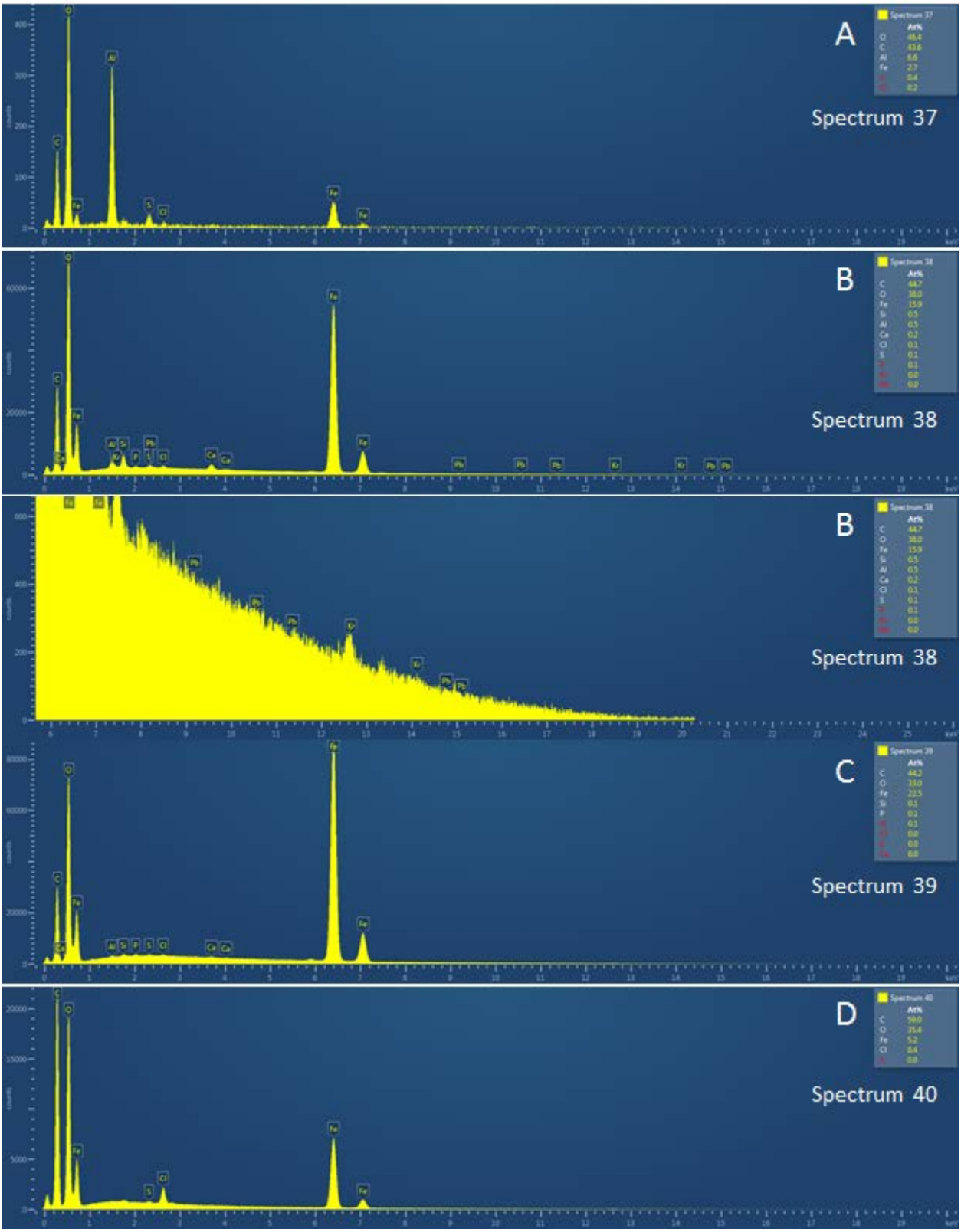

Figure 109: SEM-EDS spectra for the four sub-areas of the Capsule 5 wall segment shown in Figure 108 [Sample 5A2].

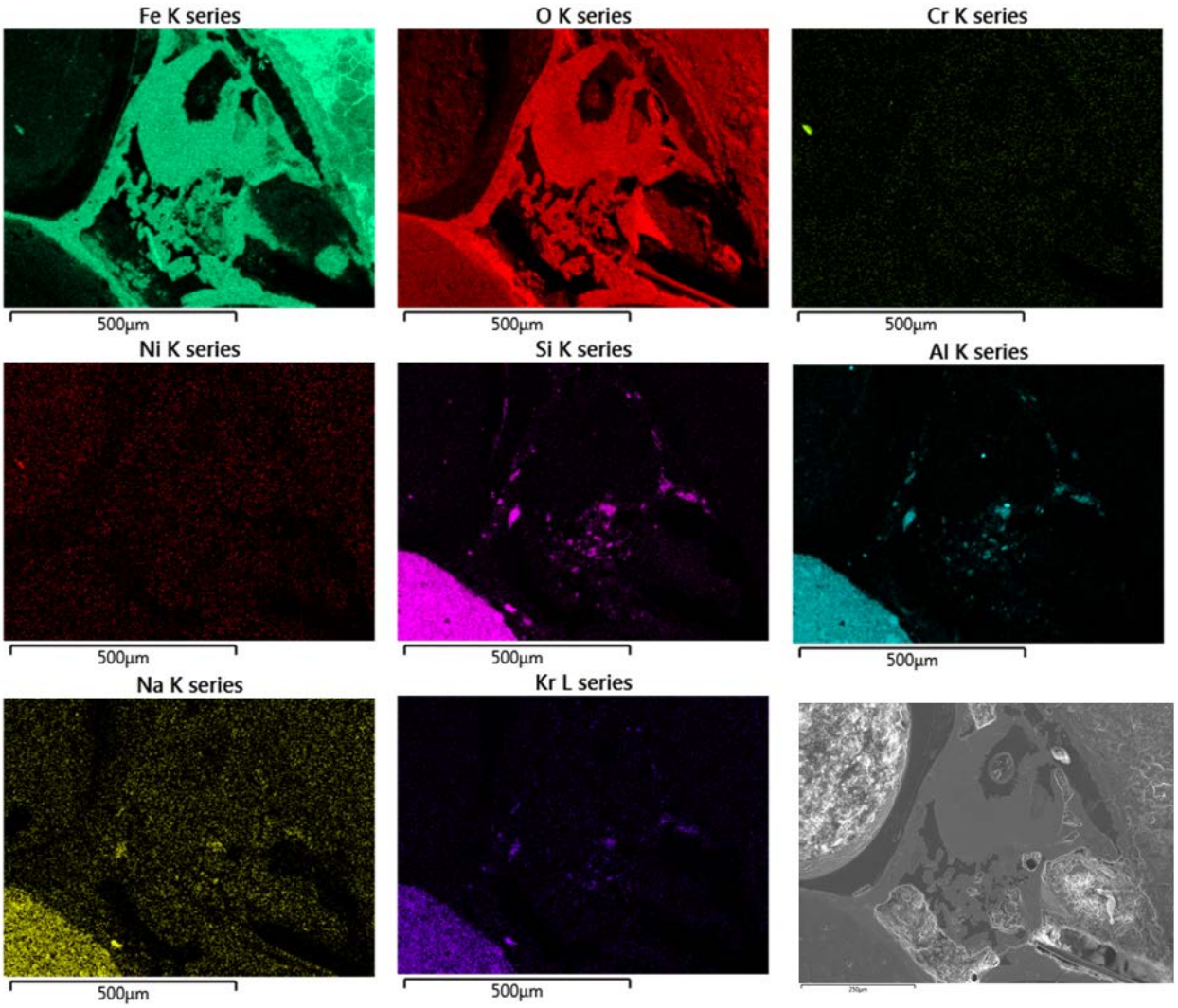

Figure 110: Elemental maps of area shown in bottom images of Figure 106B for area 9 of the exterior surface of the wall segment from Capsule 5 [Sample 5A2].

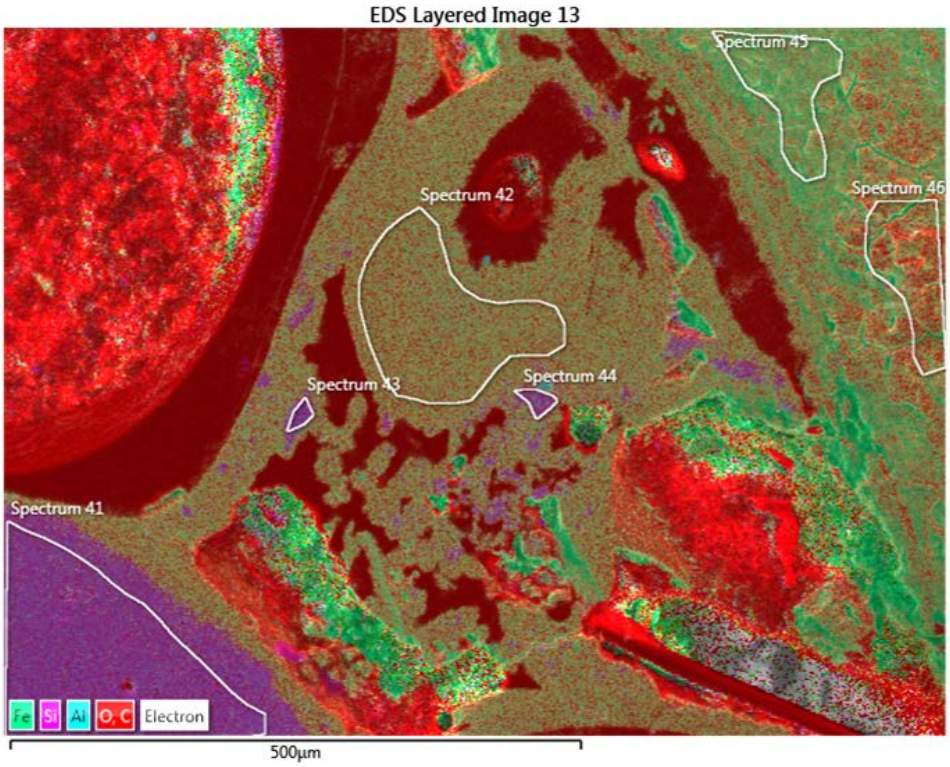

Figure 111: EDS layer image for bottom images of Figure 106B for area 9 of the wall segment from Capsule 5. Sub-areas for localized spectral analysis are annotated [Sample 5A2].

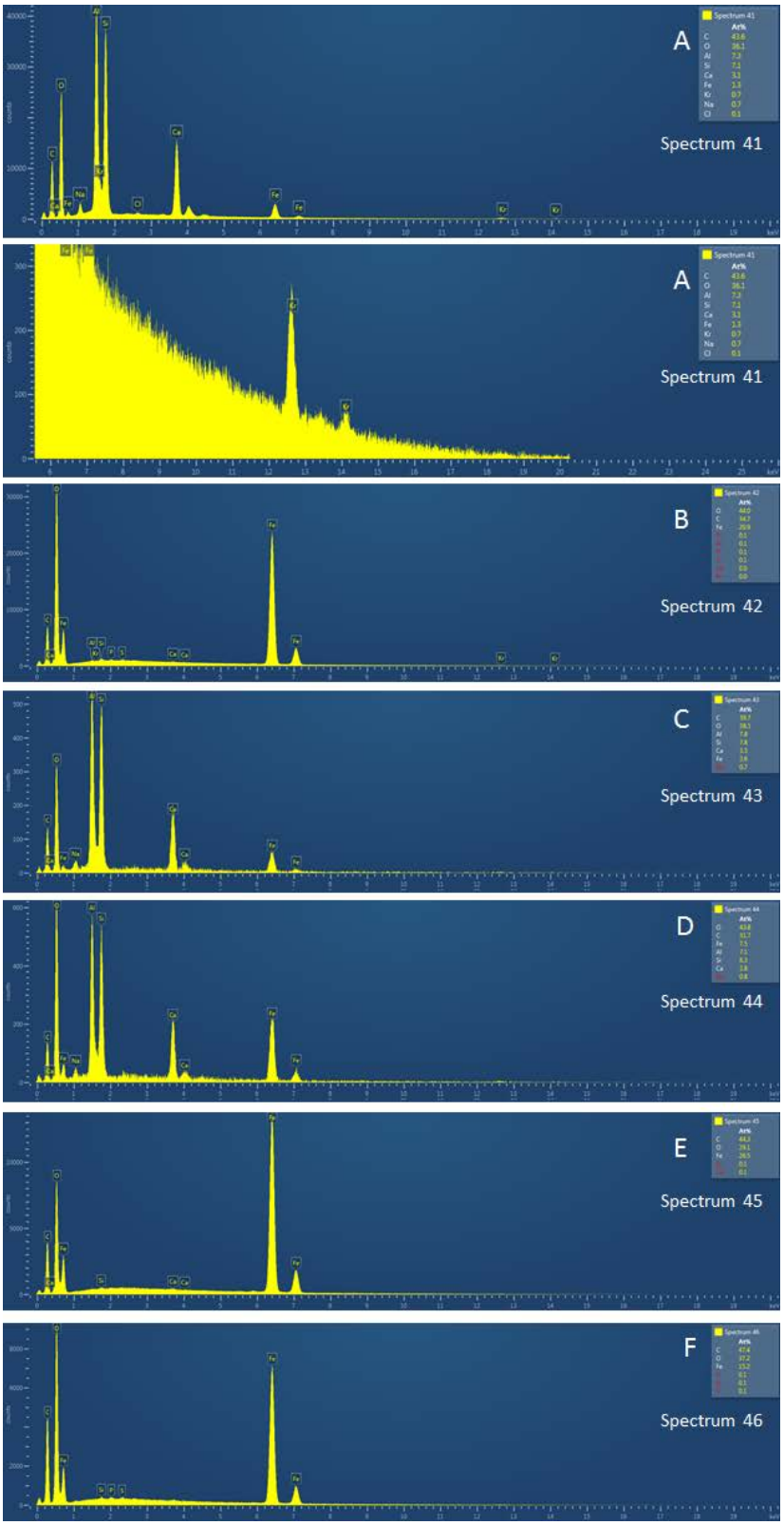

Figure 112: SEM-EDS spectra for the six sub-areas of the Capsule 5 wall segment shown in Figure 111 [Sample 5A2].

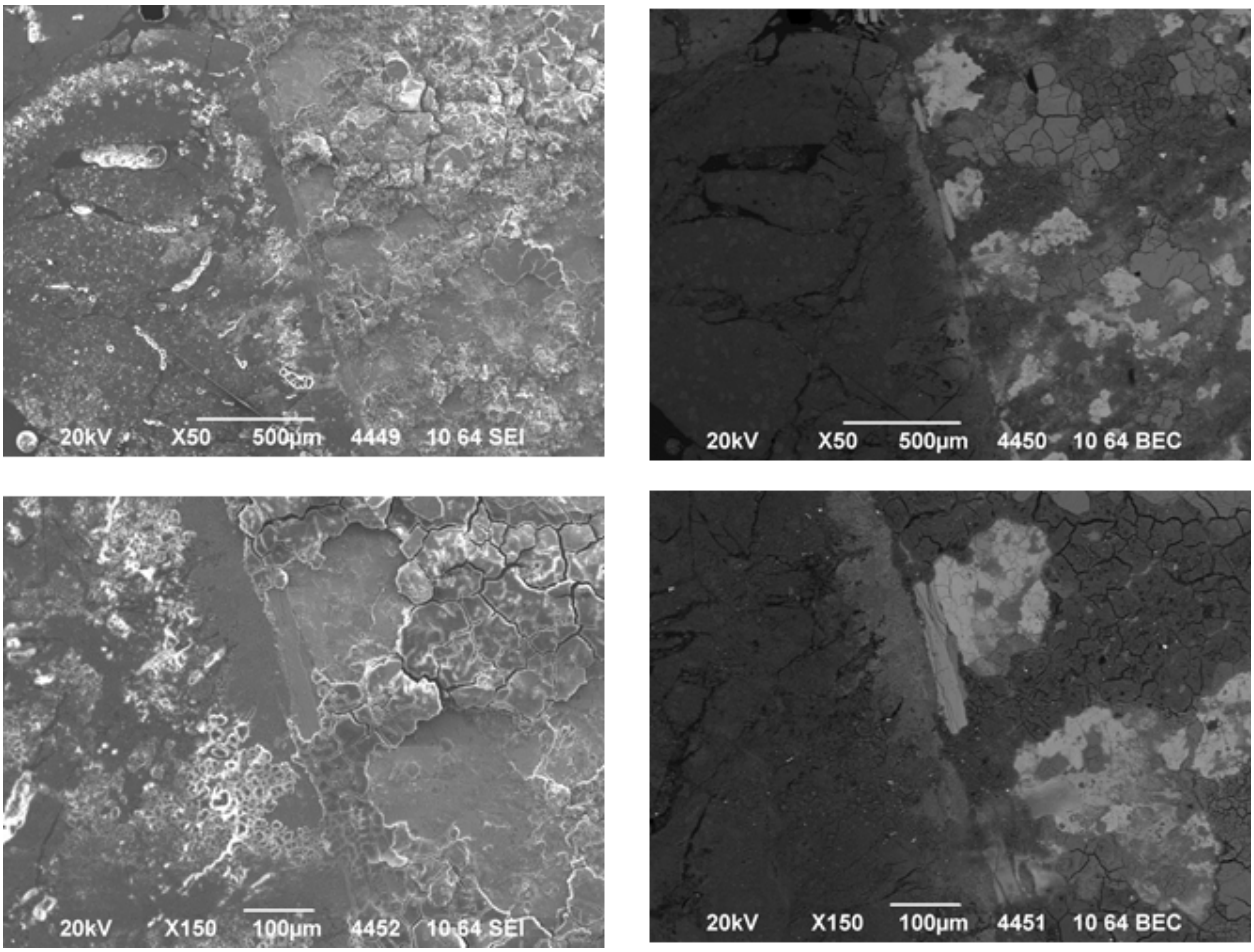

Figure 113: Detailed images of the wall of Capsule 5 at 50× to 150× magnification at location 10. SEI images on the left and BEC images on the right (Images 4449–4451) [Sample 5A2].

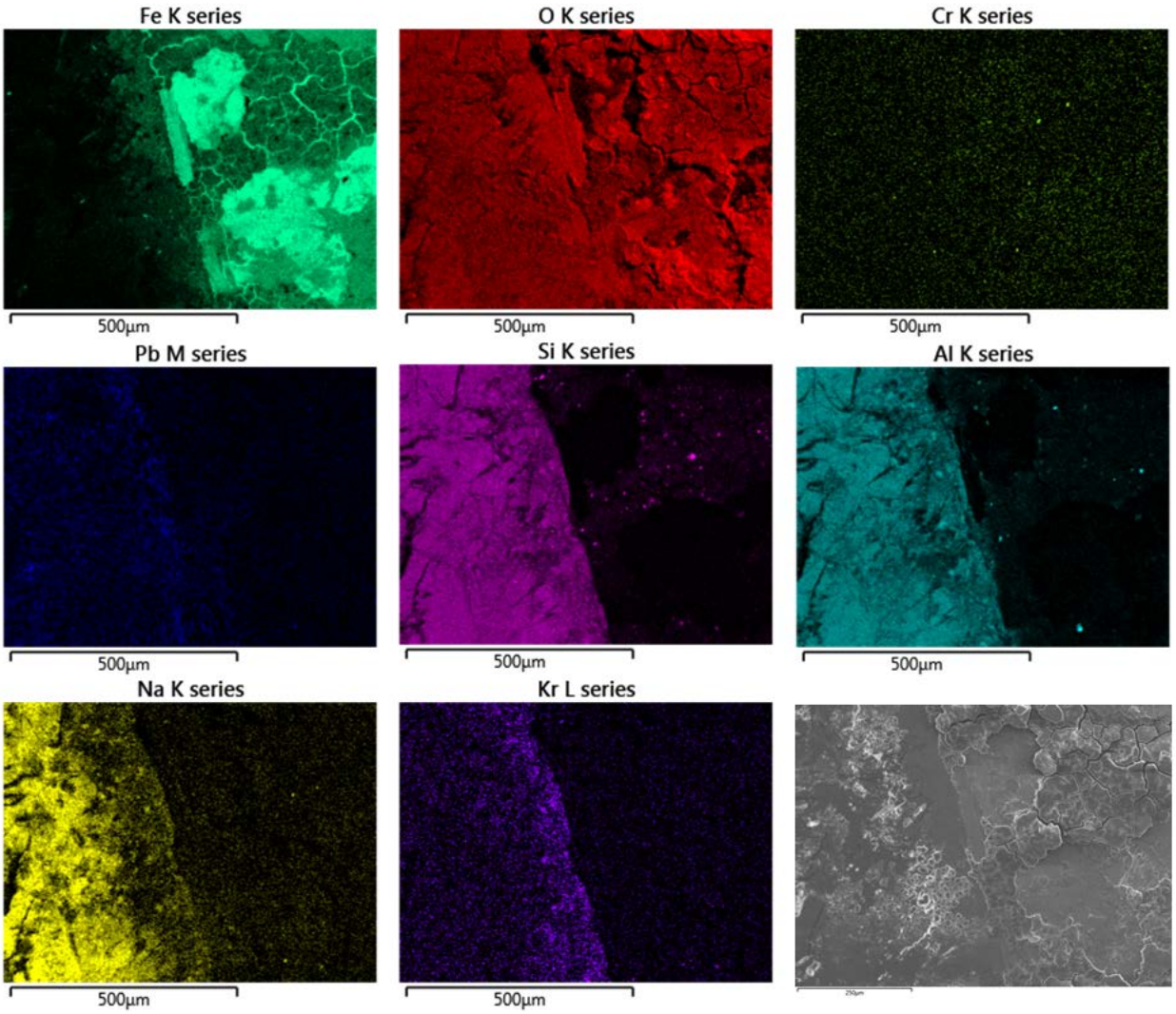

Figure 114: Elemental maps of area shown in bottom images of Figure 113 for area 10 of the exterior surface of the wall segment from Capsule 5 [Sample 5A2].

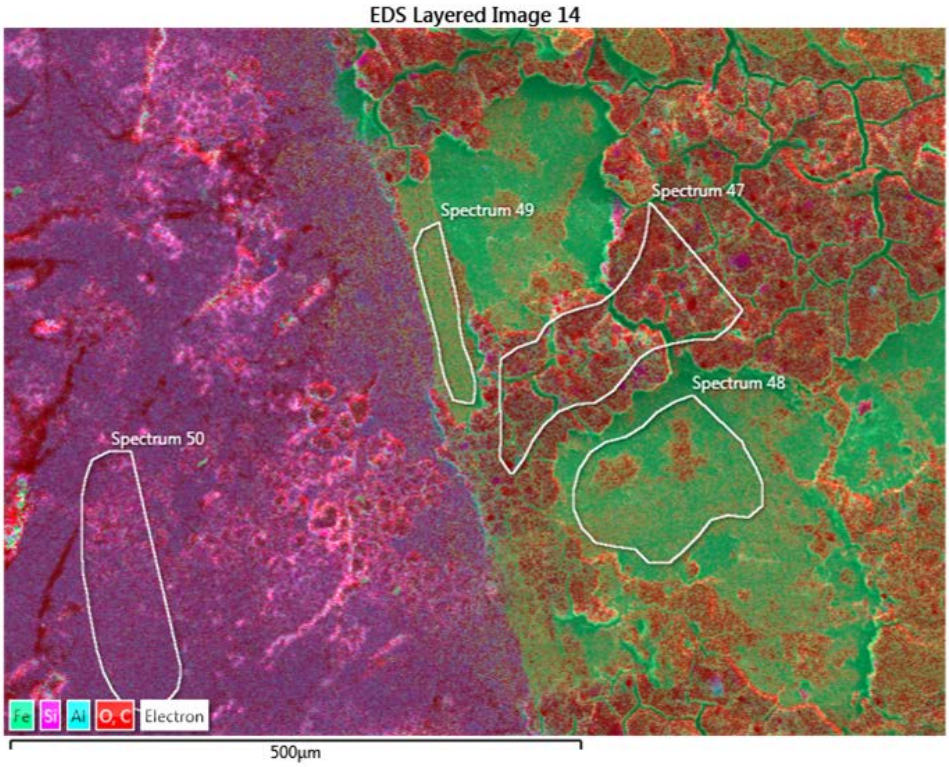

Figure 115: EDS layer image for bottom images of Figure 113 for area 10 of the wall segment from Capsule 5. Sub-areas for localized spectral analysis are annotated [Sample 5A2].

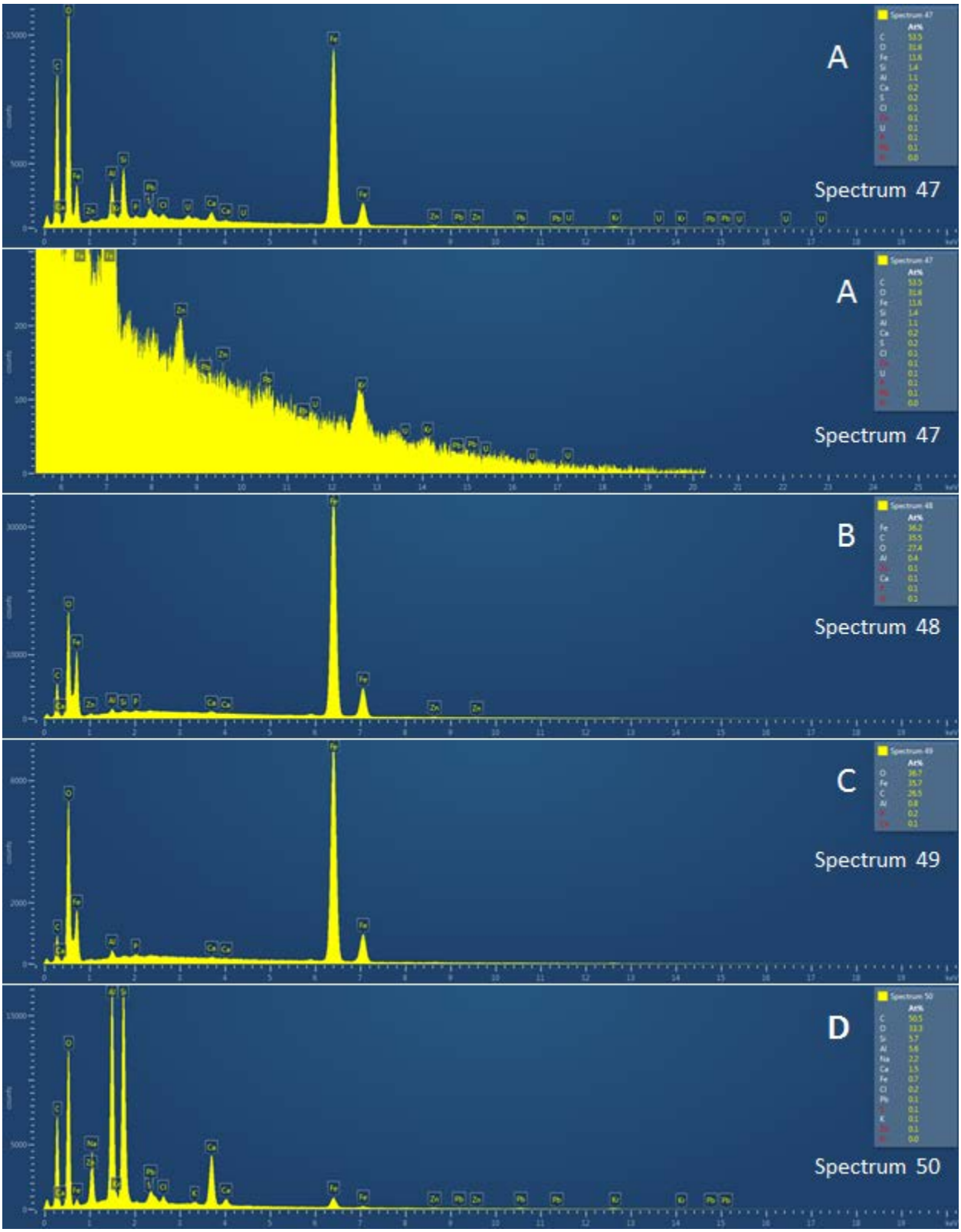

Figure 116: SEM-EDS spectra for the four sub-areas of the Capsule 5 wall segment shown in Figure 115 [Sample 5A2].

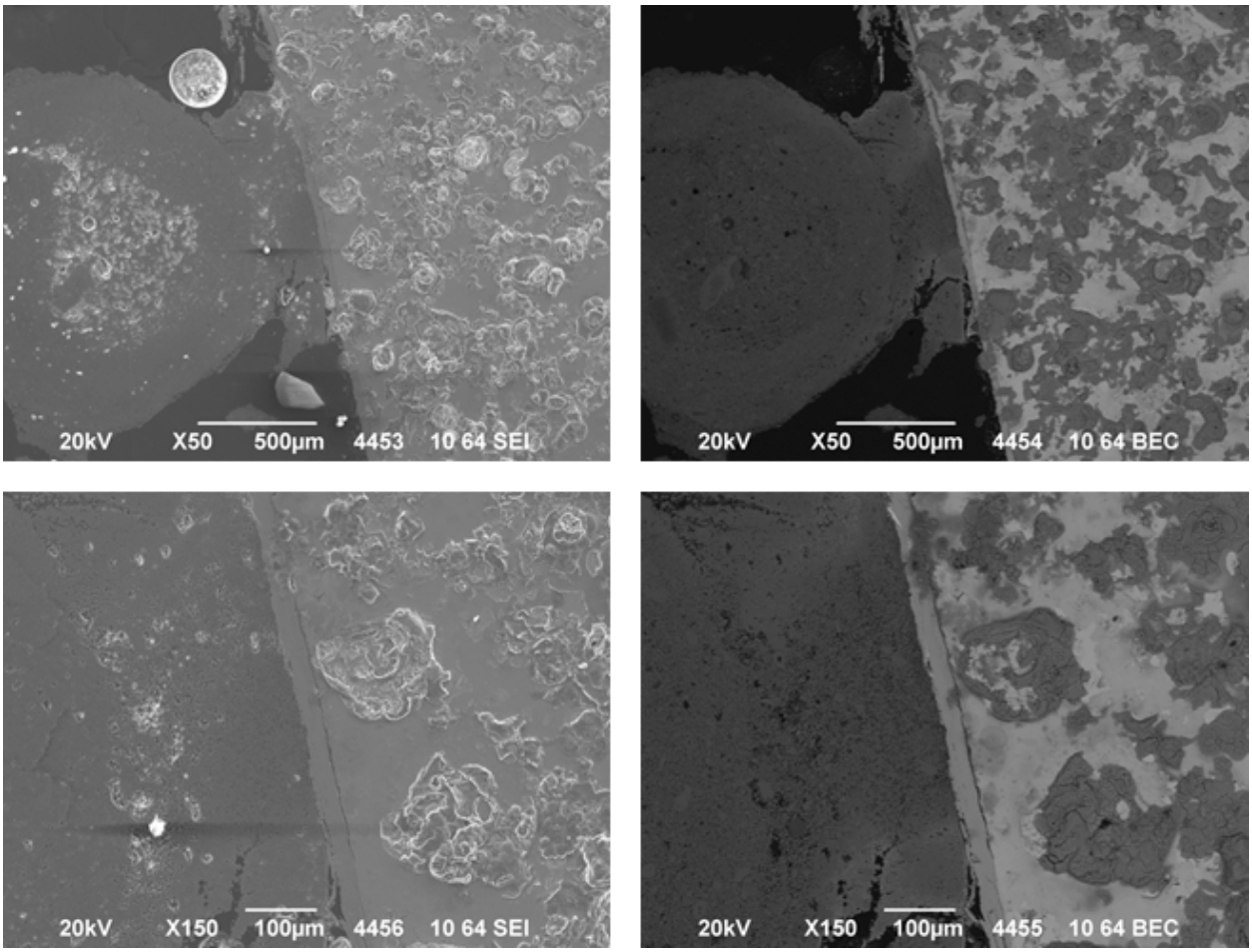

Figure 117: Detailed images of the wall of Capsule 5 at 50× to 150× magnification at location 11. SEI images on the left and BEC images on the right (Images 4452–4455) [Sample 5A2].

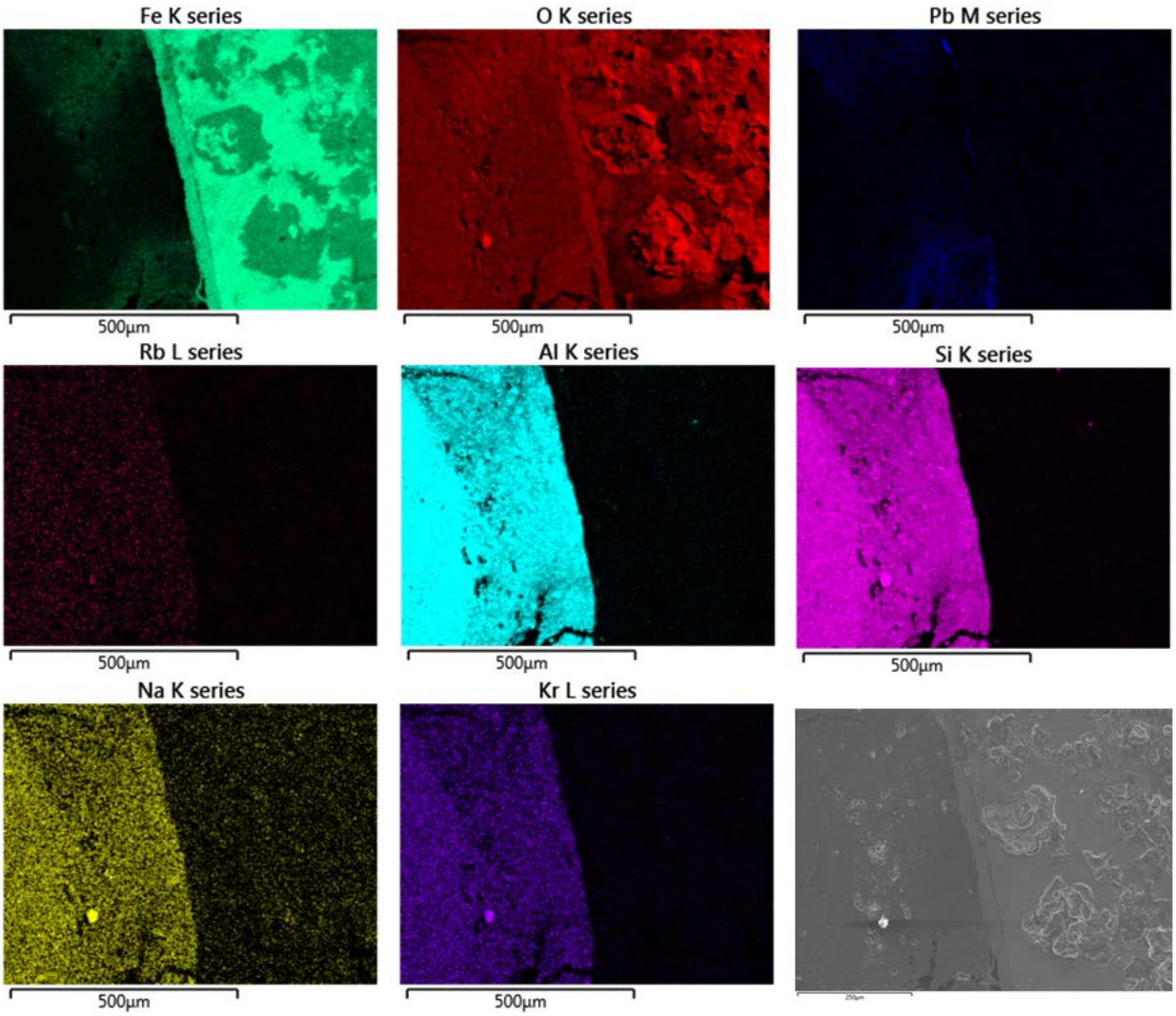

Figure 118: Elemental maps of area shown in bottom images of Figure 116 for area 11 of the exterior surface of the wall segment from Capsule 5 [Sample 5A2].

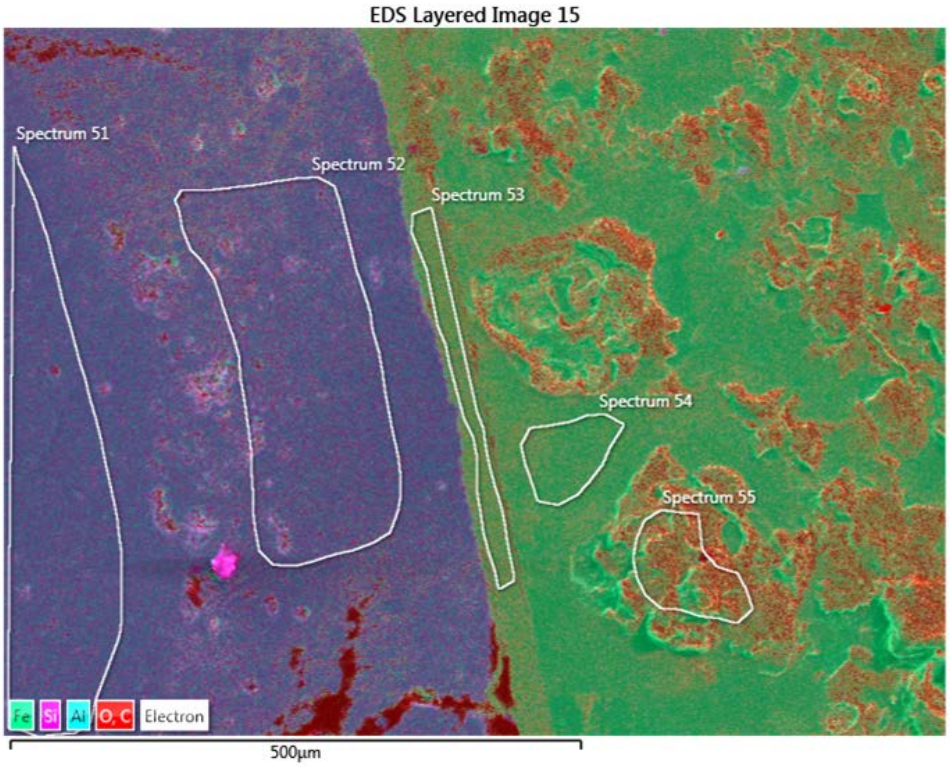

Figure 119: EDS layer image for bottom images of Figure 116 for area 11 of the wall segment from Capsule 5. Sub-areas for localized spectral analysis are annotated [Sample 5A2].

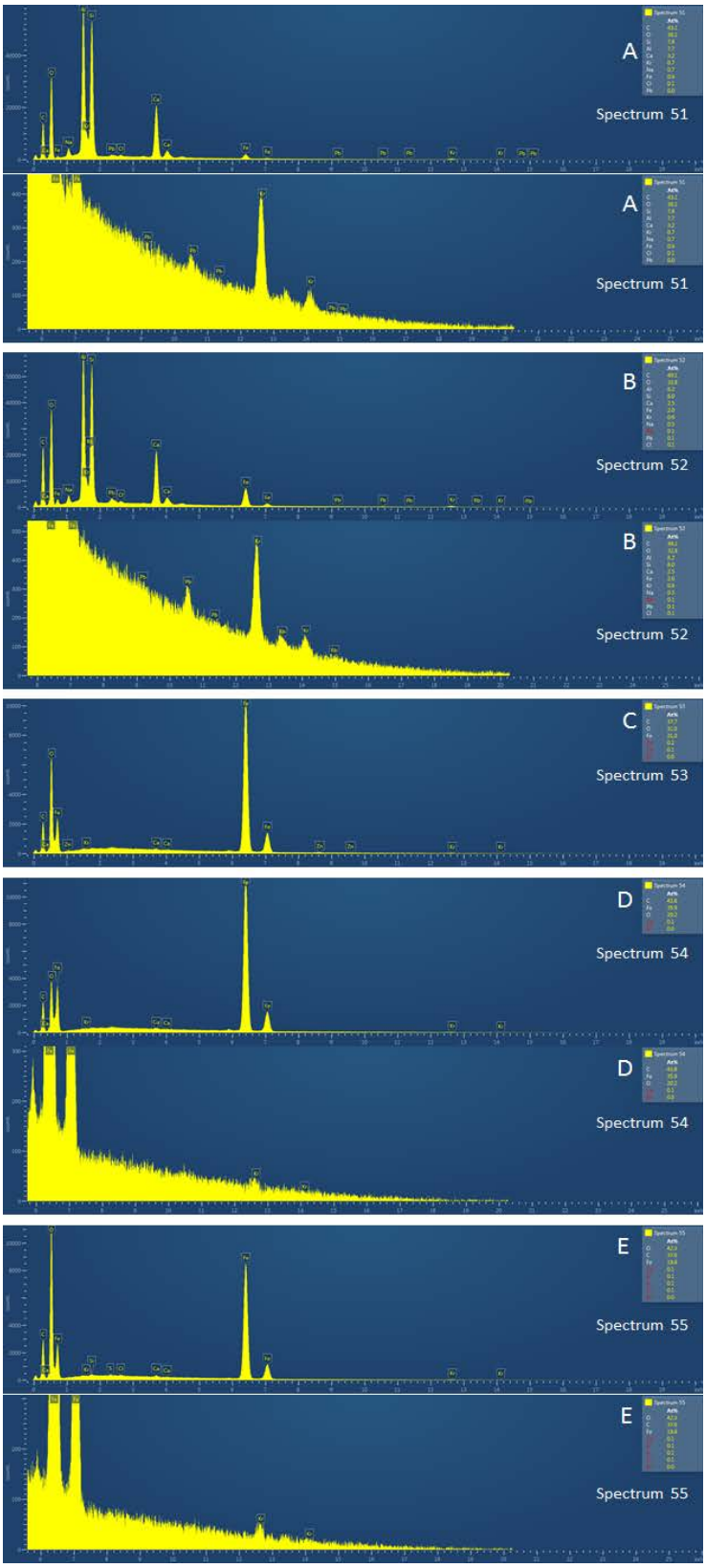

Figure 120: SEM-EDS spectra for the five sub-areas of the Capsule 5 wall segment shown in Figure 119 [Sample 5A2].

Table 4: Compositional analyis of selected area of the Capsule 5 wall sample based on EDS data

			Primary elements identified in EDS spectra														Elemental Ratios			
Image	Spectrum Area #	Feature	Fe	C	O	Cr	Ni	Mn	Si	Al	Ca	`	Rb	Pb	Kr		Fe:O	Cr:Fe	Cr:Ni	Si:Al
Area 5																				
4429	19	oxide layer	18.9	37.6	41.3									2.2			0.46			
4429	20	Interface	33.3	32.5	33.4					0.8							1.00			
4429	21	oxide pocket	21.6	35	43				0.1		0.1			0.2			0.50			
4429	22	zeolite	3.3	39.1	38.8				7.3	7.1	2.8	0.6		0.3	0.6		0.09			1.03
4429	23	base metal	36.2	39.8	24												1.51			
4429	24	base metal	37.4	42.2	20.4												1.83			
Area 6																				
4433	25	oxide pocket	19.3	41.6	38				0.1	0.1	0.1			0.7			0.51			1.00
4433	26	oxide pocket	23	32.4	44.5									0.1			0.52			
4433	27	detached oxide layer	38.4	26.1	35.6												1.08			
4433	28	zeolite	3.6	47.8	33.7				5.8	5.2	2.5	0.5		0.5	0.3		0.11			1.12
Area 7																				
4437	29	weld metal	37.9	45.3	14.4	1.6	0.6		0.1								2.63	0.04	2.67	
4437	30	weld interface	23.9	34.5	39.8	1	0.4		0.2		0.1						0.60	0.04	2.50	
4437	31	base metal	31.2	43.2	25.7												1.21			
Area 8																				
4457	32	weld metal	21.7	37.8	38.5	1.5	0.5										0.56	0.07	3.00	
4457	33	High Z in weld metal	23.3	37.6	32.1	5.5	1.1		0.2								0.73	0.24	5.00	
4457	34	weld interface	22.3	33.5	43.2	0.8	0.2										0.52	0.04	4.00	
4457	35	weld interface	29.8	33.9	34.7	1.1	0.5										0.86	0.04	2.20	
Area 9A																				
4443	37	interface	2.7	43.6	46.4					6.6							0.06			0.00
4443	38	Film pocket	15.9	44.7	38				0.5	0.5	0.2						0.42			1.00
4443	39	oxide	22.5	44.2	33				0.1								0.68			
4443	40	void?	5.2	59	35.4												0.15			
Area 9B																				
4447	41	zeolite	1.3	43.6	36.1				7.3	7.1	3.1	0.7			0.7		0.04			1.03
4447	42	high Fe interface material	20.9	34.7	44				0.1	0.1							0.48			1.00
4447	43	zeolite pocket	2.6	39.7	38.1				7.8	7.8	3.3	0.7					0.07			1.00

4447	44	zeolite pocket	7.5	31.7	43.8				7.1	6.3	2.8	0.8					0.17				1.13
4447	45	base metal	26.5	44.3	29.1				0.1		0.1						0.91				
4447	46	oxide pit	15.2	47.4	37.3				0.1								0.41				
Area 10																					
4452	47	Granular area	11.6	53.5	31.6				1.4	1.1	0.2			0.1			0.37				1.27
4452	48	base metal	36.2	35.5	27.4				0.1	0.4	0.1						1.32				0.25
4452	49	oxide film	35.7	26.5	36.7					0.8	0.1						0.97				0.00
4452	50	zeolite	0.7	50.5	33.3				5.7	5.6	1.5	2.2		0.1			0.02				1.02
Area 11																					
4456	51	zeolite	0.6	43.1	36.1				7.8	7.7	3.2	0.7			0.7		0.02				1.01
4456	52	zeolite interface	2	49.1	32.8				6.2	6	2.5	0.5	0.1	0.1	0.6		0.06				1.03
4456	53	oxide layer	31	37.7	31						0.1						1.00				
4456	54	base metal	35.9	43.8	20.2						0.1						1.78				
4456	55	oxide pit	19.8	37.6	42.3				0.1		0.1						0.47				

8. XRD ANALYSIS OF MATERIAL RECOVERED FROM CAPSULES 2 AND 5

X-ray diffraction studies were performed using a D2Phaser Benchtop (Bruker AXS, Inc.) x-ray diffractometer. Irradiated samples were mounted in epoxy and sealed using a Kapton tape to prevent any contamination of the instrument. The sample holders consisted of a plastic base, and the epoxy sample was mounted in an aluminum holder. The XRD pattern of the powdered base metal sample (5A MS) was acquired using 0.004° step size and 5–70° 2Θ range. XRD patterns of irradiated samples were acquired using the same step size, but in a 5–110° 2Θ range. However, the XRD patterns are only reported here from a 5–70° 2Θ range focusing on major peaks because no significant peak intensities were observed at high angles >70° 2Θ. The XRD pattern of an empty sample holder representing similar conditions of the actual samples was also acquired to identify the peaks coming from the sample holders and the low-angle hump due to Kapton tape. An internal silicon standard (Si SRM640d) was used with the sample holder and the base metal sample to determine sample displacement error in the XRD patterns. This displacement was corrected in the reported XRD patterns of the irradiated samples in which no internal standard was used when obtaining XRD patterns to prevent any veiling of signal coming from the relatively low peak intensity of the Kr-containing sample.

At the time the XRD analysis was completed, it was believed that the starting material for the legacy Kr samples was a 5A molecular sieve material, but this had not been confirmed. As a reference, a sample of commercially available recently procured 5A molecular sieve material containing no Kr was powdered and examined. Figure 121 shows the XRD pattern acquired for this powdered 5A MS zeolite sample. The peak positions of this XRD pattern fit well with the ICSD 15392 powder pattern of $Ca_4Na_4(Al_{12}Si_{12}O_{48})$, zeolite 5A (Ca-exchanged, dehydrated), indicating supplied commercial 5A MS contained zeolite 5A.

The XRD patterns (Figure 122) of the samples of the zeolite material recovered from Capsules 2 and 5 did not show significant peak intensities that correspond to the reflections of recently procured commercially available zeolite 5A MS material. Samples from Capsule 2 are designated K2 and K3, and those from Capsule 5 are noted as K4 and K5. K3 and K5 were coated with a thin layer of carbon to improve the SEM analysis, and samples K2 and K4 were not coated. The XRD patterns for these four samples are remarkably similar and show a significant alteration from the presumed 5A zeolite starting material.

Since most of the intense peaks of zeolite 5A lie in the range of 5–30° 2Θ, it was difficult to obtain conclusive information regarding phase stability during the zeolite loading, pore collapse (and HIPed in the case of Capsule 5), and how this may have been altered during the subsequent storage period. However, comparison of XRD patterns of the irradiated samples with the sample holder and base material sample showed that there are minor peaks with weak intensities that correspond to the samples. These positions and relative intensities of these peaks, however, do not match with zeolite 5A. The verification of the relative peak positions/intensities could not be done due to high background in the low angle region.

Two main peak broadenings were also observed in ~6–9° and ~9.7–14° 2Θ range in all four irradiated samples. A slightly higher peak broadening compared to background (sample holder) can be observed in ~24–30° 2Θ range too. The peak broadening could be due to amorphized zeolite samples, but the confirmation of this suggestion is challenging since a XRD pattern of a powder sample of the highly radioactive sample could not be performed.

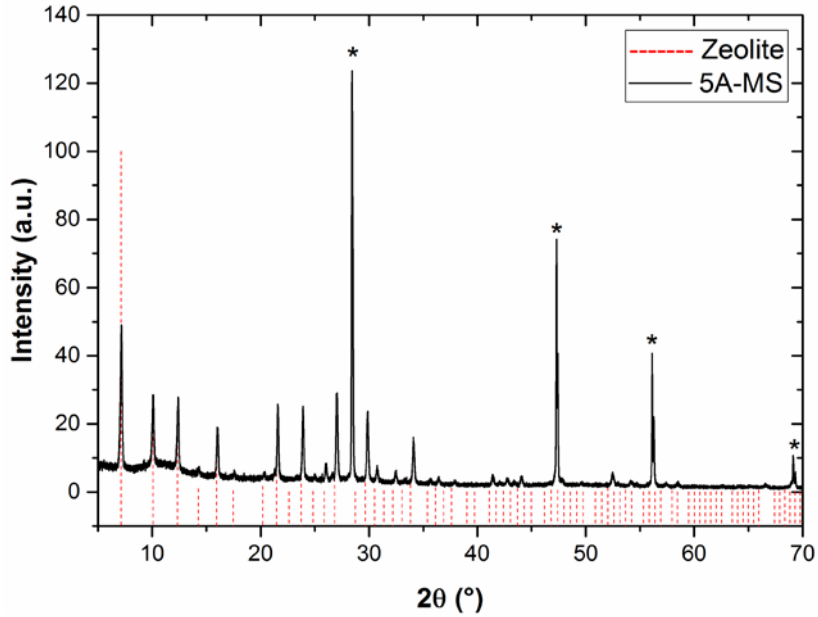

Figure 121: Experimental XRD pattern of fresh 5A zeolite sample (black color) and the reference pattern for zeolite 5A (red color lines). Asterisks indicate the reflections corresponding to Si standard.

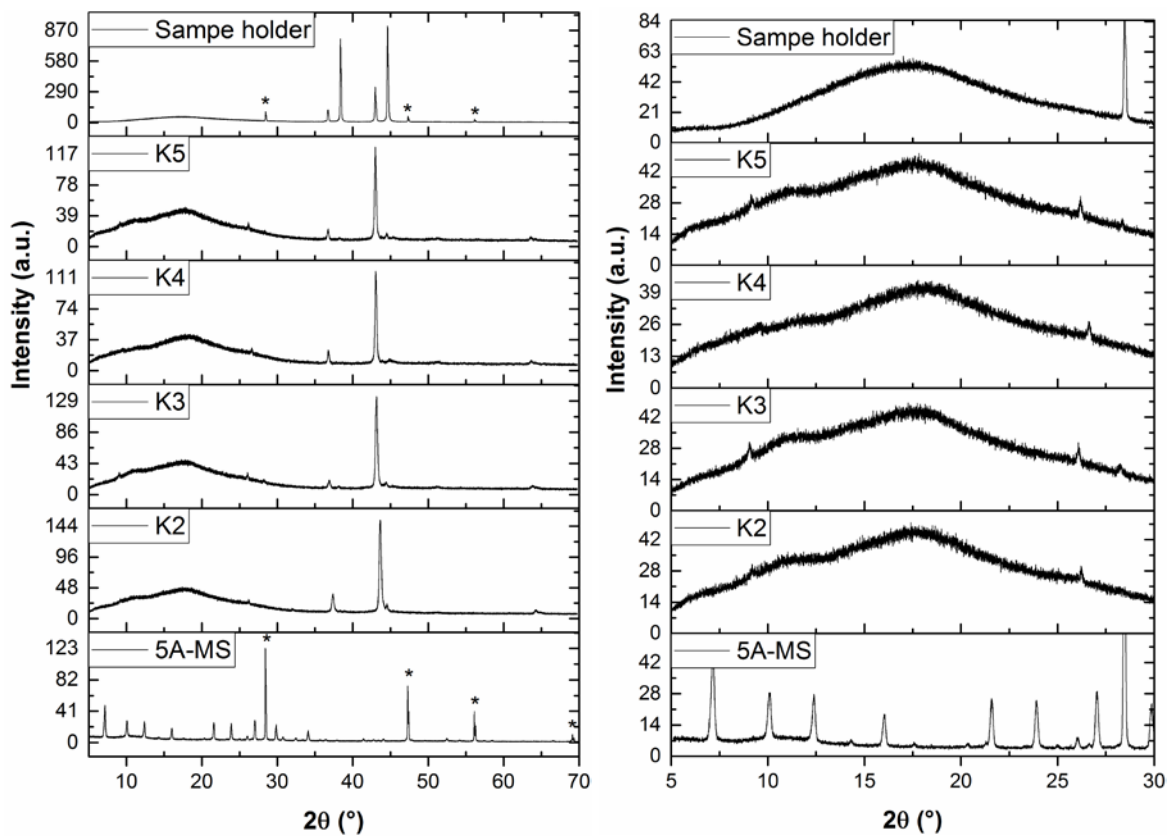

Figure 122: A comparison of XRD patterns of irradiated Kr-85 zeolite samples with 5A MS base metal sample and the sample holder. Asterisks indicate the reflections corresponding to Si standard. Full XRD patterns from 5–70° 2Θ range are shown in the left side figure, and a focused range of 5–30° 2Θ is shown on the right side.

9. DISCUSSION AND PATH FORWARD

9.1 Discussion

The analysis of the materials contained in the two breached legacy ^{85}Kr capsules has produced a significant amount of information:

- The EDS-derived chemical analysis indicates a chemical composition of the recovered materials consistent with zeolite 5A.
- The XRD analysis of the recovered materials does not show any significant structure consistent with zeolite 5A. Although it would be expected that the encapsulation and HIPing process would alter the structure, the areas of greatest interest are masked by the signal from the sample holder. As a result, very little information on the sample could be obtained from the XRD analysis. At best, these results are inconclusive.
- The elemental mapping indicates that Kr and Xe are coincident with the Si, Al, Ca, and Na, implying that the noble gases have remained within the collapsed zeolite structure. Calculations based on the EDS-derived elemental analysis show a residual Kr level within a factor of 2 from reported Kr capacities for this type of processed material.
- Rubidium was also observed at levels near the detection levels for the EDS. The Rb appeared to be coincident with the Kr.
- Lead was observed within the zeolite material contained within Capsule 5. The origin of the lead is unknown at this time.
- The initial optical analysis of the capsule material itself showed significant corrosion throughout the entire wall. EDS elemental mapping of the capsule wall material appeared to be consistent with carbon steel, and the weld material appeared to be consistent with stainless steel.
- The interior surface of the unHIPed Capsule 2 appeared to have a layer of material containing Al, Si, and Ca similar to the 5A molecular sieve.
- An iron oxide film layer was observed. EDS spectra for this film indicated an O:Fe ratio of 1. This would be consistent with wuestite (FeO). Wuestite or wüstite is gray color. Other distinct iron oxide locations were identified with an O:Fe ratio of 2. This could be consistent with FeO(OH) (rust). The formation of the FeO(OH) seemed to appear in areas where the FeO layer is broken. Portions for the FeO layer appear on the surface of the FeO(OH) on the interior surface of the capsule.
- Analysis of the pit-like features in the wall showed the presence of both iron and O with an O:Fe ratio of 2. This would be consistent with FeO(OH) or rust.
- Analysis for Rb within the corrosion sites was inconclusive. This does not mean that Rb was not present at the corrosion site, but if it was it was present at levels below 0.1 at. %.
- It could not be determined if all of the pits observed across the capsule wall thickness were interconnected in a way that would compromise the capsule integrity. It is not known if the pitting observed in the wall of these breeched capsules would be present in what are believed to be sealed capsules. It should be noted that these materials have been exposed to a number of environmental conditions during both storage and when they were sectioned in the hot cell. Thus, it is not known when the corrosion occurred.

9.2 Path Forward

There are several additional analyses that would be useful to perform on these samples prior to evaluating the "un-breached" capsules.

- Cold surrogate samples should be prepared for comparison with these hot samples. These should be made with and without Kr and with and without Rb. The Rb should be loaded as encapsulated Rb and as free Rb. The Rb-containing samples should be examined over the next several years to evaluate the corrosion effects. The Kr-containing samples should be used for both baseline reference data points and for the development of the analytical methods for analysis of the recovered zeolite materials.
- Sufficient samples should be made to provide additional practice materials for head gas sampling, which is planned for the unbreeched samples.
- Detailed Rb corrosion studies should be conducted.
- Focused ion beam study of the capsule walls should be performed to examine corrosion within the walls in locations that have not been exposed to the environment. This will also aid in the determination of linkage between the pits that would compromise the capsule integrity.
- A portion of the material recovered from Capsules 2 and 5 should be chemically analyzed by ICP-MS. This will require repackaging of the material in a glove box to control the spread of contamination. During the dissolution, the off-gas should be collected and an attempt made to quantify the amount of Kr contained within the sample.
- Micro-XRD could be attempted on the existing uncoated and mounted materials, K2 and K4. These samples may avoid the interferences posed by the Kapton tape used to seal the samples.

10. REFERENCES

1) Bruffey, S. H., D. M. Strachan, R. T. Jubin, and B. B. Spencer, *A Literature Search on the Effects of the Decay of ^{85}Kr to ^{85}Rb on Long-term Storage Options*, FCRD-MRWFD-2015-000626, ORNL/SPR/2015-575, UT-Battelle, LLC, Oak Ridge National Laboratory, September 30, 2015.
2) Garn, T., M. Greenhalgh, and J. Law, *Strategy for Analysis of Legacy Kr-85 Samples*, FCRD-SEPA-2011-000027, INL/MIS-10-20449, Dec. 23, 2010.
3) Jubin, R. T., *Multi-lab Analytical Plan for Analysis of Legacy ^{85}Kr Samples*, FCRD-MRWFD-2015-000624, ORNL/SPR-2015/188, UT-Battelle, LLC, Oak Ridge National Laboratory, April 30, 2015.
4) "Immobilization and Leakage of Krypton Encapsulated in Zeolite or Glass," Christensen, A. B.; Del Debbio, J. A.; Knecht, D. A.; Tanner, J. E., Materials Research Society Symposia Proceedings, vol. 6, pp. 525-532, 1982.
5) "Immobilization of Krypton-85 in Zeolite 5A," Christensen, A. B.; Del Debbio, J. A.; Knecht, Dieter; Tanner, J. E.; Cossel, S. C., Proceedings of the 17th DOE Nuclear Air Cleaning Conference, vol. 1, pp. 333-356, 1983.
6) "Loading and Leakage of Krypton Immobilized in Zeolites and Glass," Christensen, A. B.; Del Debbio, J. A.; Knecht, D. A.; Tanner, J.E., Scientific Basis for Nuclear Waste Management, vol. 3, pp. 251-258, 1981.
7) Technical and Economic Feasibility of Zeolite Encapsulation for Krypton-85 Storage, Benedict, R. W.; Christensen, A. B.; Del Debbio, J. A.; Keller, J. H.; Knecht, D. A., Exxon Nuclear Idaho Co., Inc., Idaho Falls, Department of Energy, Sept. 1979.
8) Personal Communications, Deiter Knecht, Oct. 2010.